



Thor Offshore Wind Farm

Hydrodynamics & Sediment
Technical report

Thor Wind Farm I/S

Date: 07 February 2024

Rev.no.	Date	Description	Prepared by	Verified by	Approved by
01	13.01.23	First version	TEB/VIMI	KLBU	RHO
02	13.10.23	Updated landfall installation	TEB	SSC	RHO
03	06.02.24	New appendices showing near-shore area	TEB	STOR	RHO

Contents

1.	Introduction.....	6
1.1.	Objective.....	6
2.	Project description	6
2.1.	Wind turbines and foundations	6
2.2.	Offshore substation platform.....	9
2.3.	Offshore cables.....	9
2.4.	Project timeline	9
3.	Methodology.....	10
4.	Background data.....	11
4.1.	Metocean data, project	11
4.1.1.	Current measurements.....	11
4.1.2.	Wave measurements.....	12
4.2.	Sediment data, project	13
4.2.1.	Surficial sediment	13
4.2.2.	Sediment samples	15
4.3.	Water level.....	17
4.3.1.	Water levels in Denmark	17
4.3.2.	Water levels in the UK.....	18
4.3.3.	Astronomical tide	19
4.4.	Temperature and salinity conditions	19
4.5.	Wind and air pressure.....	20
4.6.	Bathymetry	20
4.6.1.	MBES in the project area.....	20
4.6.2.	Cross shore profiles, Danish Coastal Authorities	20
4.6.3.	Other bathymetric data.....	22
4.7.	Nearshore morphology.....	22
4.7.1.	Danish Coastal Authority data.....	22
4.7.2.	Arial photos.....	22
4.8.	Offshore morphology	25
4.9.	Installation program, sediment disturbance.....	25
5.	Model setup	26
5.1.	Bathymetry and model mesh	26
5.2.	Numerical models	27
5.2.1.	Hydrodynamic model	27

5.2.2.	Spectral wave model	27
5.2.3.	Sediment model	27
5.3.	Boundary data, hydrodynamic and wave model.....	28
5.3.1.	Tide.....	28
5.3.2.	Wind.....	28
5.4.	Verification, hydrodynamic and wave model	28
5.5.	Project implementation	32
5.6.	Boundary data, sediment model	32
6.	Selection of simulation period	33
7.	Pressure, current and waves	36
7.1.	Current.....	36
7.2.	Waves.....	36
8.	Pressure, water exchange	38
9.	Pressure, seabed morphology.....	40
10.	Pressure, longshore sediment transport.....	41
11.	Sediment dispersal, during installation	43
11.1.	Scenario 1: cable burial with dredging, inclusive IAC and MP installation.....	43
11.2.	Scenario 2: cable burial without dredging	50
12.	Summary	52
13.	References	54

Appendices:

- Appendix 1 : DMU1035, salinity and temperature profiles
- Appendix 2 : DMU1023, salinity and temperature profiles
- Appendix 3 : DMU1072, salinity and temperature profiles
- Appendix 4 : DMU1025, salinity and temperature profiles
- Appendix 5 : Particle size distribution
- Appendix 6 : Yearly current distribution
- Appendix 7 : Yearly wave distribution
- Appendix 8 : Duration with sediment concentrations above 10 mg/l, depth average
- Appendix 9 : Duration with sediment concentrations above 50 mg/l, depth average
- Appendix 10 : Duration with sediment concentrations above 100 mg/l, depth average
- Appendix 11 : Duration with sediment concentrations above 500 mg/l, depth average
- Appendix 12 : Duration with sediment concentrations above 1000 mg/l, depth average
- Appendix 13 : Duration with sediment concentrations above 50 mg/l (bottom 10 meters)
- Appendix 14 : Duration with sediment concentrations above 100 mg/l (bottom 10 meters)
- Appendix 15 : Duration with sediment concentrations above 500 mg/l (bottom 10 meters)
- Appendix 16 : Duration with sediment concentrations above 1000 mg/l (bottom 10 meters)
- Appendix 17 : Average sediment concentrations during construction, depth average
- Appendix 18 : Average sedimentation during construction
- Appendix 19 : Duration with sediment concentrations above 10 mg/l (bottom 10 m): Nearshore
- Appendix 20 : Duration with sediment concentrations above 50 mg/l (bottom 10 m): Nearshore
- Appendix 21 : Maximum sedimentation in the construction period: Nearshore

1. Introduction

As part of the Danish Parliament's Energy Agreement of 29 June 2018, the Danish Energy Agency (DEA) agreed to the construction of three new 800 – 1,000 MW offshore wind farms (OWF), to be completed before 2030. Subsequently in 2019, the DEA initiated a screening study of Danish territorial waters to identify suitable sites for OWF development, from which the Thor Offshore Wind Farm (Thor OWF) was identified. According to the agreement, the site for Thor OWF is to be located in the North Sea, offshore Nissum Fjord, and the coastal town of Thorsminde, at a distance of at least 20 km and will be constructed and fully operational latest 31st December 2027. Thor Wind Farm I/S, owned by RWE, has been awarded the concession agreement for the construction and connection of Thor OWF to the 220 kV grid at Volder Mark, while Energinet is responsible for the conversion of the 220/400 kV substation at Idomlund.

Before offshore works commence, an environmental impact assessment (EIA) of the offshore Thor OWF project must be completed under Section III of the Danish Environmental Assessment Act. The project is also covered by section 1(2) no.1 of executive order no. 803 (BEK nr 803 af 14/06/2023), which relates to impact assessments concerning international nature conservation sites and the protection of certain species.

1.1. Objective

The purpose of the hydrodynamic study is to describe the present situation (hereafter referred to as *baseline*) and the potential impact of the construction and operation of Thor Offshore Wind Farm on:

- Spreading of sediment due to dredging, jetting, etc.;
- Changes in the general current pattern and eventual blocking;
- Changes in the wave pattern;
- Changes in the longshore sediment transport within and around the wind farm area.

2. Project description

This chapter provides a summary of the various project elements for Thor OWF, including the wind turbines and their foundations, an offshore substation as well as inter-array and export cables. An overall project timeline for offshore construction and installation is also provided.

2.1. Wind turbines and foundations

Thor OWF will have a maximum installed capacity of 1,000 MW allowing for between 72 14 MW wind turbines. The layout for the case with 72 wind turbines is shown in Figure 2.1.

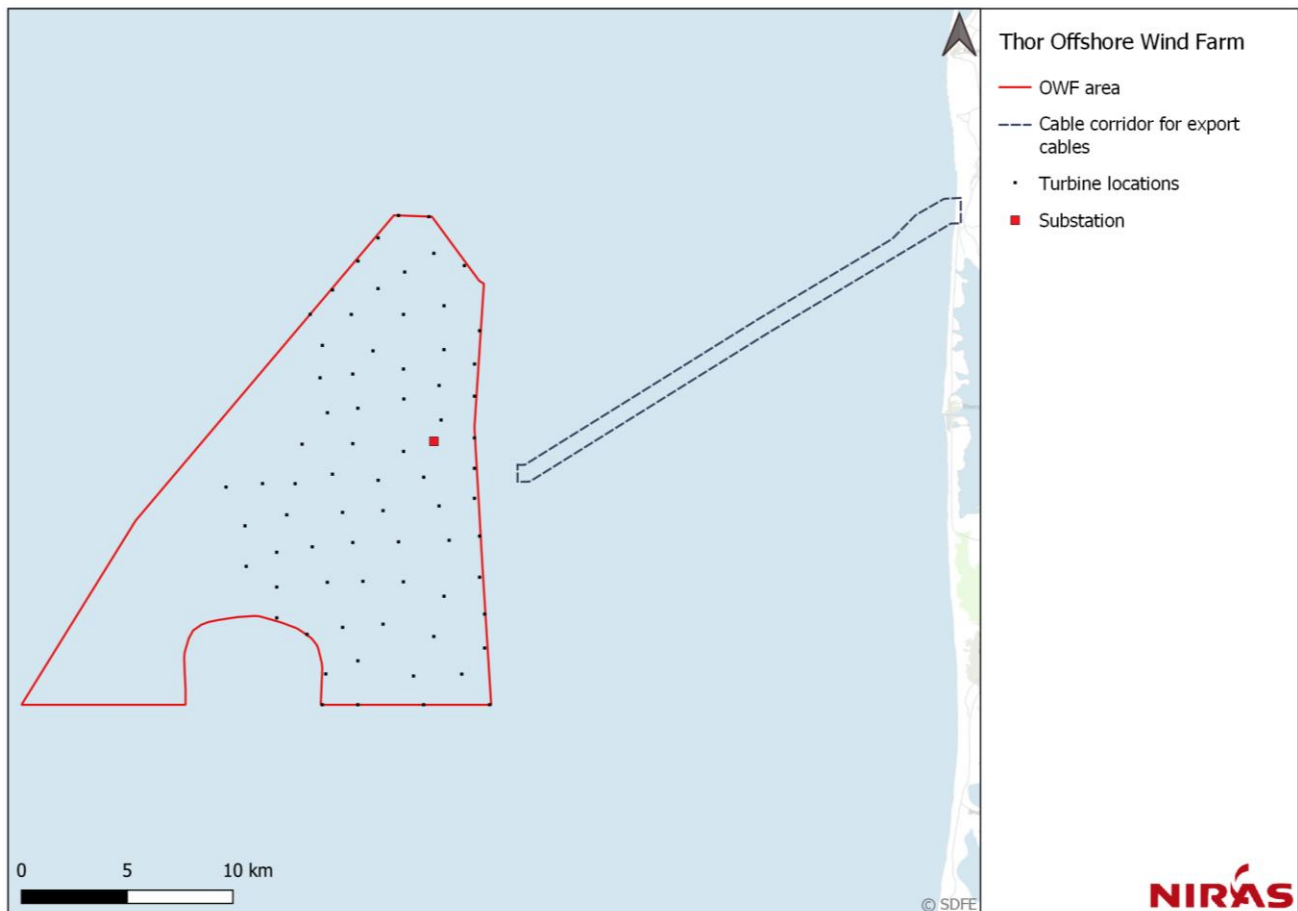


Figure 2.1: Suggested layout for Thor OWF. The total number of turbines is 72.

The wind turbines will have a rotor diameter of 236 m and a hub height of 148 m, resulting in a total tip height of 266 m (Figure 2.1). The wind turbines will be located toward the eastern part of the Thor OWF project area to account for the parameters identified during preliminary investigations and the strategic environmental assessment. The wind turbines will be installed on steel monopile foundations with a length of approximately 65–105 m and a diameter of 8.0–10.0 m. The pile will be driven into the seabed via ramming until an embedded depth of around 50 m is reached.

Based on a maximum installed capacity of 1,000 MW, Thor OWF will comprise 72 turbines with an individual capacity of 14 MW. Each wind turbine comprises a steel tower, a nacelle, and three blades (as seen in Figure 2.2), with the exact dimensions and appearances of the wind turbines dependent on the manufacturers' design.

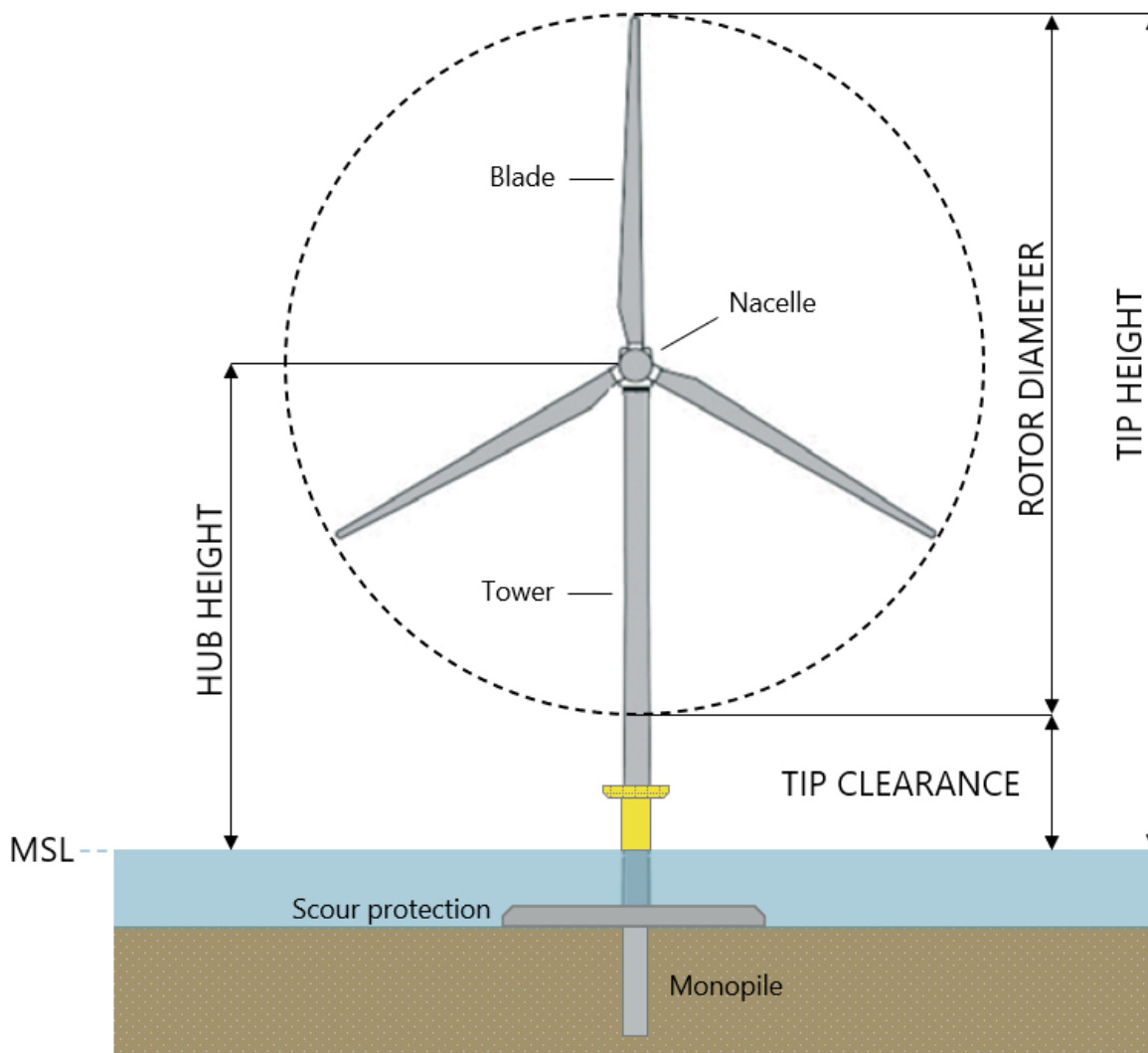


Figure 2.2: Illustration of a typical offshore wind turbine with blades, nacelle, tower, monopile foundation and scour protection. Visual explanations of hub height, tip clearance, rotor diameter and tip height are included for reference.

The dimensions of the turbines considered for the Thor OWF are summarised in Table 2-1.

Table 2-1: Dimensions of the 14 MW turbines considered for Thor OWF. The tip clearance is 30 m (the distance between the lower wing tip and the highest astronomical tide).

Dimensions	14 MW wind turbine
Rotor diameter (m)	236
Tip height (m)	266
Hub height above MSL* (m)	148
Rotor swept area (m ²)	43,743
Nacelle (length x width x height) (m)	22x11x12 – 29x12x12

* MSL = Mean sea level

The distance between the highest astronomical tide (HAT) and the lower wing tip, termed the tip clearance, must be at least 20 meters to ensure the safety of navigation for mariners (Danish Maritime Authority, u.d.). For the Thor OWF, the tip clearance will be 30 m, however, the Danish Maritime Authority will need to approve the distance between the HAT and lower wing tip before construction begins. Furthermore, offshore wind turbines with a height of 100 m or more above MSL must be reported to, and approved by, the Danish Civil Aviation and Railway Authority.

2.2. Offshore substation platform

An offshore substation will collect, stabilize and transform the electricity generated from the individual wind turbines into a higher voltage before exporting the power to land. The offshore substation comprises a topside installation containing two 275/66 kV transformers, switchrooms, earthing transformers, and a backup power source, as well various operational facilities (e.g. control room), navigation and aviation light control, fire suppression, rainwater separation, and communication antennas. The substation will be remotely operated but will be able to accommodate a normal working team of 4–6 persons and will be equipped with a heli-hoist platform, two boat landings, and two pairs of access points for motion-compensated gangways. The foundation used for the offshore substation will be a post-piled jacket.

2.3. Offshore cables

66 kV inter-array cables will connect the wind turbines via a series of 16 array strings which will be routed to the offshore substation platform and onto the cable deck. The inter-array cables will comprise three cores consisting of an aluminium conductor and an armour layer surrounded by insulating material and will have a total diameter of approximately 120–195 mm. The total length of inter-array cabling required for Thor OWF is approximately 205 km.

Two 275 kV submarine export cables will carry the generated electricity from the offshore substation platform to landfall east of Volder Mark, where they will be connected to a transition joint bay on the beach. The export cables will comprise three cores consisting of aluminium or copper conductors surrounded by insulating material encased within an armour layer and surrounded by an outer protective sheath. The export cables will have a diameter of between 286–305 mm and will each have a length of approximately 30 km.

2.4. Project timeline

The offshore construction of Thor OWF will start in 2024/2025 and the wind farm will be in full operation by the end of 2026.

3. Methodology

To estimate the dispersal of sediment during construction and the pressure on the hydrodynamics in the operation phase, 3 types of numerical models are used:

- 1) A hydrodynamic model to simulate the water level and currents.
- 2) A wave model to simulate the wave climate.
- 3) A sediment model to simulate the spread and deposit of the sediments dispersed due to the installation.

The driven forces are astronomical tides at the open boundary for the hydrodynamic model and wind fields at the surface. The wave model is forced with water levels from the hydrodynamic model and wind fields at the surface.

Before any evaluation of potential impacts the 2 base models, the hydrodynamic model and the wave model, are calibrated against the data collected by Energinet from 2020 to 2021 and publicly available water level data from the UK and Denmark.

Based on 10 years of data the baseline is described and an average year is identified for input to the Construction and Operation Phase.

The applied numerical models are MIKE21 HD, SW and PT e.g. hydrodynamic model, wave spectra model and particle tracking all developed by DHI (DHI, u.d.).

4. Background data

In the present chapter, the background data used in the numerical modelling and the description of the morphological, oceanographic, and hydraulic conditions at the site and along the cable corridor are presented. This includes metocean data, sediment grab samples and morphological surveys, coastal profiles, and shoreline evolution.

4.1. Metocean data, project

Currents and waves have been measured in the project area from May 2020 to May 2021. The data is measured at latitude 56.3489N and longitude 7.60647E. The location of the measurement station relative to the project area is illustrated in Figure 4.1.

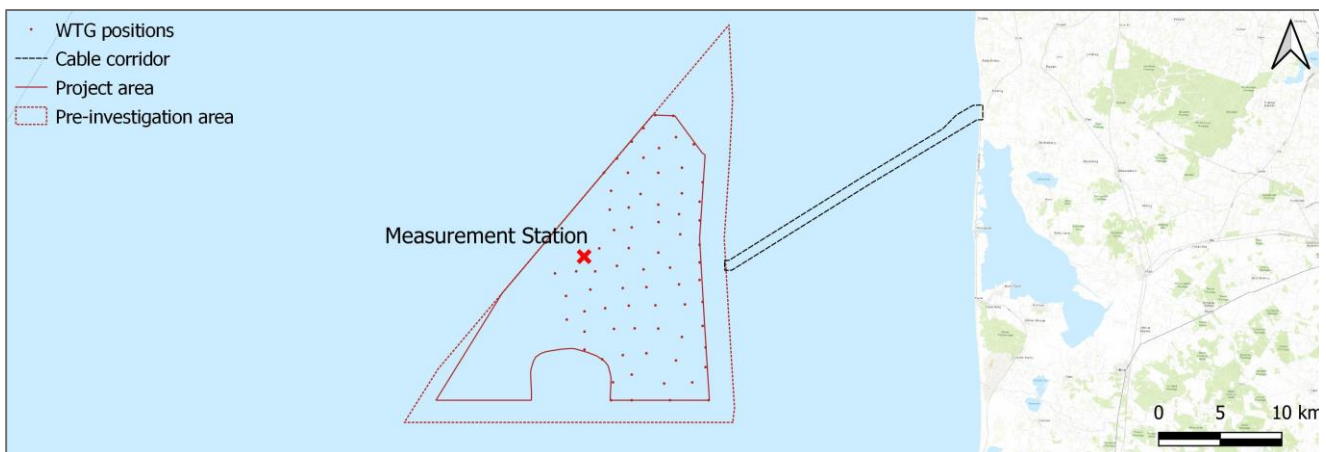


Figure 4.1: Location of measurement station.

4.1.1. Current measurements

The current speed and direction are measured through the water column at five-meter intervals from 5 to 30 m water depth. An example of the horizontal velocity profile through the water column is illustrated in Figure 4.2. The figure shows the U (east to west) and V (north to south) components of the current velocity.

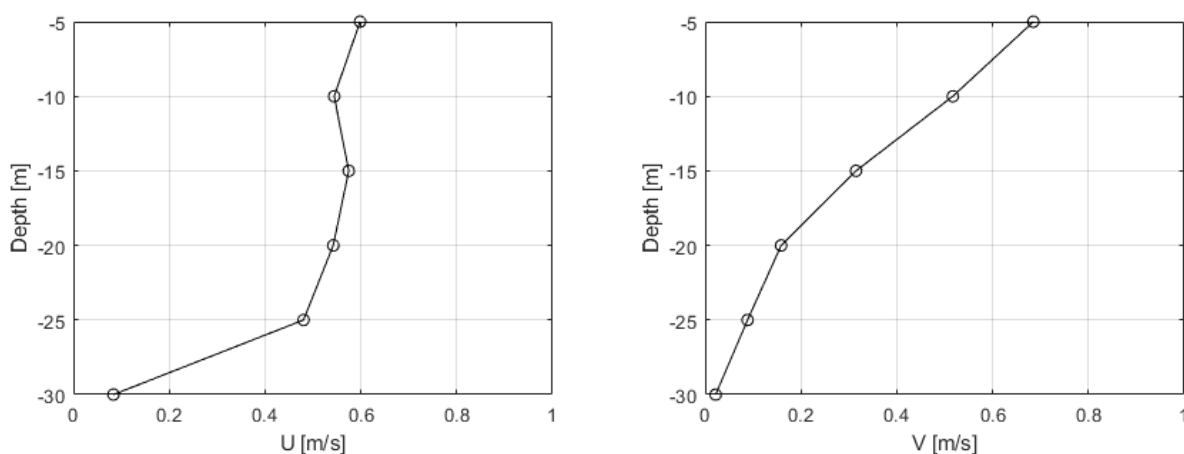


Figure 4.2: Examples of horizontal velocity profiles through the water column. Left: East/West components. Right: North/South components.

Since the hydrodynamics are modelled in a 2D model, the depth-averaged current speeds are calculated from the velocity profiles. A time series showing the depth-averaged current speeds during the year of measurements is illustrated in Figure 4.3. The figure shows, that the highest current speeds generally are observed in the wintertime. The figure furthermore shows that the measurements have gaps between November 2nd to November 9th and January 22nd to February 1st.

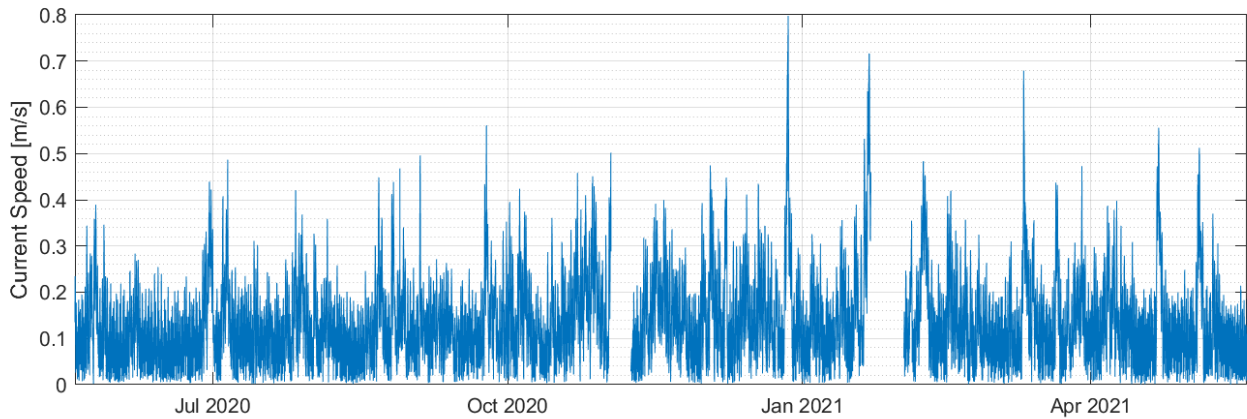


Figure 4.3: Timeseries of depth-averaged current speeds at the measurement station.

4.1.2. Wave measurements

The measurement station also measured the wave climate in the year from May 2020 to May 2021. The magnitude and direction of the significant wave height (H_{m0}) and mean wave period are illustrated in Figure 4.4. The figures show that the waves primarily are coming from WNW.

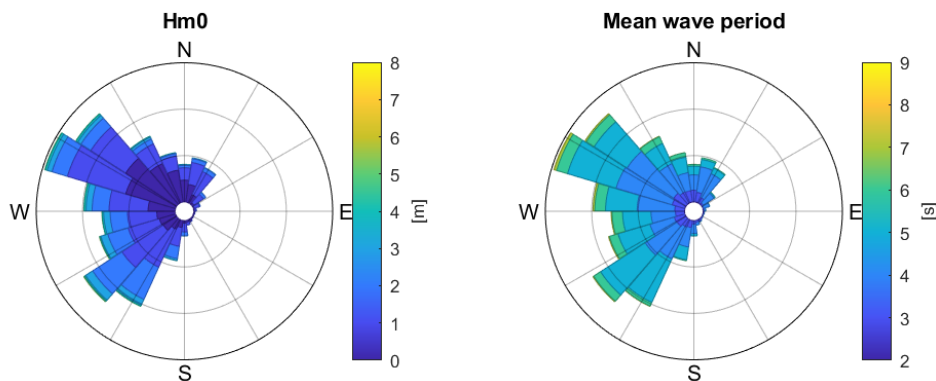


Figure 4.4: Rose plots showing significant wave height (left) and mean wave period (right) at the measurement station.

A time series showing the significant wave height during the year of measurements are illustrated in Figure 4.5. The figure shows, that the highest waves generally are observed during winter. Just like the current data, the wave measurements have gaps from November 2nd to November 9th and January 22nd to February 1st.

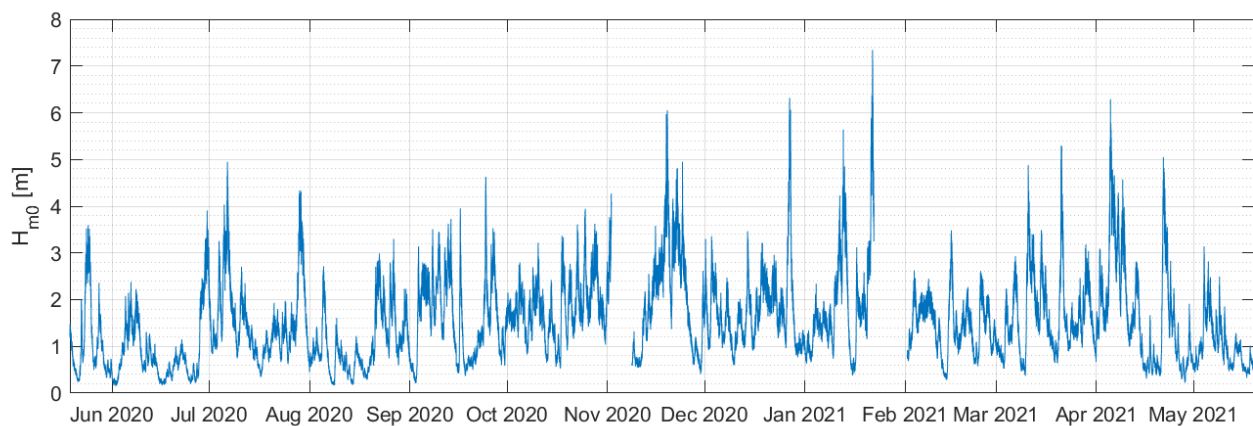


Figure 4.5: Timeseries of significant wave height at the measurement station.

4.2. Sediment data, project

In the following sections, there will be distinguished between the area where the offshore wind turbines are located (hereafter referred to as the OWF area) and the area of the proposed export cable corridor (hereafter referred to as the ECC area). Since four potential cable corridors were outlined in the early phases of the project, surveys were carried out at four cable corridors as seen in Figure 4.6. It is, however, only the third cable corridor (counting from the south toward the north), that will be used as an export route. The three other cable corridor surveys will therefore be disregarded in the following sections.

The surficial soil at the OWF area and ECC area is described based on the surficial geology by (MMT, 2020a; MMT, 2020b) and the classification of samples collected also in 2019.

4.2.1. Surficial sediment

The surficial soil in the 442 km² pre-investigation area for Thor OWF as well as along the four considered ECC areas are illustrated in Figure 4.6. The surficial soil is categorized into five different soil types:

1. Clay
2. Sand
3. Gravelly sand to sandy gravel
4. Gravel
5. Diamicton

From Figure 4.6 it is seen, that the seabed primarily consists of sand and gravelly sand to sandy gravel in the OWF area. Besides the areas with sand and sandy gravel, there are smaller areas with diamicton and gravel. Given the small areas with diamicton and clays in the OWF and ECC areas, and given the fact that no grab samples were made in these areas, they will not contribute to the sediment dispersal modelling.

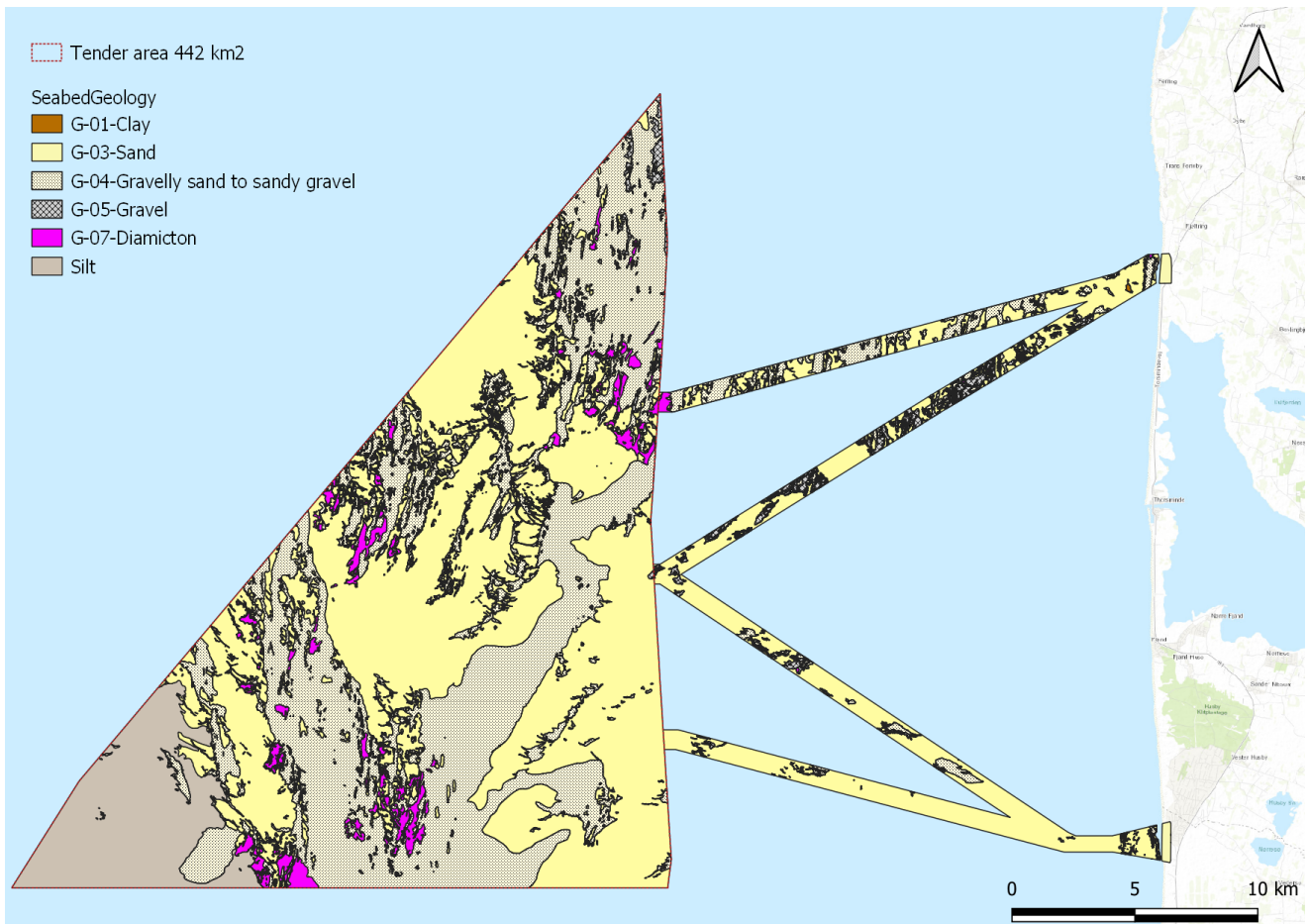


Figure 4.6: Surficial soil geology in the pre-investigation area and cable corridors (MMT, 2020b; MMT, 2020a).

A more detailed view of the surficial soil in the proposed ECC area is illustrated in Figure 4.7. The figure shows, that the surficial soil in the cable corridor primarily consists of sand and gravel. There are also small areas with diamicton and clay along the cable route, however, no grab samples were taken in these areas.

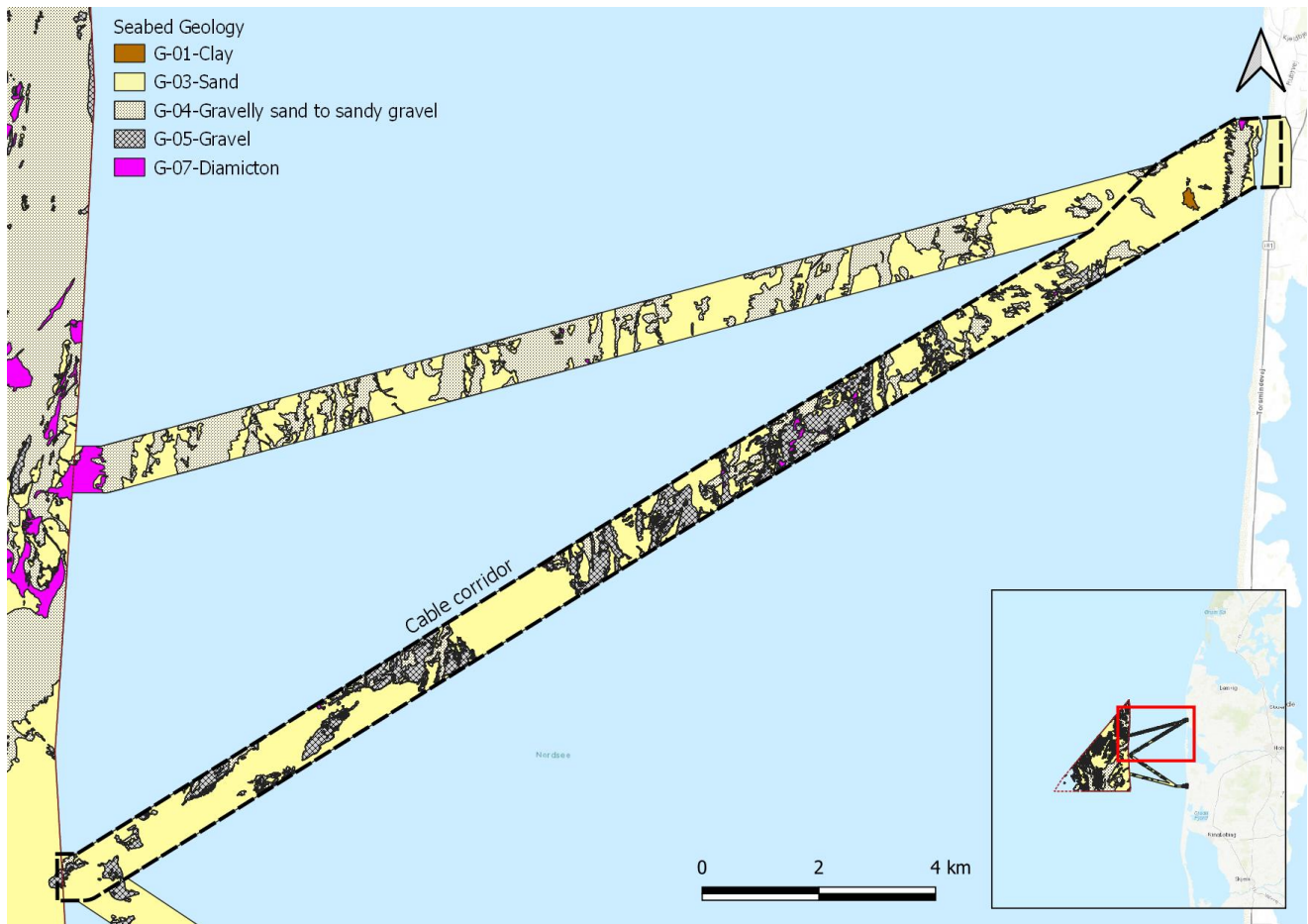


Figure 4.7: Surficial soil geology in the cable corridor (MMT, 2020b). The relevant cable corridor is marked with a black dashed line.

4.2.2. Sediment samples

A total of 94 grab samples were successfully carried out in the OWF and ECC areas. 82 of the samples were taken in the OWF area and 12 of the samples were taken in the ECC area. The particle distribution from the grab samples is used to calculate the average particle distribution for each of the analyzed types of surficial soils (i.e. sand, gravelly sand to sandy gravel and gravel). Based on the average particle distribution, the spill of the dredging/jetting works carried out in the areas with sand, gravelly sand to sandy gravel and gravel can be modelled. Not all 82 grab samples in the OWF area are analyzed. Many of the grab samples are taken in areas with surficial soil categorized as sand or gravelly sand to sandy gravel. For each of these two soil types, 10 grab samples are randomly chosen and analyzed. A figure showing the location of the grab samples along with the randomly selected grab samples used to calculate the average sediment distribution in the OWF area is seen in Figure 4.8. The location of the grab samples from the ECC area is seen in Figure 4.9.

The particle size distribution for each of the grab samples in the OWF and ECC area is shown in Appendix 5. The figures also show the average sediment distribution, used for modelling purposes.

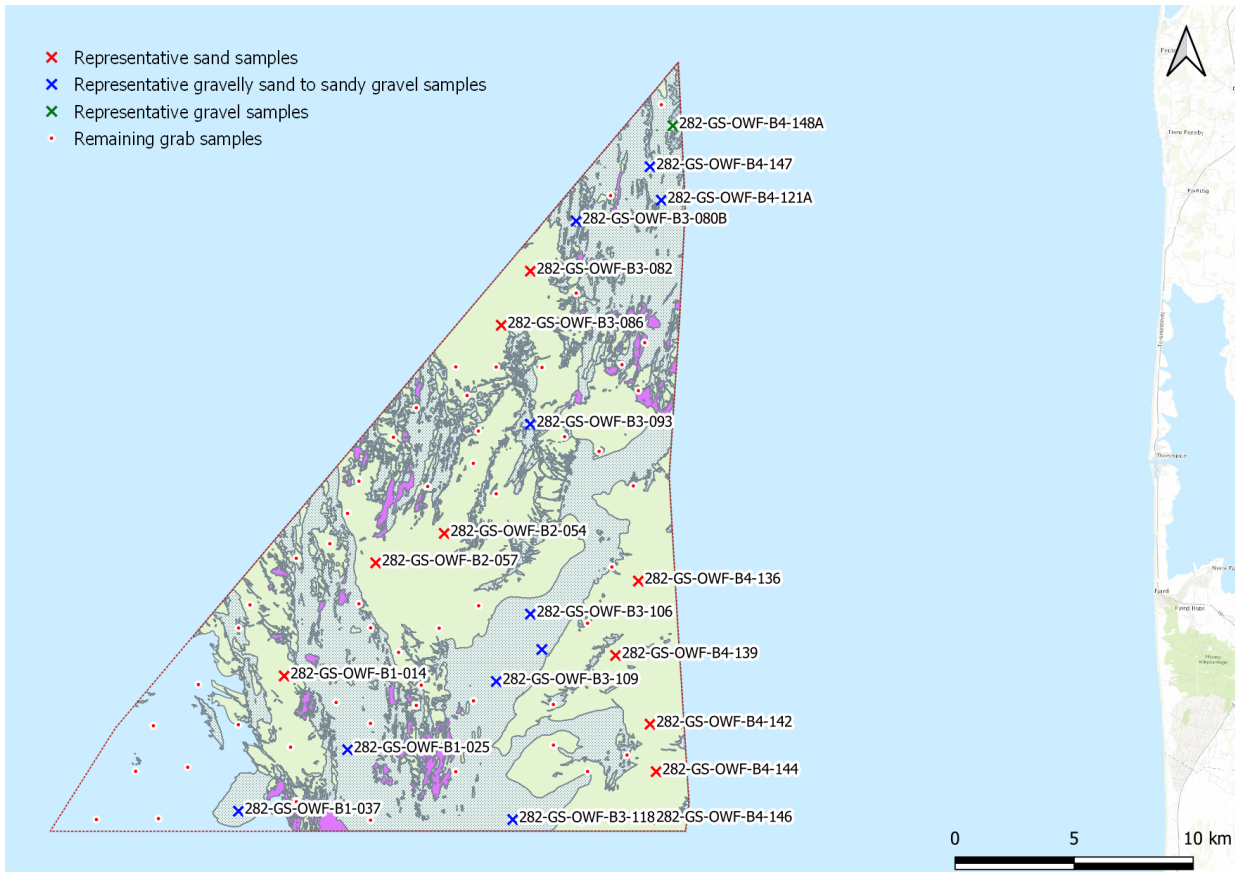


Figure 4.8: Grab samples used to calculate the average particle size distribution in the OWF area.



Figure 4.9: Grab samples used to calculate the average particle size distribution in the ECC area.

It is only the relatively fine sediments that are relevant when analyzing the environmental impact of dredging/jetting since these can be brought into suspension in the water column. The coarser sediments will just fall through the water column and deposit on the seabed close to where they are dropped. The percentage content of fine particle fractions for the three sediment types (sand, gravelly sand to sandy gravel and gravel) in the OWF and ECC area is seen in Table 4-1.

Table 4-1: Percentage content of fine sediment fractions for three surficial soil classifications in the OWF and ECC areas.

Area	Sediment classification	Very fine				
		Sand [%]	sand/coarse silt [%]	Medium silt [%]	Fine silt [%]	silt/Clay [%]
OWF	Sand	21.6	2.4	1.4	0.0	0.9
	Sandy gravel	6.6	0.0	0.0	0.0	0.0
	Gravel	0.0	0.0	0.0	0.0	0.0
ECC	Sand	22.3	1.2	0.5	0.0	0.2
	Sandy gravel	4.5	0.0	0.0	0.0	0.0
	Gravel	7.5	0.0	0.0	0.0	0.0

4.3. Water level

The numerical hydrodynamic model is verified with measured tidal data from two stations in Denmark and three stations in the UK. At the model boundaries, astronomical tides have been applied. In the following sections, the measured water levels in Denmark and the UK are presented along with the predicted astronomical tidal levels at the model boundaries.

4.3.1. Water levels in Denmark

Along the Danish Westcoast, two measurement stations are used to verify the numerical model — one in Hvidesande and one in Thorsminde. The measured water levels in Hvidesande and Thorsminde are illustrated in Figure 4.10 and Figure 4.11 respectively.

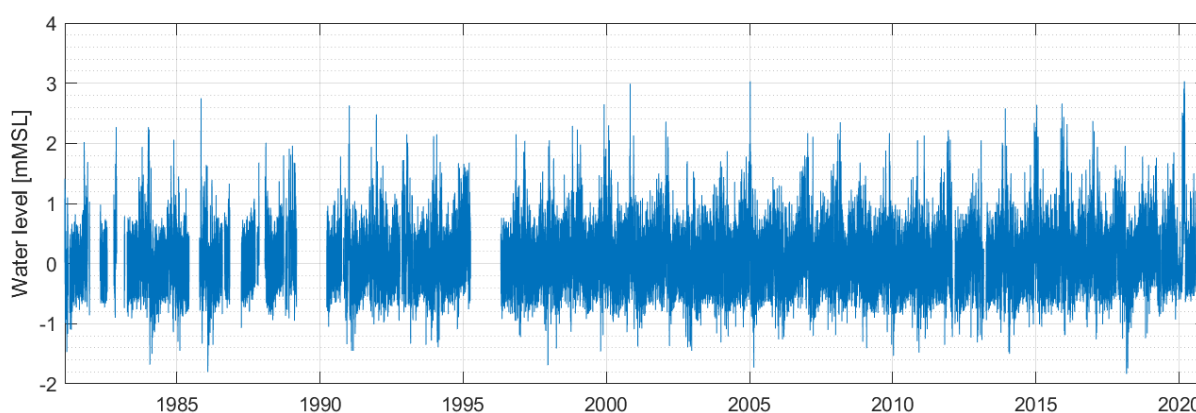


Figure 4.10: Measured water levels in Hvidesande (DMI, 2022).

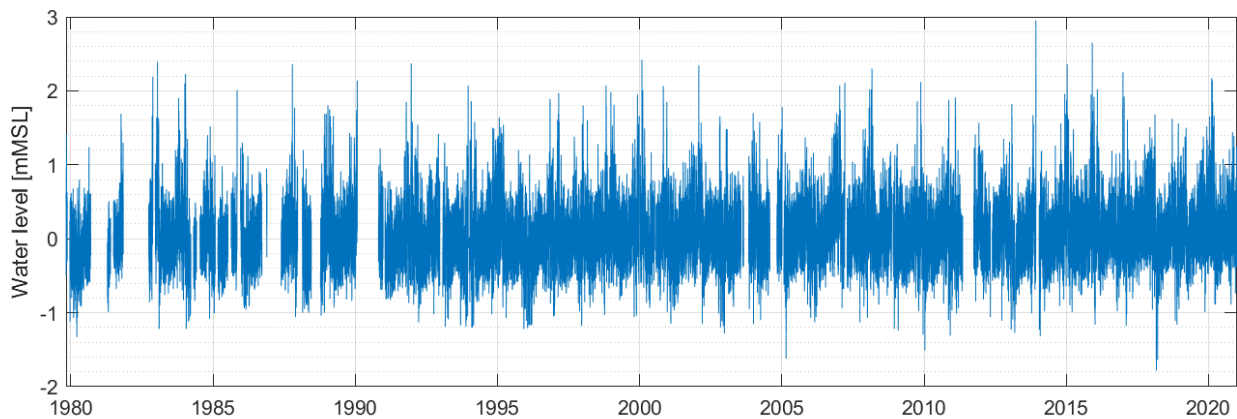


Figure 4.11: Measured water levels in Thorsminde (DMI, 2022).

4.3.2. Water levels in the UK

The hydrodynamic model is furthermore validated against water level measurements from Aberdeen, Whitby and Dover along UK's east coast. The water levels at the three measurement stations are illustrated in Figure 4.12, Figure 4.13, and Figure 4.14.

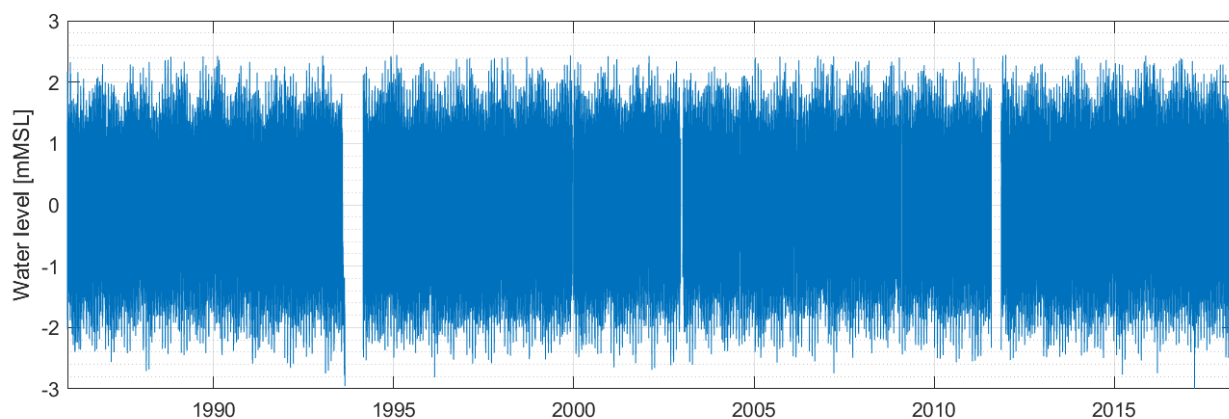


Figure 4.12: Measured water levels in Aberdeen (British Oceanographic Data Centre, 2022).

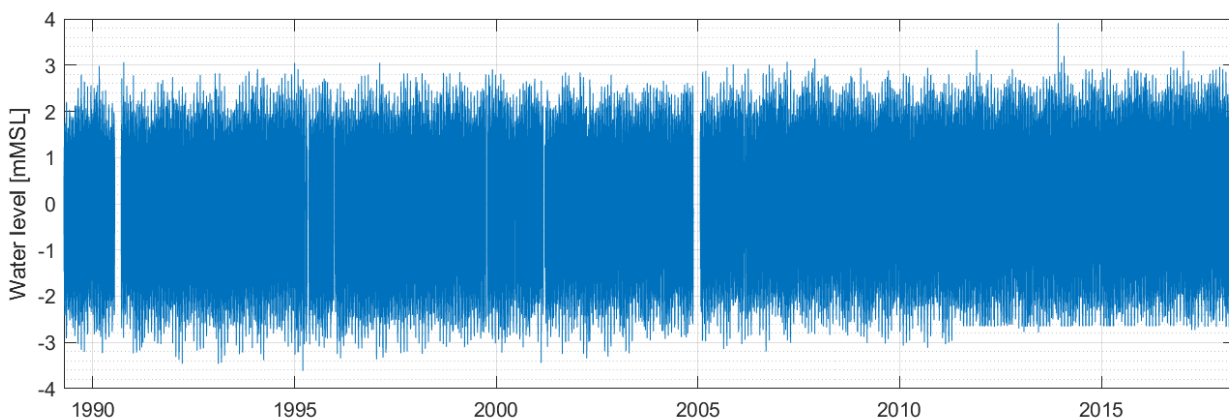


Figure 4.13: Measured water levels in Whitby (British Oceanographic Data Centre, 2022).

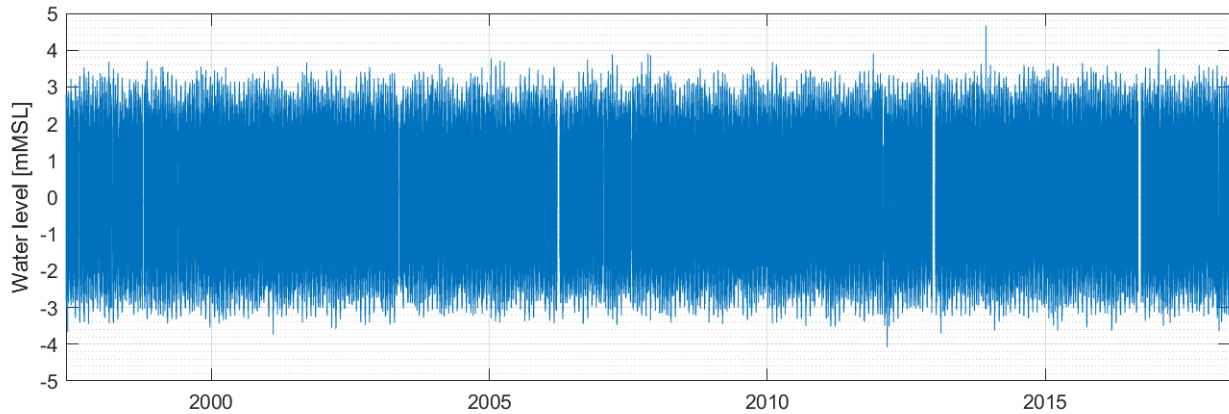


Figure 4.14: Measured water levels in Dover (British Oceanographic Data Centre, 2022).

4.3.3. Astronomical tide

On the model boundary, astronomical tides are applied. The tides have been extracted from the MIKE toolbox provided by DHI.

4.4. Temperature and salinity conditions

Water temperature and salinity profiles have been extracted from Overfladedatabasen (Miljø- og Fødevarerministeriet, 2022) at the locations illustrated in Figure 4.15.

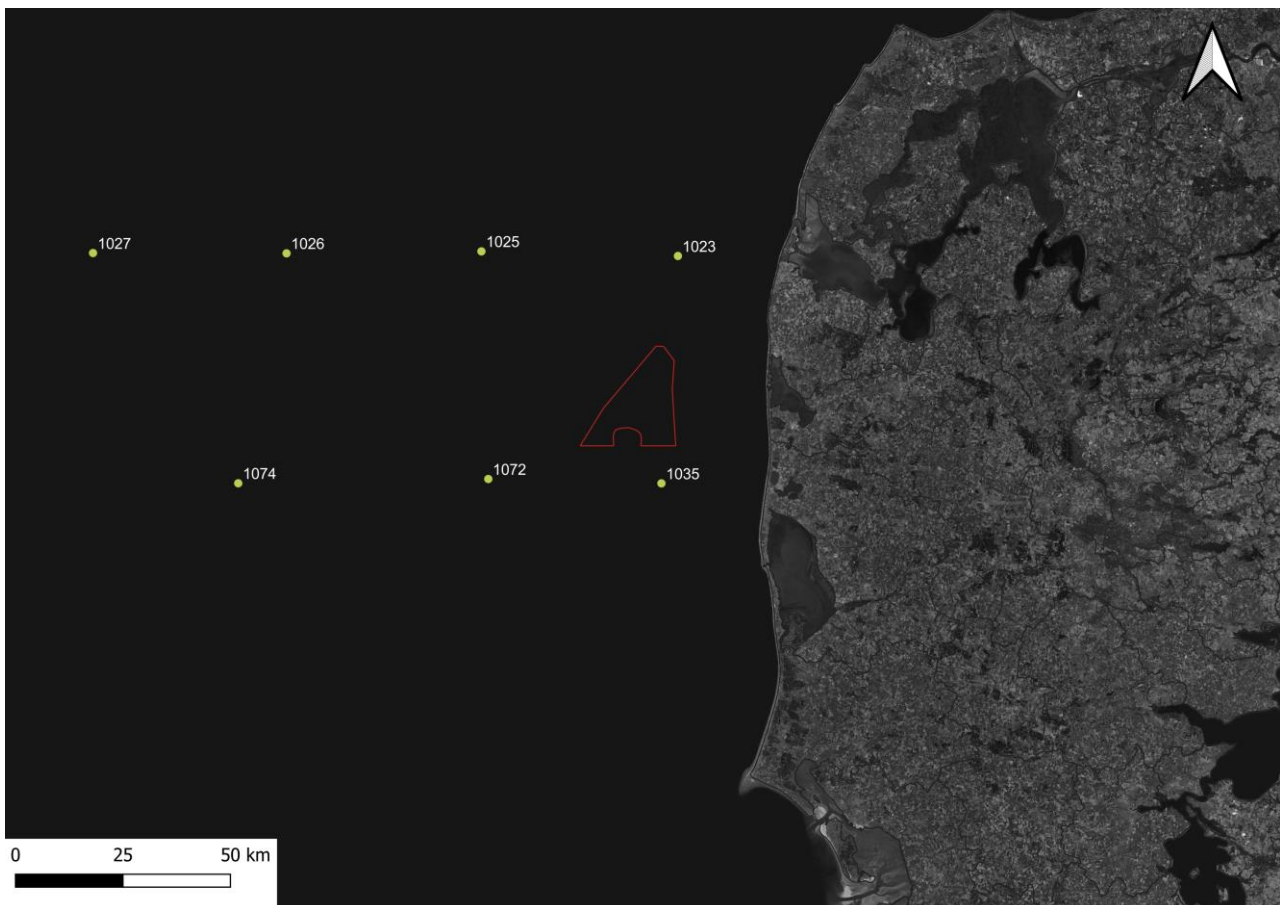


Figure 4.15: DMU profiles station in the vicinity of Thor OWF.

Stratification in the salinity and temperature profiles is observed, however, based on the available profiles, this is considered to be a rare phenomenon. Since stratification occurs only rarely, it is estimated that the influence of the general stratification in this part of the North Sea at the wind farm is negligible.

At station 1035 two events with a strong halocline are observed on February 05 2018 and January 30 2021, and one event with a thermocline on July 18 2018. The day before both a halocline and a thermocline are observed at station 1023. A halocline on February 05 2018 and February 01 2021 is also observed at station 1023. At station 1072 a thermocline is only confirmed on July 18 2018.

Salinity and temperature profiles from stations 1035, 1023, 1072 and 1035 are presented in Appendix 1, Appendix 2, Appendix 3 and Appendix 4.

4.5. Wind and air pressure

Atmospheric data in the form of wind speed at 10 mMSL in x- and y-directions and air pressure at the surface has been extracted from ECMWF (ECMWF, 2019). Data has a horizontal resolution of 0.25 degrees and a 1-hour temporal resolution.

4.6. Bathymetry

The bathymetry is based on various data sources. In the project area and along the export cable route, a multibeam echosounder (MBES) survey is carried out. Close to the landfall position, coastal profiles have been measured since 1938 by the Danish Coastal Authority.

4.6.1. MBES in the project area

The results of the bathymetric MBES surveys can be found in geophysical and hydrographical survey reports (MMT, 2020a; 2020b; 2020c; 2020d).

4.6.2. Cross shore profiles, Danish Coastal Authorities

The Danish Coastal Authority has measured beach profiles in the area since 1938 (Danish Coastal Authority, 2022). The three profiles closest to the landfall are analysed. The location of the three profiles and the profile IDs are illustrated in Figure 4.16. The beach profiles after beach nourishment was initiated in 1983 are illustrated in Figure 4.17, Figure 4.18, and Figure 4.19.

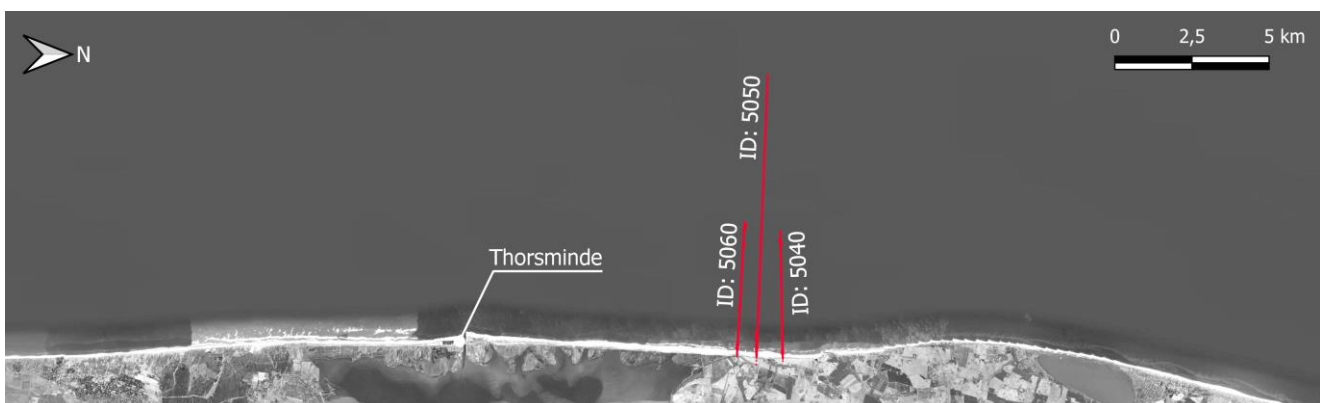


Figure 4.16: Measured beach profiles.

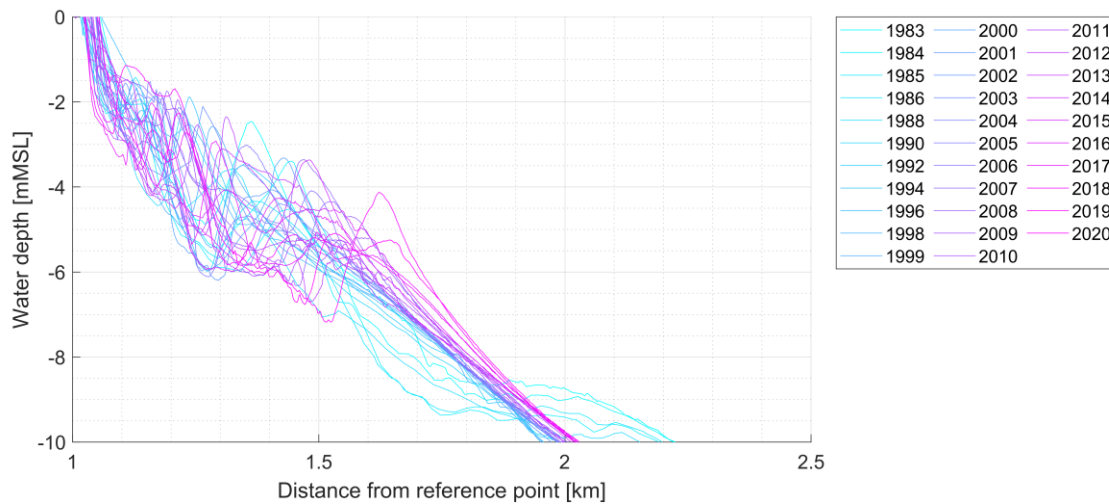


Figure 4.17: Changes in beach profiles after nourishment was initiated for profile 5040 (profile furthest north).

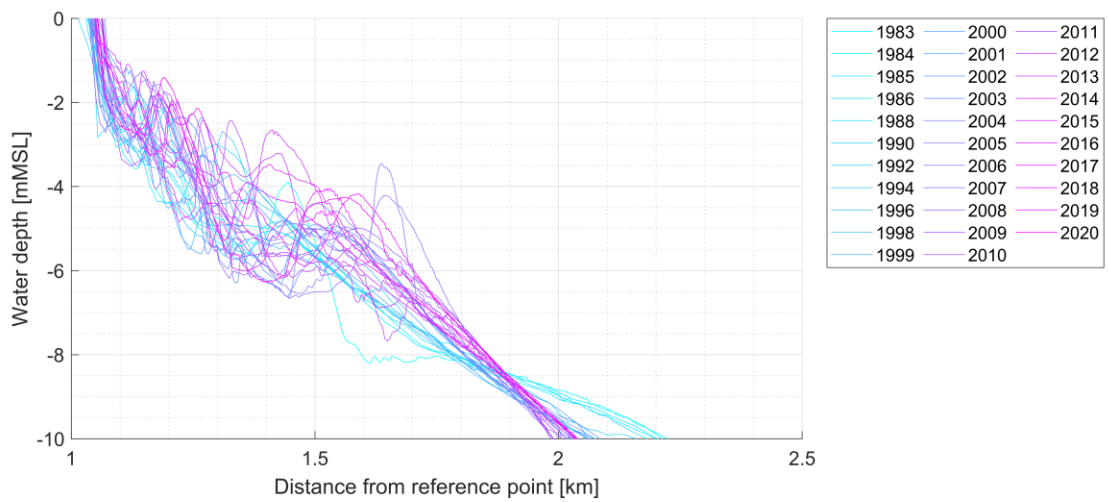


Figure 4.18: Changes in beach profiles after nourishment was initiated for profile 5050 (profile closest to landfall).

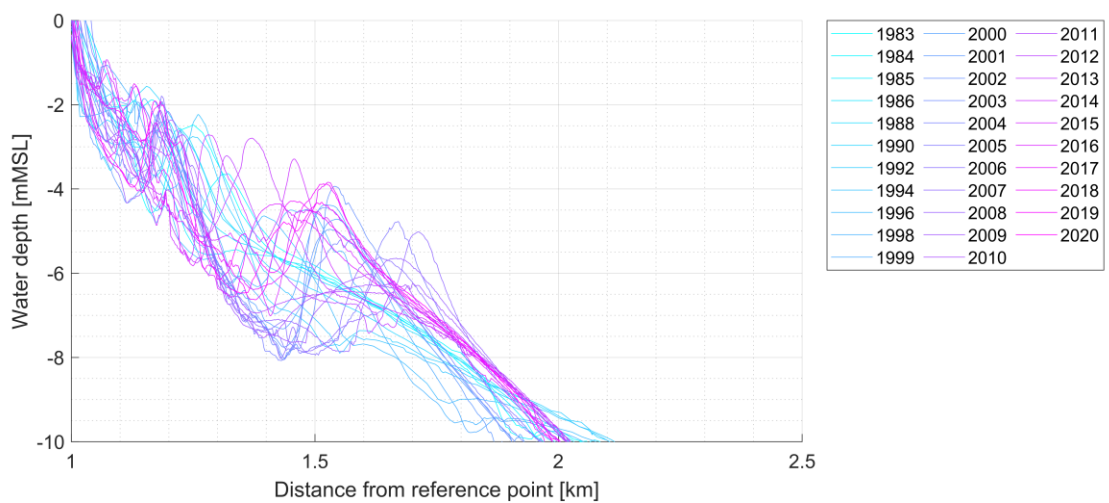


Figure 4.19: Changes in beach profiles after nourishment was initiated for profile 5060 (profile furthest south).

As can be seen from the figures, the beach profiles within the active depth are highly dynamic, due to the large sediment transport in the area. The retreat of the profile is, however, mitigated by the beach nourishment.

4.6.3. Other bathymetric data

The main input to the numerical model is based on the following two datasets:

- C-CMAP (C-map, 2019)
- EMODnet (EMODnet, 2021)

4.7. Nearshore morphology

Many coastlines along the Danish West coast have large south-going sediment transportation. This includes the project area from the north of Thorsminde to Hvidesande.

4.7.1. Danish Coastal Authority data

The direction of the net sediment transportation is illustrated in Figure 4.20. From the figure it is seen, that the net direction of the sediment transportation in the project area is south.

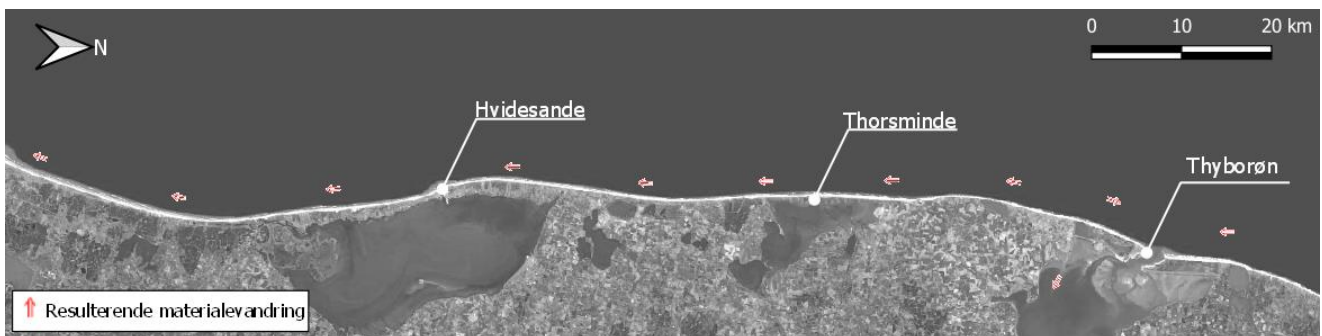


Figure 4.20: The direction of the net sediment transportation is illustrated in Figure 4.20 (Danish Coastal Authority, 2022b).

The shoreline evolution from 1872 to 2005 is illustrated in Figure 4.21. The Figure shows, that the coastline has been retreating significantly during the period. The coastline, however, has been stable since 1983 when beach nourishment was implemented to avoid further erosion.

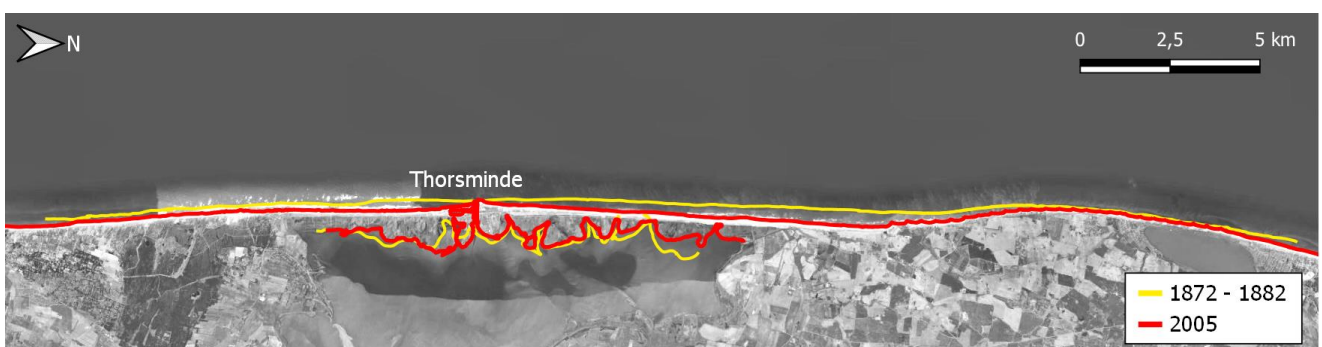


Figure 4.21: Shoreline evolution from 1882 to 2005. Beach nourishment was initiated in 1983 (Danish Coastal Authority, 2022b).

4.7.2. Aerial photos

Orthophotos in the years 1954, 1995, 2007, 2010, 2013, and 2021 are illustrated in Figure 4.22 to Figure 4.27. A stationary reference line is plotted on the figure to illustrate the shoreline evolution over time. The figures show, that the shoreline was retreating drastically in the years between 1954 and 1995. In the years between 2007 and 2021, the shoreline seems to be stable due to the beach nourishment.



Figure 4.22: The year 1954.

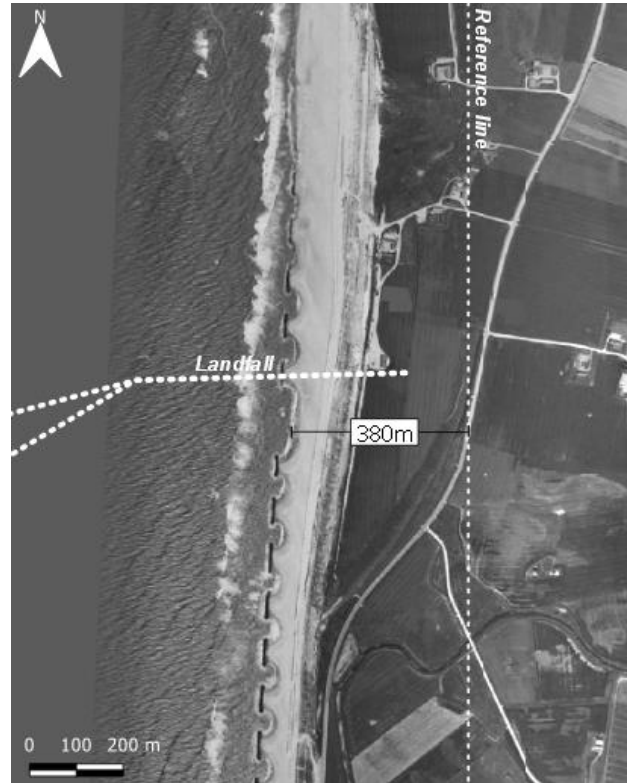


Figure 4.23: The year 1995.



Figure 4.24: The year 2007.



Figure 4.25: The year 2010.



Figure 4.26: The year 2013.



Figure 4.27: The year 2021.

4.8. Offshore morphology

MarineSpace has (in collaboration with DHI) carried out an assessment of the seabed morphology across Thor OWF and associated export cable corridors (MarineSpace, 2022). The assessment is based on the MBES surveys described in section 4.2 (MMT, 2020a; MMT, 2020b). The conclusion of the seabed morphology assessment is, that the majority of the Thor OWF and ECC areas are dominated by stable, large-scale ridge and runnel features, with a dominant orientation of northeast to southwest. In MarineSpaces own words, ridges and runnels are defined as:

"... linear features [that] have an along axis length of several kilometres, with the ridges having widths of 0.5 – 2 km whilst the runnels (associated linear depressions) have widths < 1 km. The amplitude from the base of the troughs to the apex of the ridges varies between 2 – 4m. The ridges are frequently asymmetric in cross-sectional profile. The depressions represent coarser sediments (coarse sands to gravels) sometimes with small-scale bedforms (wavelengths < 2 m and amplitudes of < 0.2 m. The ridges are made up of finer uniform sand with sharp discrete boundaries"
(MarineSpace, 2022)

The study furthermore finds, that oscillatory movement can occur at the sharp margins of these ridges and runnel structures. The associated bed level change of this oscillatory movement is up to one meter. On top of these large-scale sand formations, the study concluded that transverse bedforms migrating in a north, north-northeast or north-eastward direction at speeds of 15.5 m/yr down to < 10 m/yr are seen. In total, these mobile bedforms result in bed level changes of 1.2 to 1.75 meters, within a relatively short period.

4.9. Installation program, sediment disturbance

For the simulation of sediment dispersal, an indicative installation program excluding weather downtime has been defined considering time and space for the various activities involving disturbance of the sediments, such as dredging and jetting of cables. Sediment disturbance for activities such as installation of scour protection, piling and, for example, the use of jack-ups are considered to be insignificant.

The activities considered include the installation of export cables, infield cables and the drilling of 1 monopile. Two separate scenarios for the installation of export cables are considered to account for the presence of mobile sediment in the nearshore area:

Export cable, scenario 1 - cable burial with dredging:

- Seabed preparation, removal of mobile sand between Kilometer Point (KP) 0.46 (landfall) to KP 3.3:
 - o From KP 0.46 to approx. KP 1.0 with a Backhoe Dredger, estimated amount of 40.000 m³ sand in total for the 2 cables;
 - o From approx. KP 0.5 to KP 3.3 with e.g. a Trailing Suction Hopper Dredger, estimated amount of 300.000 m³ in total for the 2 cables. The sediment will be stored temporarily inside the cable corridor approx. 800 m north of the cable at 15 m water in an area with a sandy seabed. After the cables have been jetted the material will be recovered and used to reestablish the cable corridor (included in the modelling but in reality expected to happen naturally).;
- Cable burial:
 - o From KP 0.46 to KP 1.19, jetting to 2 m below the seabed and 2 m wide;
 - o From approx. KP 1.1 to KP 1.6, CFE (Controlled flow excavation) in the transition between nearshore and offshore jetting. Width x depth = 8.5 x 1.5 m;
 - o KP 1.50-28.4, jetting to 2 m below the seabed. Width: 1 m in clay and 2 m in sand (the design depth of burial is increased from 1.5 m to 2 m to include any spill from potential seabed preparations);
 - o CFE the first 75 m of the cables next to the offshore substation.

Export cable, scenario 2 - cable burial without dredging:

- Cable burial:
 - o From KP 0.46 to KP 1.2, jetting to 3 m below seabed and 2 m wide;
 - o From approx. KP 1.2 to KP 1.7, CFE. Width x depth = 8.5 x 3 m;
 - o KP 1.7 to KP 3.5, jetting to 2.5 m below seabed. Width: 1 m in clay and 2 m in sand;
 - o KP 3.5 to KP 28.4, jetting to 1.5 m below seabed. Width: 1 m in clay and 2 m in sand;
 - o CFE the first 75 m of the cables next to the offshore substation.

Infield cable:

- Cable burial:
 - o Jetting to 2 below the seabed, width: 1 m in clay and 2 m in the sand (the design depth of burial is increased from 1.5 m to 2 m to include any spill from potential seabed preparations);
 - o CFE the first 75 m of the cables next to the offshore substation.

Monopile:

- Drilling of 1 monopile with a diameter of 8.6 m to a depth of 50 m;

5. Model setup

In the following sections, the setup of the three numerical models (the hydrodynamic model, the spectral wave model, and the sediment model) is described. This includes the model domain, mesh, boundary conditions, and verification.

5.1. Bathymetry and model mesh

The mesh is divided into different regions with different element sizes depending on the area of interest. The model domain and bathymetry are illustrated in Figure 5.1. The model has three open boundaries: Two boundaries north of the North Sea, and one in the English Channel where the North sea meets the Atlantic Ocean. The mesh has the highest resolution (62500 m²) in the area around the OWF and ECC.

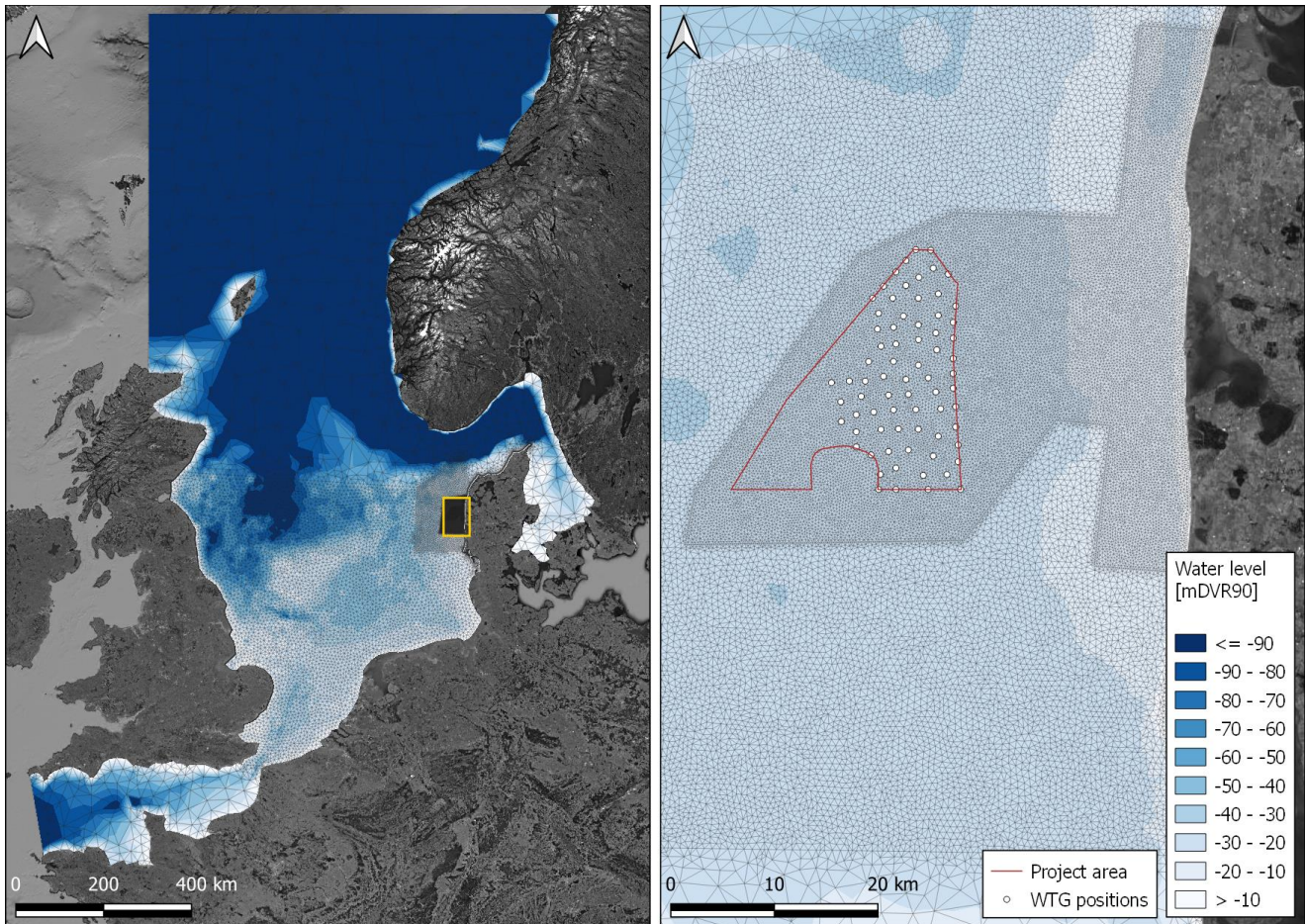


Figure 5.1: Model mesh, domain, and bathymetry.

5.2. Numerical models

The numerical models used to simulate the baseline and the pressure from the wind farm are described shortly below and further information can be found here: <https://www.mikepoweredbydhi.com/products>.

5.2.1. Hydrodynamic model

MIKE 21 HD FM (Hydrodynamics) is a hydrodynamic model with a flexible mesh. Based on tidal and current inputs along the open boundaries together with the wind conditions at the sea surface, the model simulates tide and depth-integrated current speed and direction throughout the model domain. The benefit of a flexible mesh is the possibility of using varying sizes of the mesh across the domain. Therefore, the focus area can have a high resolution, and areas further away can have a coarser resolution. This makes the model run faster, with a negligible impact on the simulation results.

5.2.2. Spectral wave model

MIKE 21 SW FM (Spectral Waves) is a spectral wave model which models wave growth and decay due to wind forcing, wave transformation, wave dissipation (from white capping, bottom friction, and depth-induced wave breaking), refraction, and shoaling.

5.2.3. Sediment model

MIKE 21/3 PT (Particle Tracking) is a so-called Lagrangian model which over time considers both the position and properties of the particles e.g. keeping track of the particle position in both x,y- and z-direction according to the mean current field. This is the opposite of an Eulerian model which does it cell-wise where e.g. the concentration will

be an average of the volume over each cell. This type of model is extremely sensitive to the model resolution both horizontally and vertically, whereas the Lagrangian approach is independent of cell sizes.

The selection of MIKE 21/3 PT for the modelling of the sediment dispersal is due to the nature of the plumes created by dredging, drilling, ploughing and jetting. The plumes are initially narrow and occur in various depths of the water column. This is difficult to describe in a standard model mesh while maintaining a reasonable calculation time.

5.3. Boundary data, hydrodynamic and wave model

The hydrodynamic model is forced by tide and wind fields. The spectral wave model is forced by wind fields. Moreover, the two models feed into each other: The hydrodynamic model provides tidal data to the wave model and the wave model provides wave radiation to the hydrodynamic model.

5.3.1. Tide

Hourly astronomical tide at the open boundaries as presented in chapter 4.3.3.

5.3.2. Wind

Hourly wind fields as described in chapter 4.5.

5.4. Verification, hydrodynamic and wave model

The hydrodynamic model results in the project area are verified by comparing the simulated depth-averaged current speeds at the offshore measurement station (location illustrated in Figure 4.1) with the observed depth-averaged current speed. The observed and modelled current speeds are illustrated in Figure 5.2. The modelled current speed is in good agreement with the observed current speed. The mean difference (bias) between the modelled and measured current speed is 0.0 and the correlation coefficient is 0.9. This was achieved with default MIKE21 HD parameters except for a modification of the bed resistance; a Chezy Number of $60 \text{ m}^{0.5}/\text{s}$ reduced to $30 \text{ m}^{0.5}/\text{s}$ along the shore from the English Channel to Skagen.

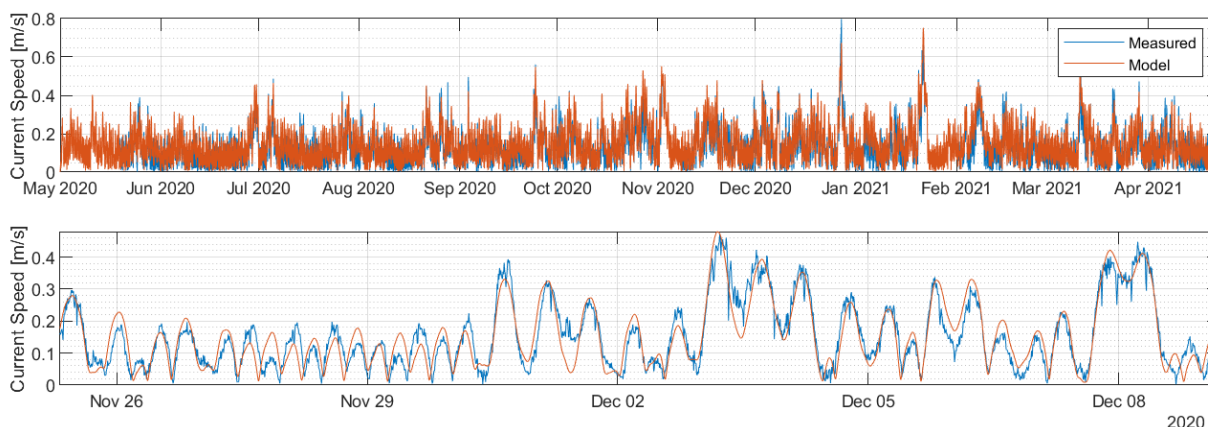


Figure 5.2: Model verification of depth-averaged current speed at the offshore measurement station. Legend applies to both figures. Bias is 0.0 and R is 0.9.

The hydrodynamic model is also verified against the water levels in Aberdeen, Whitby and Dover on the UK coast, and Hvidesande and Thorsminde on the Danish west coast. Figures showing the modelled water levels compared to the observed water levels for the 5 different stations are illustrated in Figure 5.3 to Figure 5.7. The figures show a good agreement between the modelled and observed data, with a bias ranging from -0.07 to 0.04 and a correlation coefficient between 0.90 and 0.98.

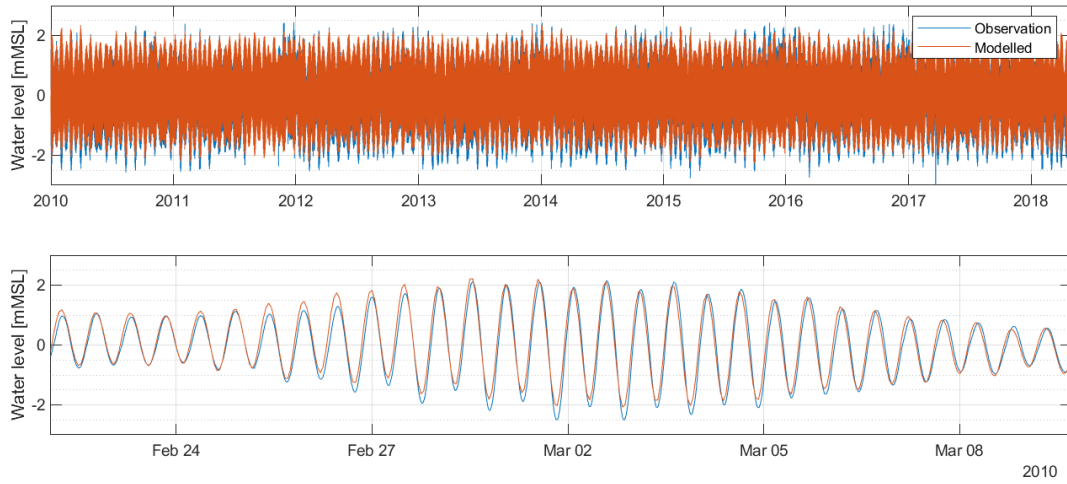


Figure 5.3: Model verification of water levels in Aberdeen. Legend applies to both figures. Bias is 0.00. and R is 0.96.

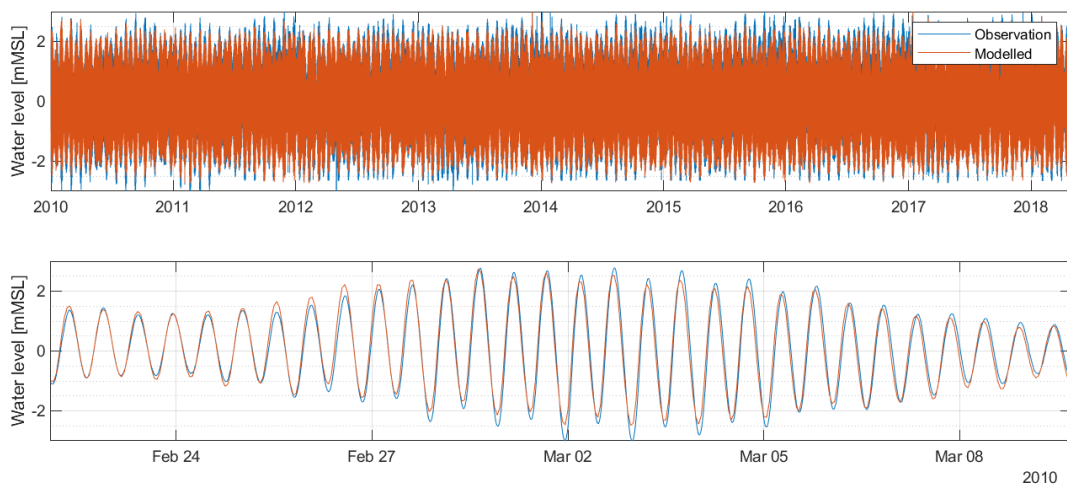


Figure 5.4: Model verification of water levels in Whitby. Legend applies to both figures. Bias is -0.07 and R is 0.98.

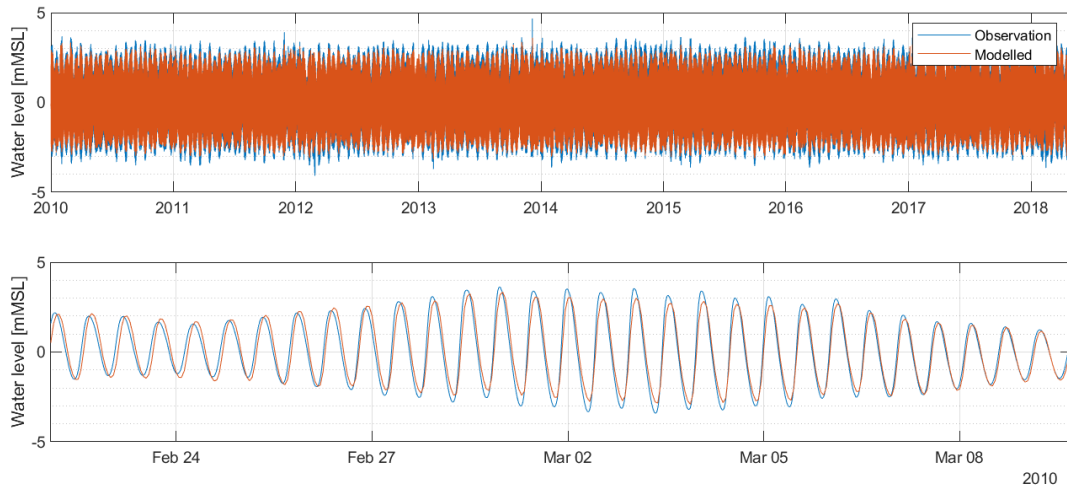


Figure 5.5: Model verification of water levels in Dover. Legend applies to both figures. Bias is -0.01 . R is 0.96

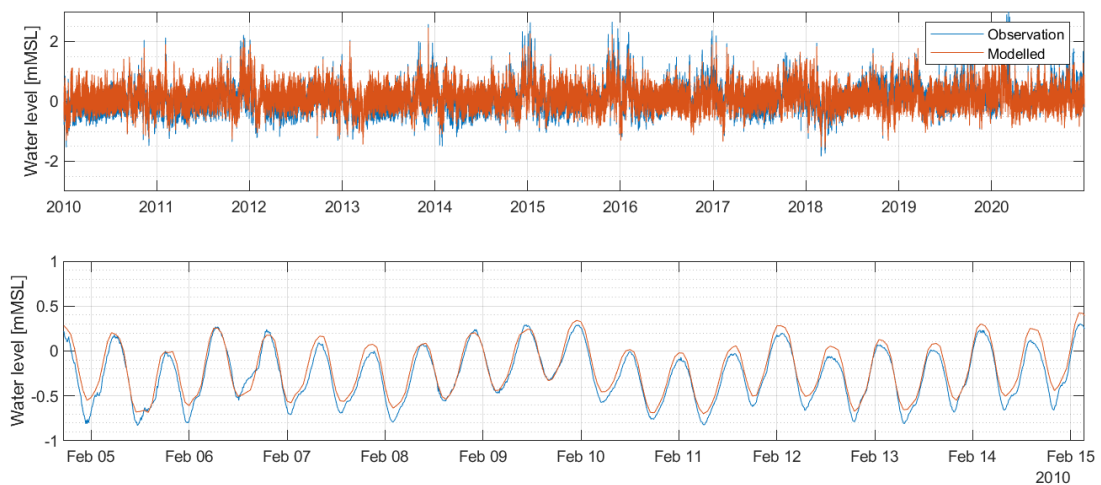


Figure 5.6: Model verification of water levels in Hvidesande. Legend applies to both figures. Bias is 0.012 . R is 0.90 .

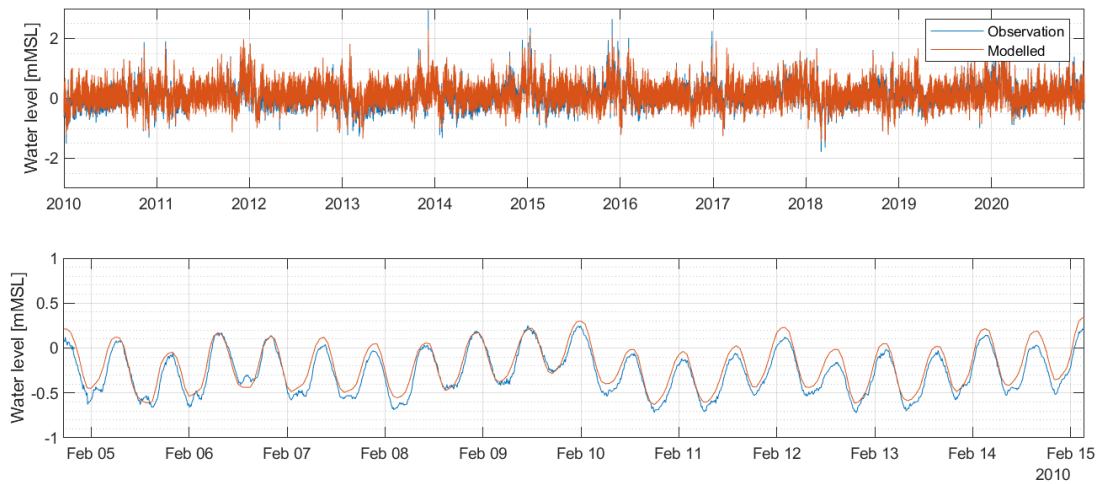


Figure 5.7: Model verification of water levels in Thorsminde. Legend applies to both figures. Bias is 0.04. R is 0.94

The spectral wave model is verified against the observed significant wave height and mean wave direction at the measurement station described in section 4.1.2. The measured and modelled significant wave heights at the measurement station in the project area are illustrated in Figure 5.8. The model has a bias of 0.14 meters, and the correlation coefficient between the time series is 0.91. Achieved with the default MIKE21 SW parameters with a modification of the Wind Forcing “Growth parameter” and “Wave age tuning parameter”; changed from 1.2 to 1.4 and 0.008 to 0.015.

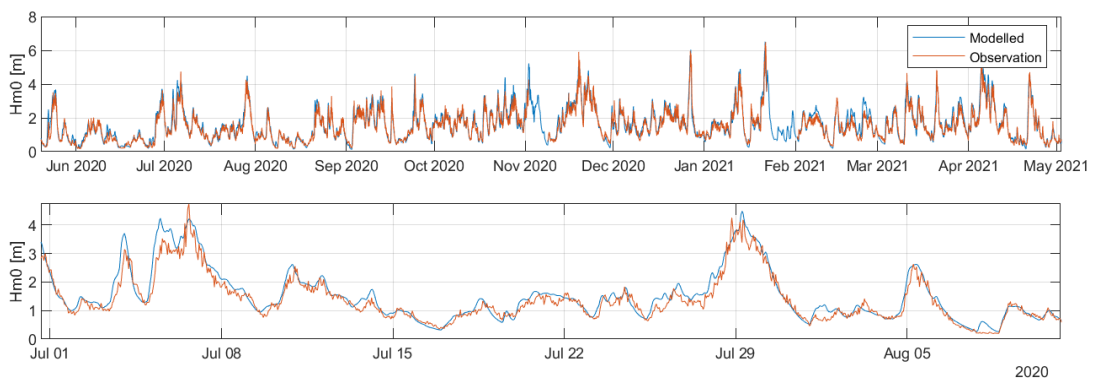


Figure 5.8: Model verification of significant wave height at the measurement station. Legend applies to both figures. Bias is 0.14. R is 0.91.

The measured and observed mean wave directions are illustrated in Figure 5.9. The verification shows, that the model is representing the metocean conditions in the project area well.

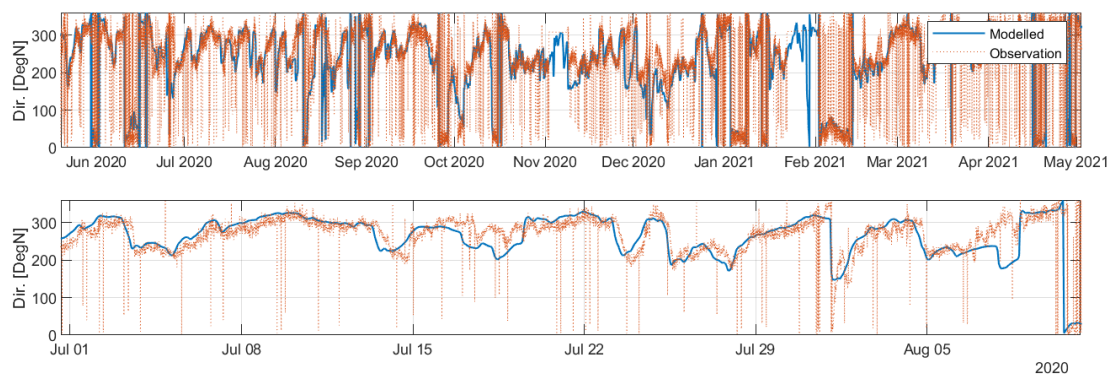


Figure 5.9: Model verification of mean wave direction at the measurement station. Legend applies to both figures.

5.5. Project implementation

The investigated project is one consisting of 72 wind turbines fixed to the seabed via a monopile as well as one off-shore substation placed on a 4-legged platform.

To simulate the impact due to the project the following has been implemented to the wind field, in the HD and SW models:

- i. Wind turbines: The wind field downstream of the wind farm has been modified with the use of a wake function (Jensen, N.O., 1983) considering the roughness (0.001m), hub height (150m), rotor diameter (240m) and the trust coefficient (c_t) for wind speeds of below 5, 5 to 11 and above 15 m/s at each turbine position. To capture the presence of the turbines the resolution of the wind fields was changed from 0.25° to 0.01aprox. 0.65 km) and the effect of the wake was imprinted based on a wind direction in steps of 5°.
- ii. Substructure: In the hydrodynamic model the blocking from the substructures is described with a simple drag-law to increase the resistance at each position.
- iii. Substructure: For the wave model a source term has been introduced at each turbine position.

5.6. Boundary data, sediment model

The sediment model is an add-on to the hydrodynamic and wave model thus current data and shear stress are transferred by time step for advective transport of the sediment and deposition/resuspension of near-bottom sediments.

The sediment model itself contains information about:

- 1) The sediment types are here divided into 5 categories (Table 4-1);
 - a. Sand,
 - b. Fine sand,
 - c. Coarse silt
 - d. Fine Silt and
 - e. Clay
- 2) Settling velocity for each sediment type;
- 3) For erosion a critical shear stress per type;
- 4) Dispersion, both horizontal and vertical;
- 5) A description of the sediment source in time and space.

6. Selection of simulation period

For evaluation of the hydrodynamic pressure, the years within the period 2010–2019 coming closest to the average current at the centre of the wind farm have been identified based on magnitude persistence for the current in the west-east and south-north direction (Figure 6.1) and the current roses (see Figure 6.2 and Appendix 6).

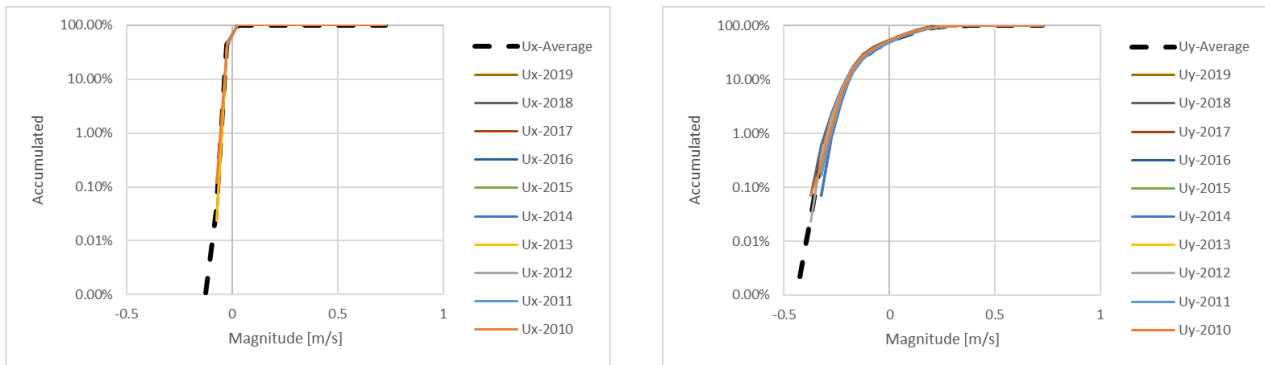


Figure 6.1: Persistence of magnitude for the current in west-east (left) and south-north (right) for the years 2010 to 2019 compared to the average for the period

The general impression is a current pattern with only a limited yearly variation. From the persistence curves, the year-to-year variation can't be distinct but from the current roses, some variations are visible. North going current dominates for 26% of the time and south going for 19%. The strongest current speeds are also related to the dominating directions with depth average speeds up to 0.8 m/s towards the north and 0.5 m/s towards the south. The average northerly current speed is 0.19 m/s, to the south 0.17 m/s, and for both directions 0.03 m/s towards the north.

Also, the wave climate has been analyzed and the year 2019 is reasonably close to the average for the period, see Figure 6.3 and Appendix 7. In the period 2010 to 2020, the average significant wave height is found to be 1.7 m, and the maximum significant wave height is 8.5 m. For the year 2019, the same numbers are 1.7 m and 7.0 m. In the same order for the average but slightly lower for the maximum.

Thus based on the limited yearly variation in the current and that the waves in 2019 come closest to the yearly average for the period 2010 to 2020 it was decided to go with the year 2019 for the evaluation of the impact on the hydrodynamics.

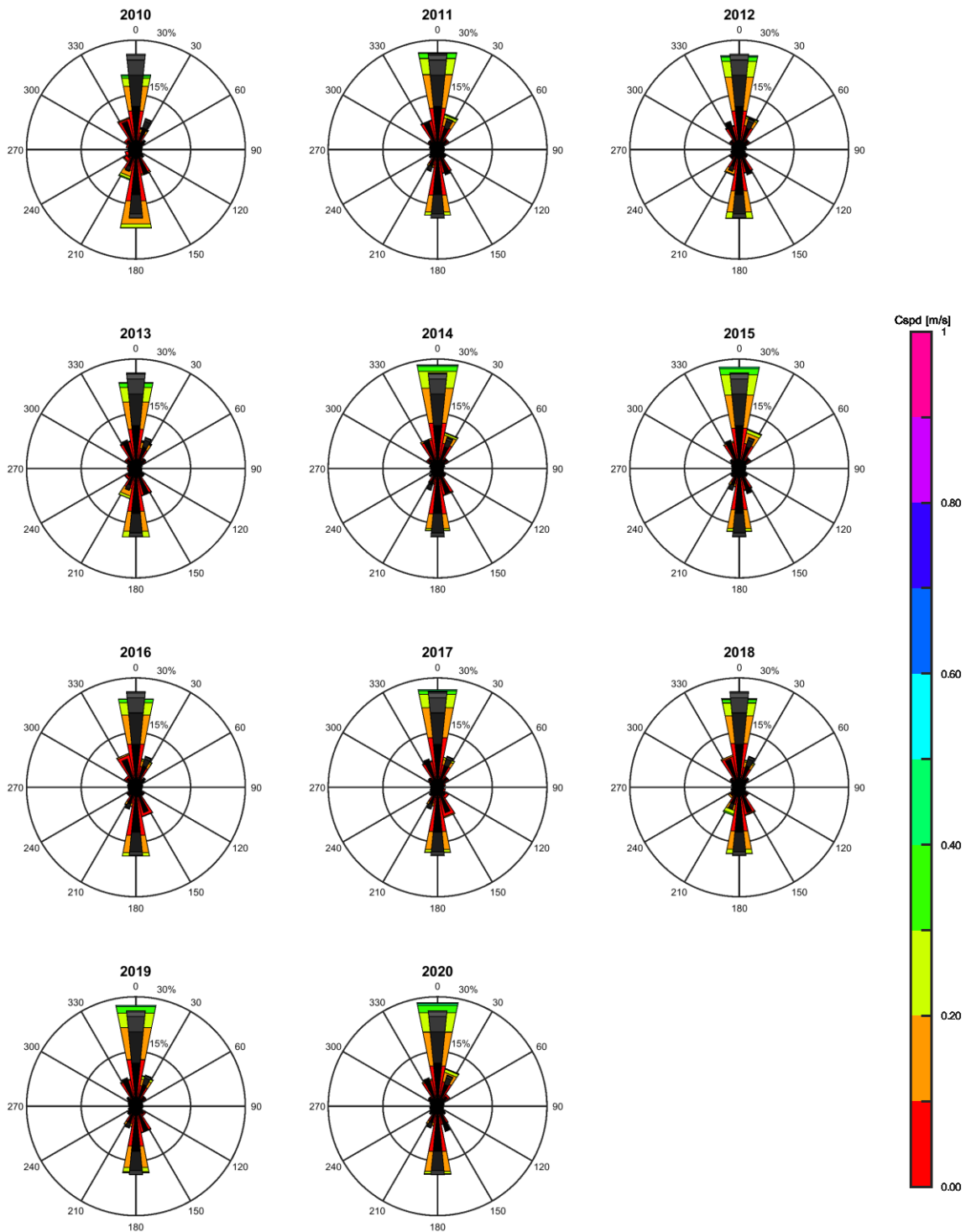


Figure 6.2: Yearly current roses for the location of the Thor OWF for 2010 to 2020 compared to the average (grey).

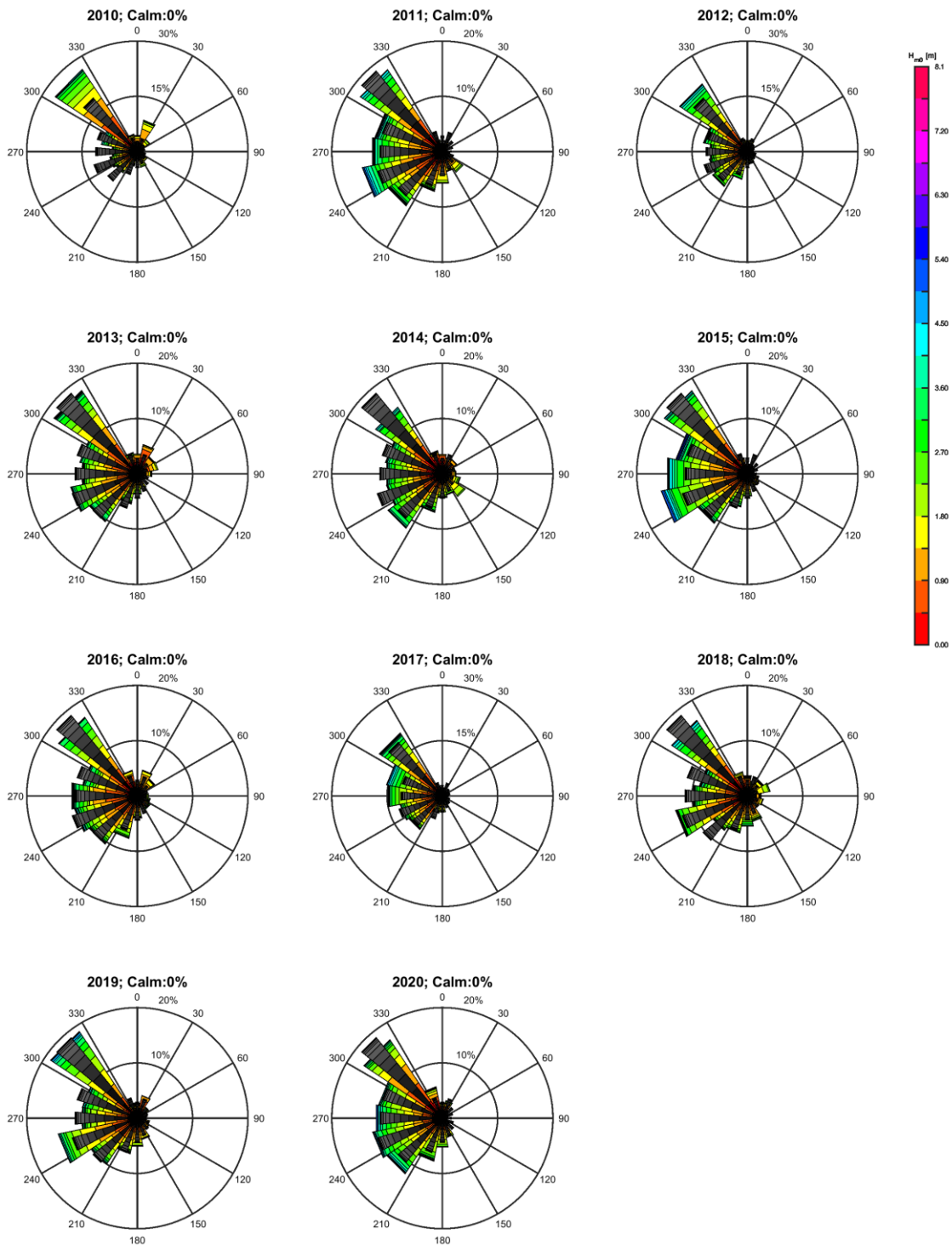


Figure 6.3: Yearly wave roses for the location of the Thor OWF for 2010 to 2020 compared to the average (grey).

7. Pressure, current and waves

7.1. Current

The average current speed will be slightly affected in the area around the wind farm, where both increases and decreases in the average current speed are expected. The presence of wind turbines will increase the current speed by up to 0.8 cm/s in parts of the water strait between the wind turbines and the coastline. The model also shows a slight increase in the current speed around the southwestern tip of the project area. The average current speed will decrease up to 1.4 cm/s north of the wind farm. The difference in average current speed between the baseline model and the model with Thor is illustrated in Figure 7.1. The arrows in the figure illustrate the mean flow direction from the baseline model. The figure shows, that the average flow direction in the area around Thor is N to NNE.

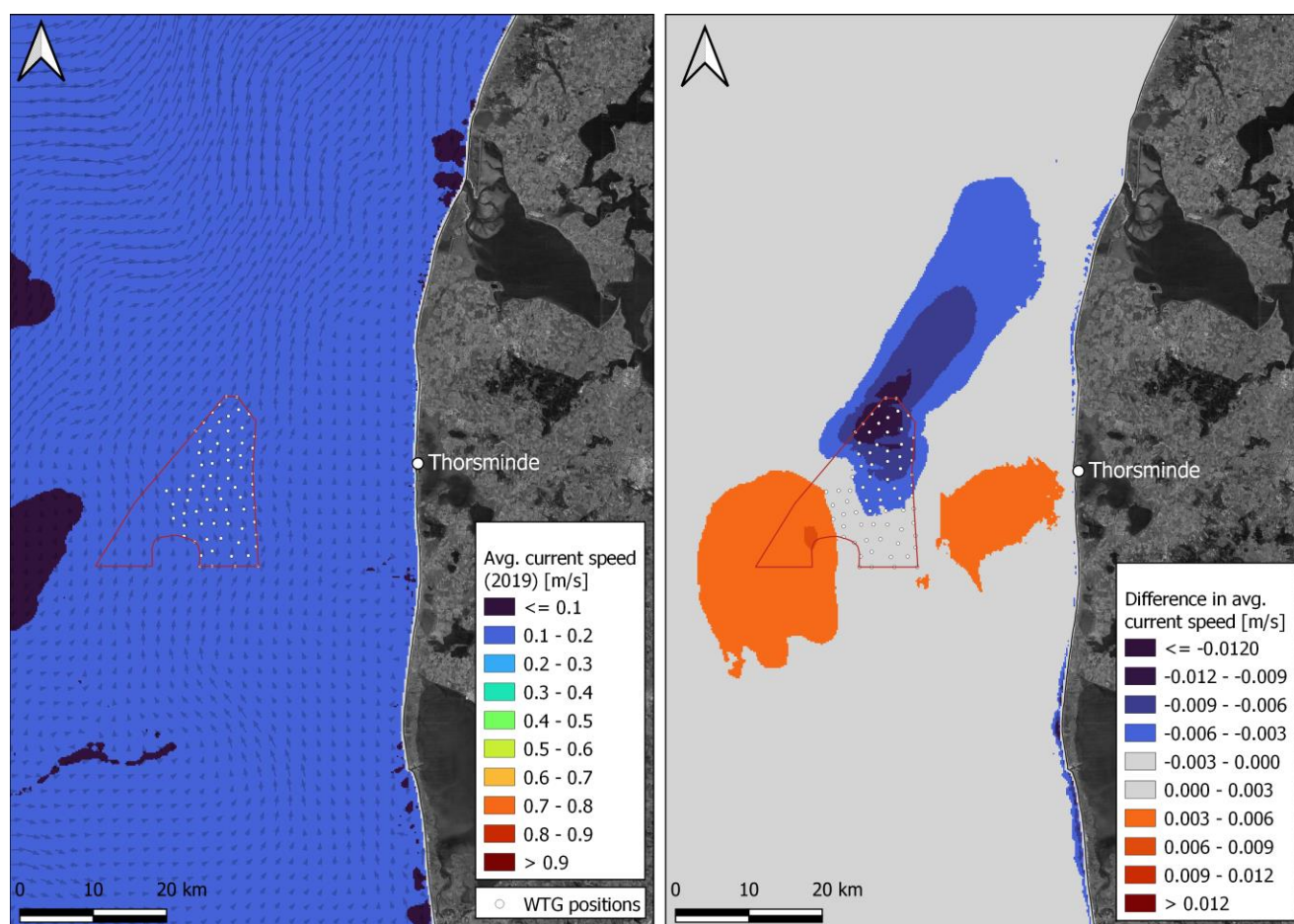


Figure 7.1: Left: Baseline depth-averaged current speed. Arrows indicate the average flow direction. Right: Difference in average current speed between the baseline model and the model with Thor OWF.

7.2. Waves

The change in the yearly average significant wave height is illustrated in Figure 7.2. From the figure, it is seen that the presence of the wind farm is reducing the average significant wave height on the coast from Nymindegab to Thyborøn. The largest coastal impact on the average significant wave height is found around 12 km north of Hvidesande. Here the average significant wave height is reduced by 2 to 3 cm. The largest offshore impact on the average significant wave height is found on the eastern border of the wind farm, where the significant wave height is reduced by 6 to 7 cm. The daily change in wave height is small and many times smaller than the natural variation, Figure 7.3.

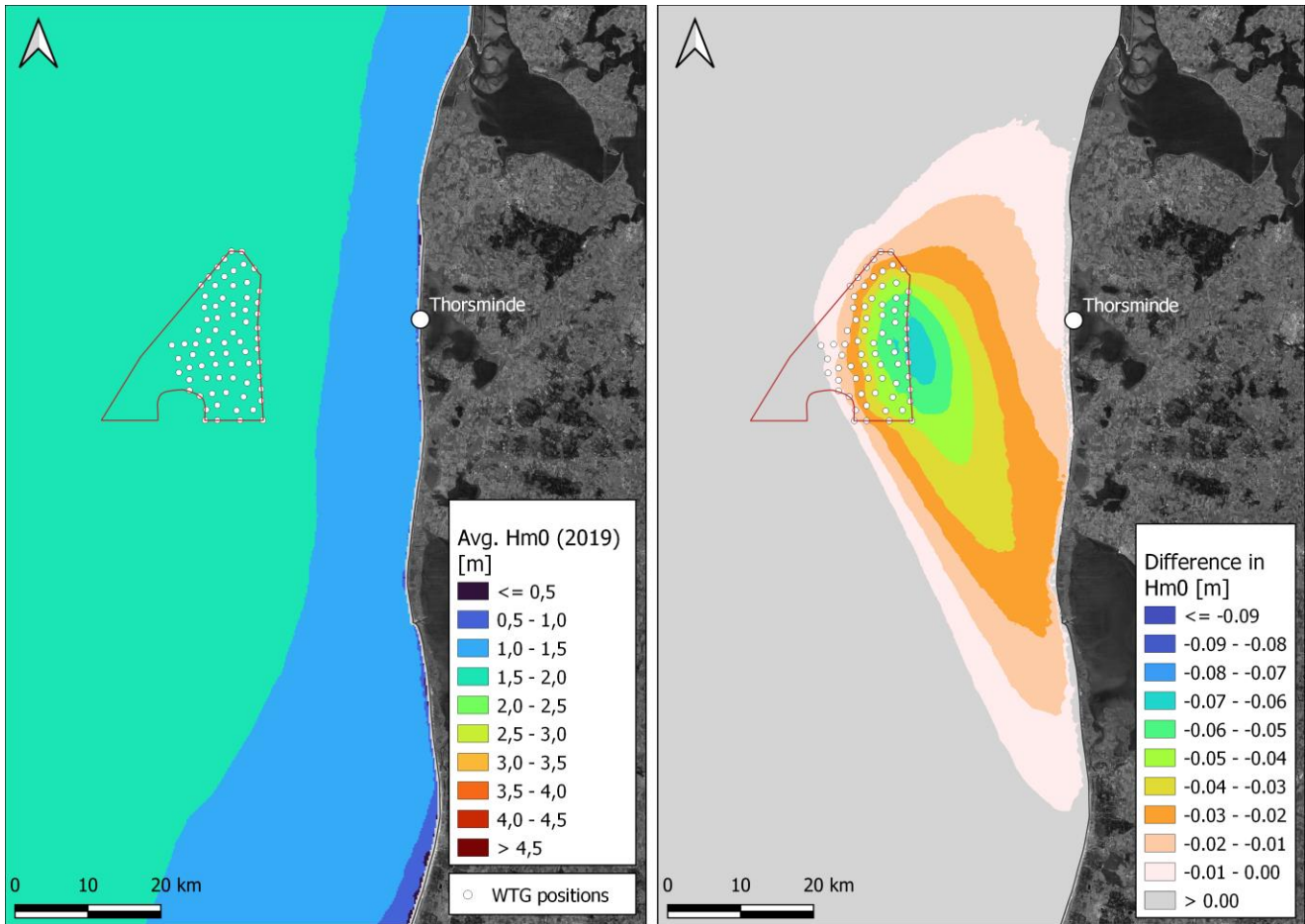


Figure 7.2: Left: Baseline average significant wave height. Right: Difference in yearly average H_{m0} between the baseline model and the model with Thor OVF.

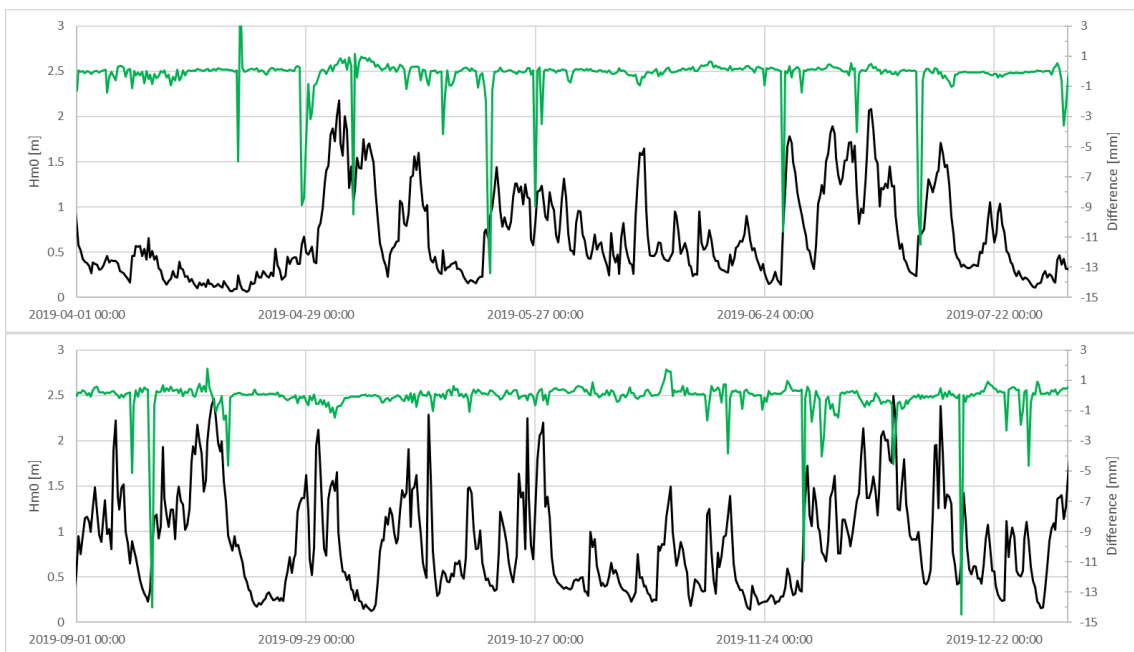


Figure 7.3: Wave climate approx. 1 km offshore north of Hvidesand. Black: Significant wave height (Baseline) and Green: Difference.

8. Pressure, water exchange

The water flow is controlled by the resistance that the flowing water feels (the hydraulic resistance) and the forces that drive the system. When establishing Thor OWF, the flow resistance increases locally due to the monopiles. As such, some blocking of the water flow in the vicinity of the OWF can be expected. The effect on the retention time is quantified by modelling the exchange of water particles for 5 areas; one covering the wind farm and one west, east, north and south of the OWF as illustrated in Figure 8.1. The particles are equally distributed within the areas and released on day 1 whereafter the number of particles within the area is compared on an hourly basis.

The general current pattern shows an average reduction of up to 5 mm/s inside the wind farm area, a reduction of up to 2 mm/s at a distance of 18 km north of the wind farm, and 1 mm/s up to a distance of 26 km. Towards the south, the effect of the wind farm is less pronounced. Here a reduction of 2 mm/s is visible up to a distance of 3 km and a reduction of 1 mm/s up to around 26 km.

Despite that the increased resistance from the foundations is visible in the current pattern the effect on the exchange of water only affects the wind farm area; at its maximum by up to 15%. But the impact on the neighbouring areas is extremely small and only visible on the second decimal, Figure 8.2.

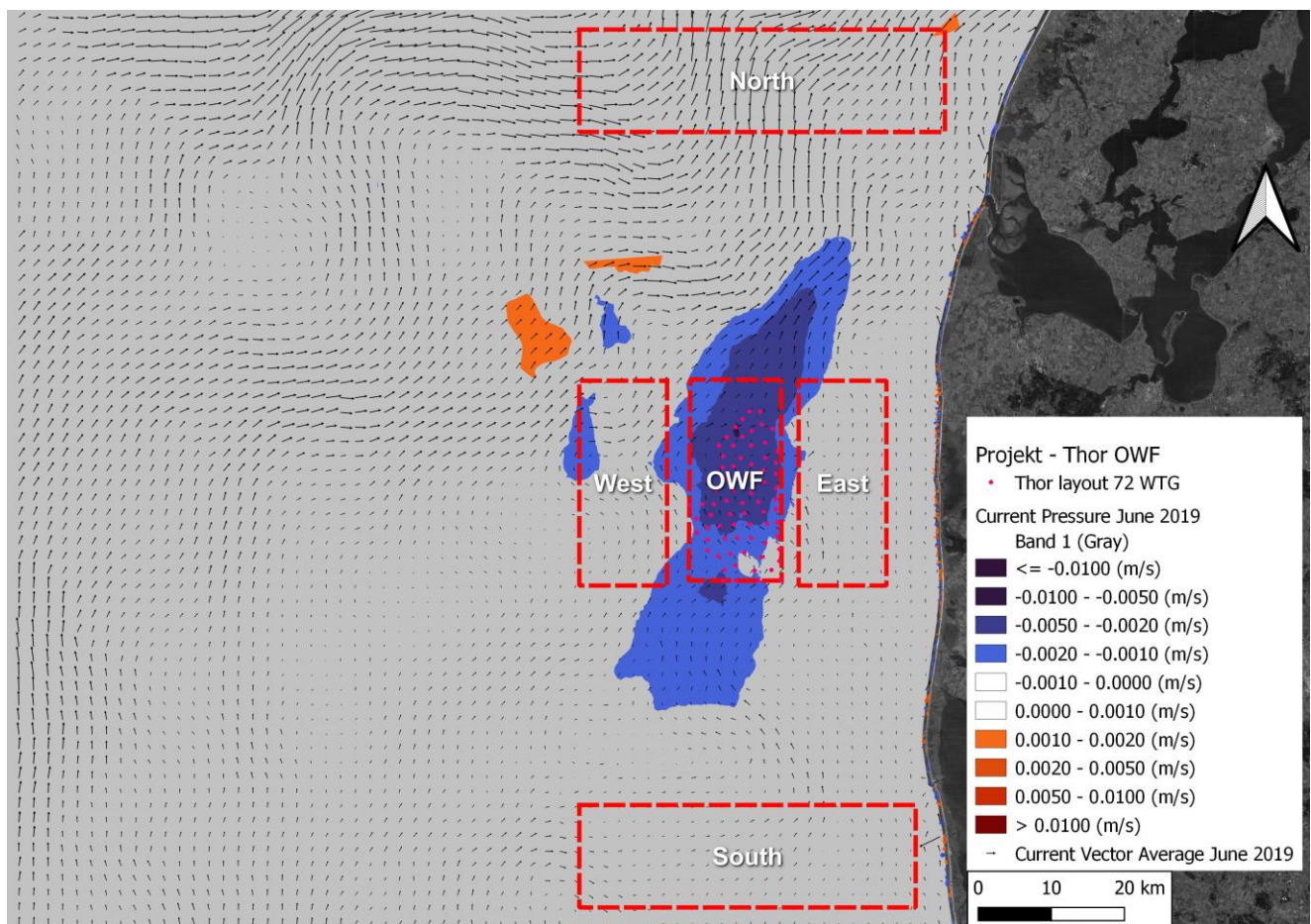


Figure 8.1: Water exchange areas on top of the average current pressure in June 2019. WTG represents wind turbine generators.

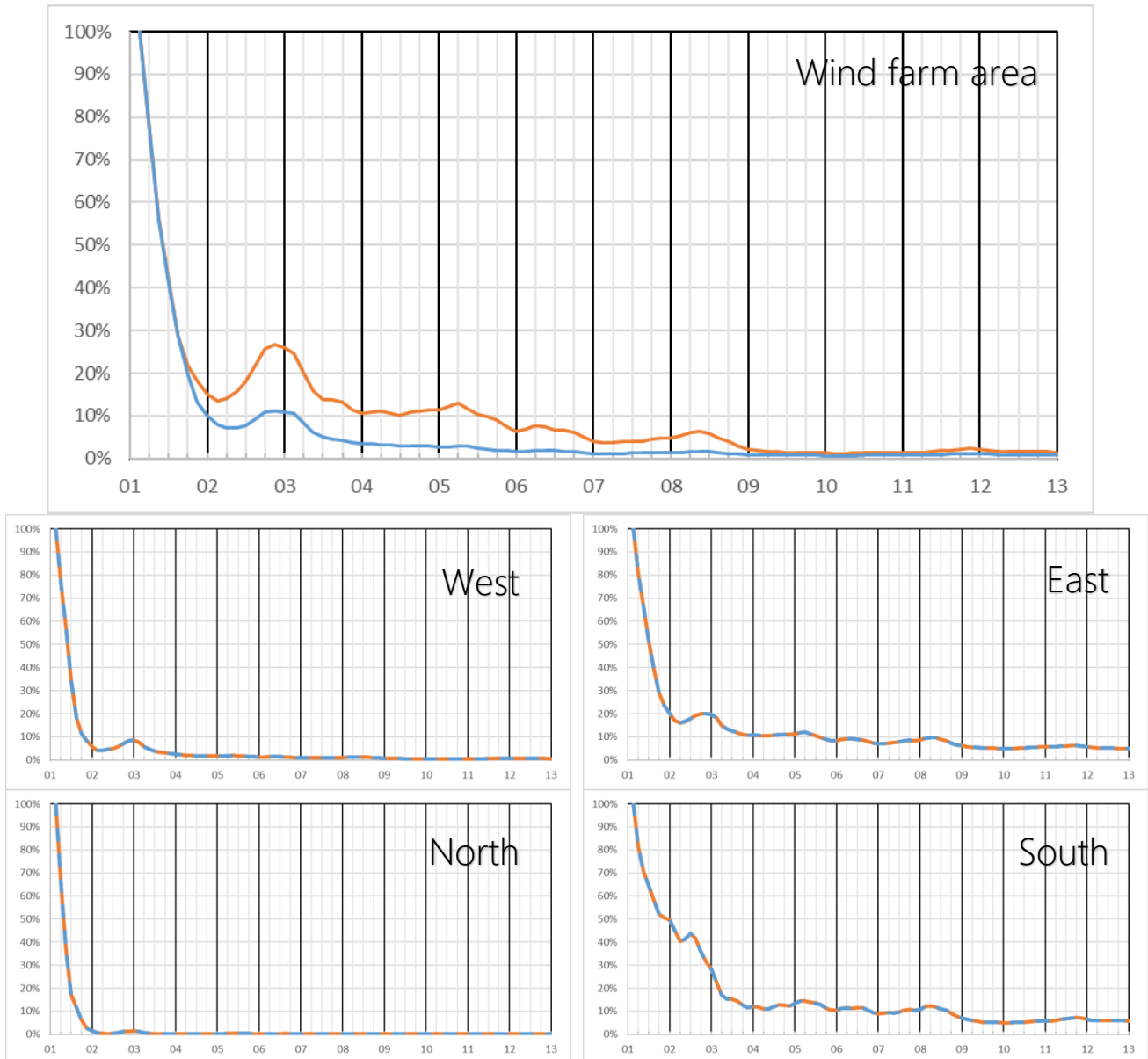


Figure 8.2: Retention time over 12 days for the wind farm area (top), west and east of the wind farm (mid left and right) and north and south of the wind farm (bottom left and right). Blue: Baseline, Orange: Project.

9. Pressure, seabed morphology

As a rule of thumb, sediment transport along the Danish west coast occurs at bed shear stresses of around 0.3 N/m^2 . A previous study of seabed mobility in Øresund has concluded that the seabed material starts to move when the shear stress exceeds 0.3 N/m^2 (Lumborg, 2005). Most of the time, the bed shear stress in the area of interest (except for the area close to shore) will be well below 0.3 N/m^2 . Only in more severe weather, will the maximum limit be exceeded; 2% of the time for the northeasterly corner and 1% of the time for the whole wind farm area except for the southwesterly corner.

The maximum bed shear stress and the difference in the maximum shear stress are illustrated in Figure 9.1. The figure shows, that the maximum bed shear stress comes above the limit of 0.3 N/m^2 throughout the entire OWF area; around 0.4 N/m^2 in the southwesterly corner and up to 0.6 N/m^2 towards the east. This is also indicated in the geophysical survey where bedforms are observed.

As seen in Figure 9.1, the change in the average bed shear stress is much smaller than 0.3 N/m^2 , thus the changes in the bed shear stress are not expected to have an impact on sediment transport outside the OWF area. Local scouring may occur, max. +/- 100 m, due to the obstruction caused by the foundations and the scour protection which potentially may result in a lowering of the seabed and sorting of the sediments.

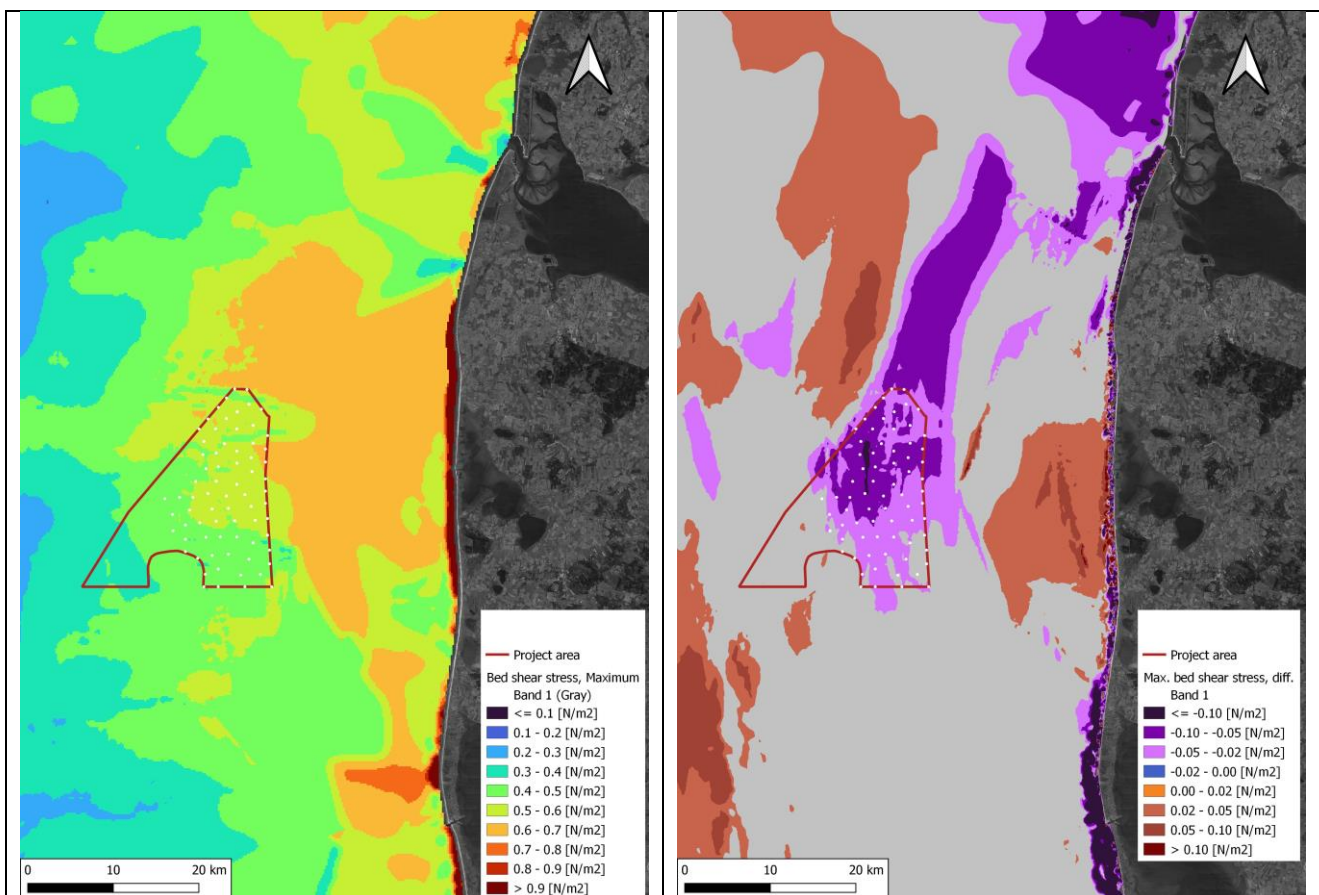


Figure 9.1: Maximum bed shear stress (left) and the difference between project and baseline (right).

10. Pressure, longshore sediment transport

The longshore sediment transportation is driven by the wave-induced longshore currents (i.e. wave radiation from breaking waves). Changes in the wave climate can therefore potentially result in changes in sediment transportation. The changes in sediment transportation before and after the installation of Thor OWF are illustrated in Figure 10.1.

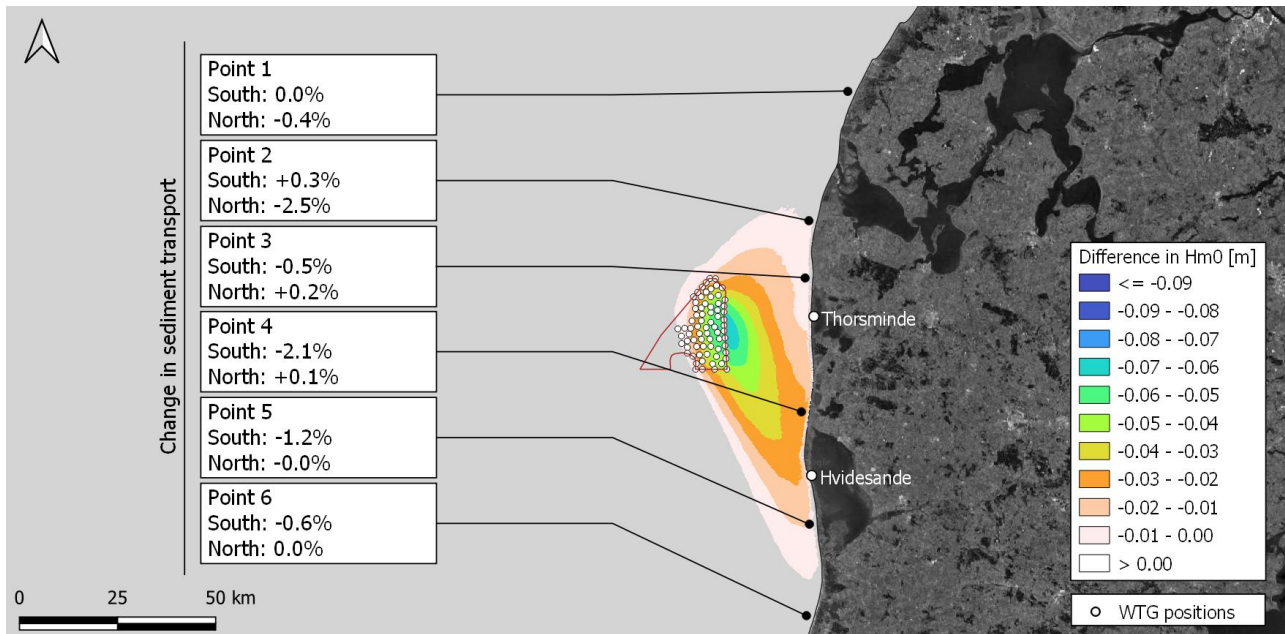


Figure 10.1: Annual impact on the longshore sediment transport and the annual significant wave height.

The changes in longshore sediment transportation are estimated with the CERC formula (Coastal Engineering Research Center, 1984). From Figure 10.1 it is seen, that small changes in sediment transportation are observed in both northern and southern directions. The changes in sediment transportation, however, are less than the yearly variations in sediment transportation capacity rates. To illustrate this, the total sediment transportation is calculated on a yearly and monthly basis by using the CERC formulation (Coastal Engineering Research Center, 1984) at a point close to landfall north of Thorsminde.

The yearly and monthly sediment transportation capacity is seen in Table 10-1. The table shows a highly volatile sediment transportation capacity from year to year; +236% to -195% according to the average. It should be mentioned that the transportation capacity from the CERC formulation is strongly dependent on the coastal orientation in the given area. On average the net longshore sediment transport is south going.

Table 10-1: Sediment transportation capacity [m³] divided by year and month. Colour bars indicate magnitude (by length) and direction (blue is northbound and red is southbound).

Month	Year										
	2010	2011	2012	2013	2014	2015	2016	2017	2018	2019	2020
1	-101279	2882	-221029	19467	160771	86354	168214	-153576	151016	-504347	211066
2	-26368	71560	-164739	94258	518368	-16339	45420	55768	105937	121828	236670
3	-145820	-54611	-319513	56518	20565	90942	-28154	-41118	-15547	-42863	200822
4	-63420	-138528	-48717	85201	-100589	-216397	-162593	-338926	16185	-6659	-225177
5	-285678	76328	-195892	31358	-134214	1704	-87615	-57289	-33018	-314031	-247488
6	-273934	-77462	-180139	-178022	-350351	-168122	-64159	-74708	-292186	8976	62459
7	23076	-168576	-39611	-131113	-2204	-179199	-53101	-105579	-197318	-261313	-85190
8	-37255	-43340	-110956	-49364	19838	90561	-99437	-13165	8545	212603	34705
9	-138951	138405	-41713	-125526	-138645	-14392	106576	44952	38485	-236018	20870
10	-44471	-74654	-69450	178602	292134	-16445	-62631	-269716	-217701	74025	176175
11	14122	136123	166684	-137875	130482	84940	-44837	-216836	191484	-4026	191082
12	-157209	9718	166592	384830	-67483	473537	-68780	-97174	-184802	151157	216166
Sum	-1237188	-122154	-1058484	-135933	348672	213737	-351097	-1267368	-428919	-800669	792160

11. Sediment dispersal, during installation

The following (sub)chapter presents the outcome of the sediment simulations in the form:

- Duration of suspended depth average sediment concentrations (SSC) above 10 mg/l, 50 mg/l, 100 mg/l, 300 mg/l, 500 mg/l, 1000 mg/l and the average concentrations over the installation period in mg/l,
- Duration of suspended sediment concentrations for the lower 10 m of the water column above 10 mg/l, 50 mg/l, 100 mg/l, 300 mg/l, 500 mg/l, 1000 mg/l and the average concentrations over the installation period in mg/l and
- Average sedimentation in mm over the installation period.

All data presented in the following are average values for an area of around 50 x 50 m (2,500 m²) and the concentrations are depth-averaged unless otherwise specified.

The type of sediment to be drilled, dredged or jetted for the different activities are as presented in chapter 4.2.

The case that has been simulated (14 MW layout) presents results with sediment being released:

- 2 m below the water surface for the drilled monopile;
- 2 m above the seabed for jetting and CFE;
- at the surface for dredging.

For the export cable burial near landfall, two cases are modelled and presented:

Scenario 1 - cable burial with dredging:

From KP 0.46 to KP 3.3, sediment is removed prior to jetting and CFE follow:

- KP 0.46 to approx. KP 1.0 an excavator (Backhoe Dredger) is used. The estimated sand volume is 40,000 m³ (total for the 2 export cables).
- KP 0.5 to KP 3.3 a Trailing Suction Hopper Dredger is used. The estimated sand volume is 300,000 m³ (total for the 2 export cables). The sediment will be temporarily stored in an area with a sandy seabed approximately 800 metres north of the cable. After the cables are flushed, the sediment will be moved back and used to re-establish the cable corridor. In practice, this is only done if the trench is not back-filled naturally.

Scenario 2 - cable burial without dredging:

- From KP 0.46 to KP 3.3, the cables are buried to 3 m below the seabed by jetting and CFE.

The chosen installation scenario will depend on the nature of mobile sediments within the nearshore area of the cable corridor, although Scenario 2 is the preferred method. For details please see the technical project description for the offshore facilities of Thor Offshore Wind Farm, which is appendix 2 to the environmental impact assessment report (NIRAS, 2023).

11.1. Scenario 1: cable burial with dredging, inclusive IAC and MP installation

The estimated depth average concentrations for different durations are presented in Appendix 8 to Appendix 12, while the concentrations for different durations as an average for the lowest 10 m of the water column are presented in Appendix 13 to Appendix 16. The average sediment concentration for the construction period is shown in Appendix 17

and the average sedimentation for the construction period is shown in Appendix 18. Lastly, close-ups showing duration of suspended sediment concentrations of 10 mg/l and 50 mg/l in the lower 10 m of the water column in the near-shore area are presented in Appendix 19 and Appendix 20, while maximum sedimentation in the construction period is shown in Appendix 21.

Increased concentrations of 10 mg/l are found along the export cables and the infield cables (Figure 11.1) with the longest duration of 45 days found closest to the shore at landfall. This is slightly longer than the spill-related activities but due to the current and the wave activities, the sediments are kept in suspension before they are transported either along the shore or offshore. The former will be included in the natural longshore transport and will only contribute to an increased level of concentration close to the working area. The material which settled offshore will go through a similar process.

Table 11-1 and Table 11-2 show the duration and area affected for selected concentrations during the full installation scope; as depth average SSC in Table 11-1 and as an average for the lower 10 m of the water column in Table 11-2. The depth average SSC for the export cable is illustrated in Table 11-3. At the point of landfall, maximum values of approximately 20,000 mg/l are recorded momentarily, while in the wind turbine area, maximum values of approximately 3,500 mg/l are momentarily recorded. The duration of values such as these will be less than 1 hour.

Table 11-1: Total scope, Selected depth average concentrations as duration and affected areas (measured in hectares) in the entire water column (seabed to sea surface).

Concentration (from seabed to sea surface)		Duration										
		6 [hour]	12 [hour]	1 [day]	2 [day]	1 [week]	2 [week]	3 [week]	4 [week]	8 [week]	12 [week]	16 [week]
10 mg/l	Area [ha]	16280	11588	4665	2215	296	64	39	14	0	0	0
50 mg/l	Area [ha]	8537	5436	2166	1193	209	62	38	13	0	0	0
100 mg/l	Area [ha]	6871	4413	1828	1059	198	60	37	13	0	0	0
300 mg/l	Area [ha]	4448	2643	1280	808	157	58	34	11	0	0	0
500 mg/l	Area [ha]	2592	1548	922	630	132	54	32	11	0	0	0
1000 mg/l	Area [ha]	849	685	529	366	93	42	24	7	0	0	0

Table 11-2: Total scope, Selected average concentrations for the lower 10 m of the water column as duration and affected areas (measured in hectares).

Concentration (from sea bed to 10 meters above seabed)		Duration										
		6 [hour]	12 [hour]	1 [day]	2 [day]	1 [week]	2 [week]	3 [week]	4 [week]	8 [week]	12 [week]	16 [week]
10 mg/l	Area [ha]	27011	19737	7837	2669	328	64	39	14	0	0	0
50 mg/l	Area [ha]	11202	7196	2572	1239	213	62	38	13	0	0	0
100 mg/l	Area [ha]	8760	5574	2097	1140	204	60	37	13	0	0	0
300 mg/l	Area [ha]	6405	4064	1654	968	167	58	34	11	0	0	0
500 mg/l	Area [ha]	5310	3282	1442	857	148	54	32	11	0	0	0
1000 mg/l	Area [ha]	3469	1953	974	606	111	42	24	7	0	0	0

Table 11-3: Export cable, Selected depth average concentrations as duration and affected areas (measured in hectares) in the entire water column (seabed to sea surface).

Concentration (from seabed to surface)		Duration										
		6 [hour]	12 [hour]	1 [day]	2 [day]	1 [week]	2 [week]	3 [week]	4 [week]	8 [week]	12 [week]	16 [week]
10 mg/l	Area [ha]	4548	3940	3061	2149	292	63	39	14	0	0	0
50 mg/l	Area [ha]	2313	1984	1604	1175	209	62	38	13	0	0	0
100 mg/l	Area [ha]	1949	1721	1415	1056	198	60	37	13	0	0	0
300 mg/l	Area [ha]	1534	1350	1099	808	157	58	34	11	0	0	0
500 mg/l	Area [ha]	1286	1119	880	630	132	54	32	11	0	0	0
1000 mg/l	Area [ha]	808	676	528	365	93	42	24	7	0	0	0

The duration of suspended average sediment concentrations above 10 mg/l during construction for the lower 10 meters of the water column is illustrated in Figure 11.1. The figure shows, that the concentration is exceeding 10 mg/l in the OWF area for up to 1 to 2 days during construction. Concentration of 10 mg/l exist for longer durations in the areas around the cable corridor (Figure 11.2).

The duration of suspended depth average sediment concentrations above 10 mg/l during construction for the entire water column is illustrated in Figure 11.3.

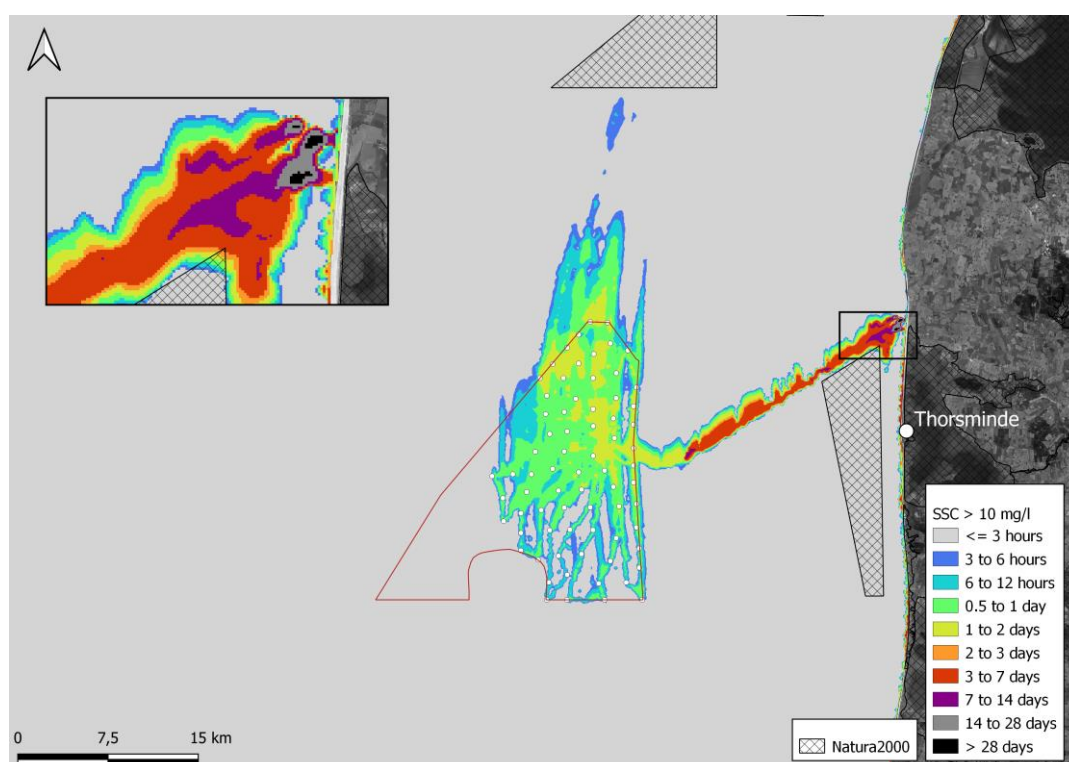


Figure 11.1: Total scope, Duration with concentrations above 10 mg/l (average for the lower 10 m of the water column).

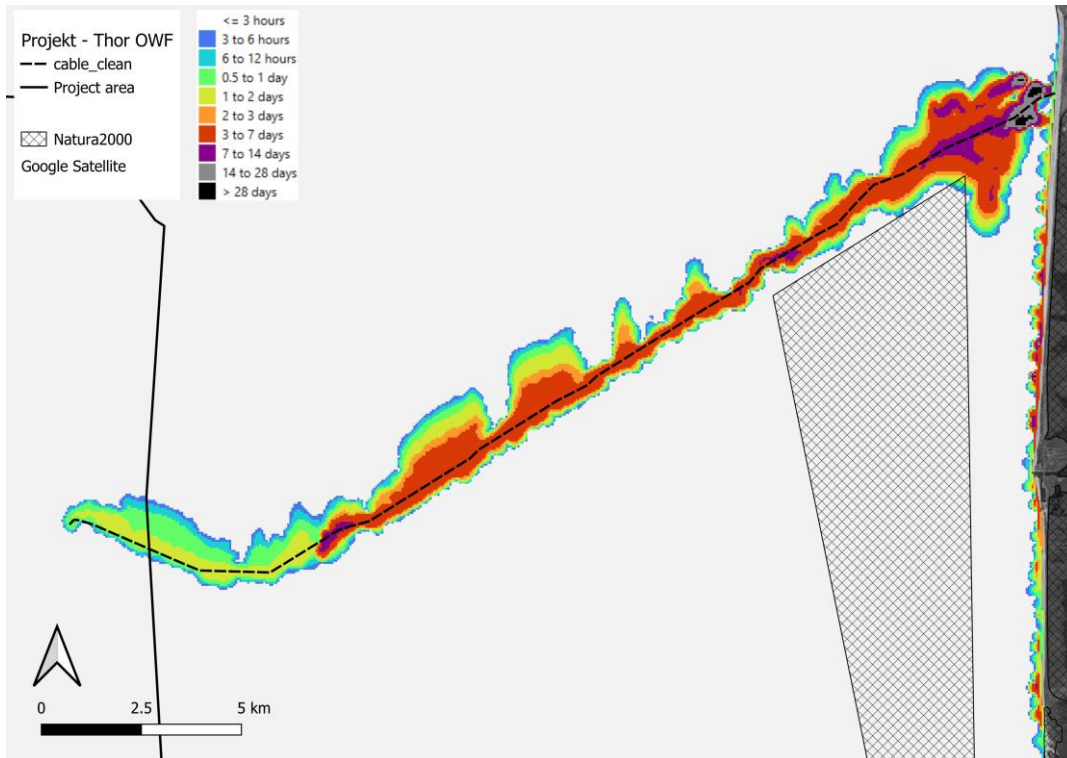


Figure 11.2: Export cable, Duration with concentrations above 10 mg/l (depth average).

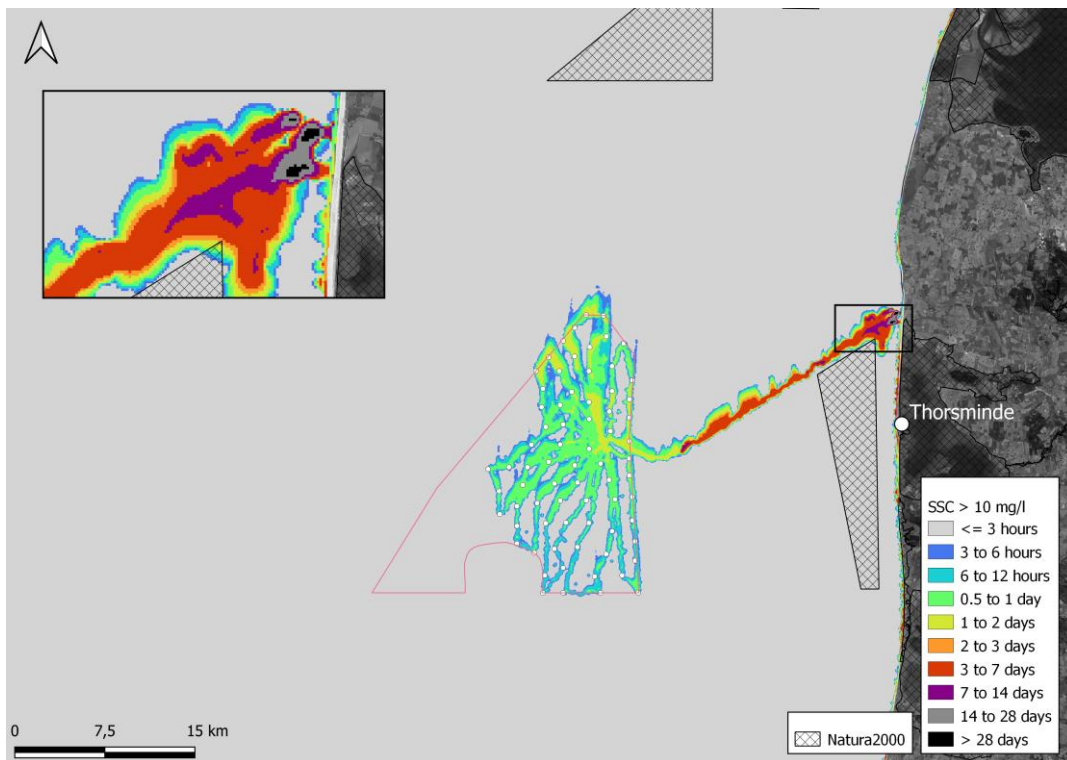


Figure 11.3: Total scope, Duration with concentrations above 10 mg/l (depth average)

The thickness of the deposited material is a few centimeters deep and thus very limited in dept. The maximum sedimentation in the construction period is around 45 mm (Figure 11.5), observed close to landfall. At the end of the construction period, the maximum sedimentation is up to 43 mm close to the shore, along the section where the export cable was dredged before jetting and in the area where the export cable was buried with the CFE next to the offshore substation, Figure 11.4 and Figure 11.6.

After the end of construction, the deposited sediment will be exposed to current and waves bringing the sediment into suspension. The movement of sediment after one month is illustrated in Figure 11.7, showing a north-going transport trend both inside the wind farm and along the export cables. Duration of deposited sediment for various thicknesses and belonging areas are illustrated in Table 11-4 for the full scope and for the export cable in Table 11-5. From the table, it is seen that the deposit sediments are not stationary and will be brought into suspension due to waves and currents. E.g. for the full scope sedimentation of 20 mm will 6 hours after the construction has finished cover an area of 398 ha but after 16 weeks the area is reduced to 2 ha and for the export cable it is 327 ha after 6 hours and 1 ha after 16 weeks.

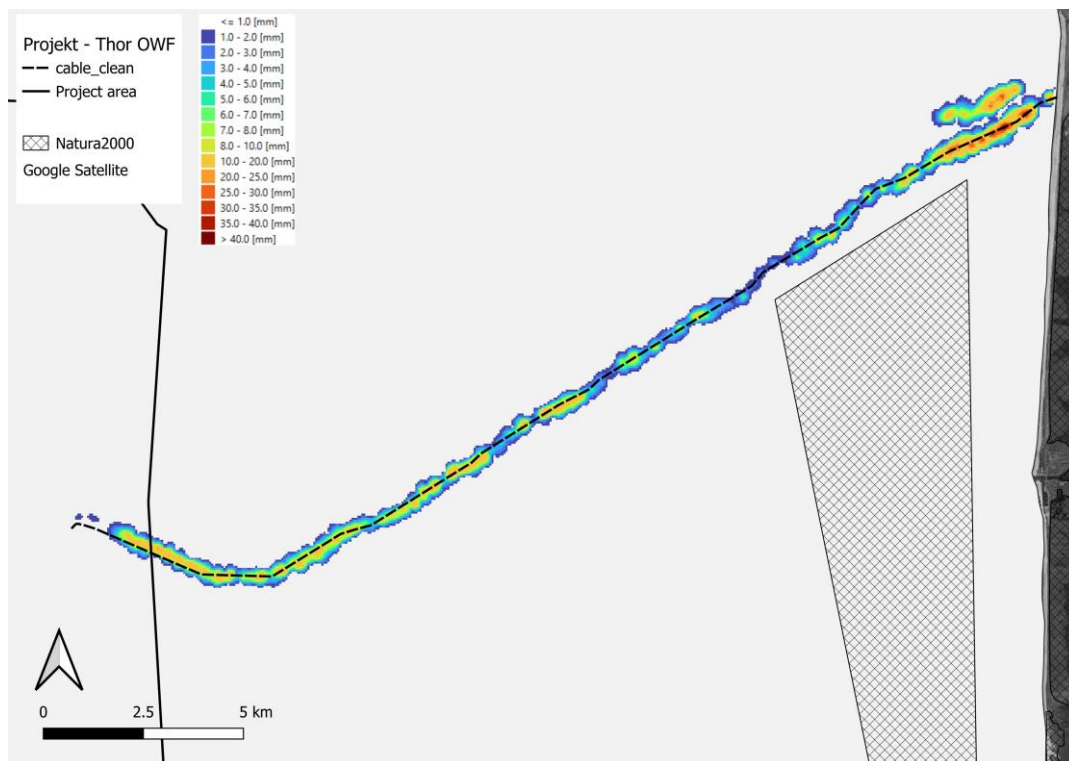


Figure 11.4: Export cable, Sedimentation at the end of the construction period.

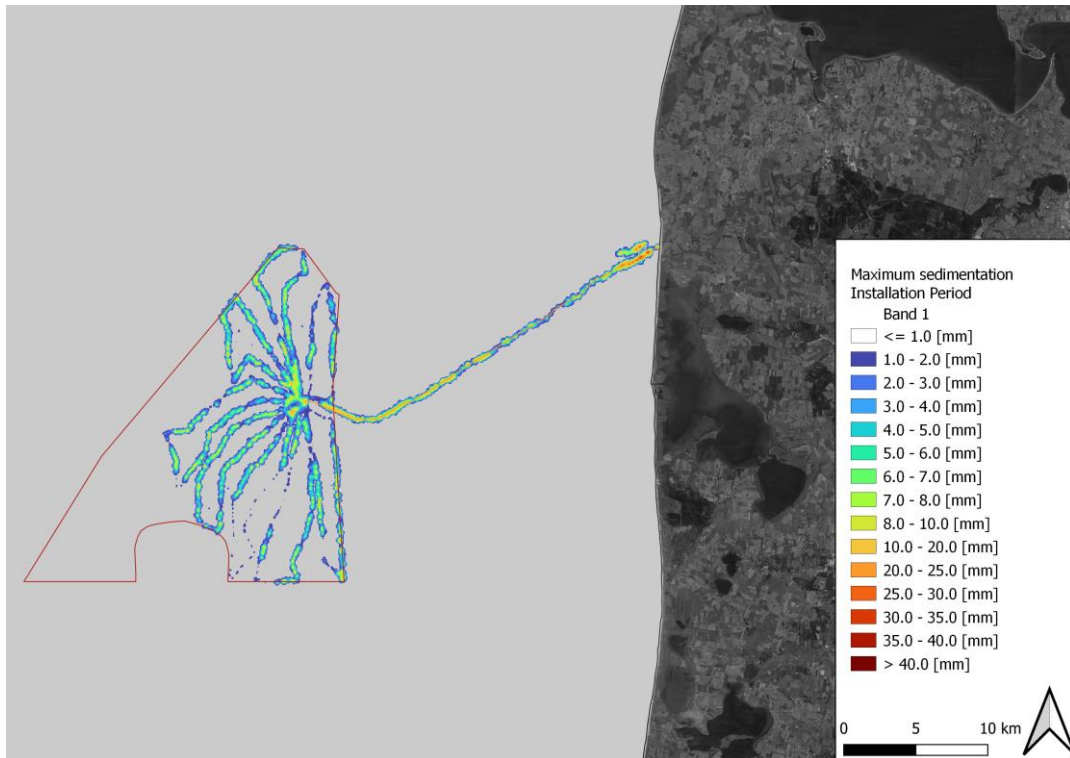


Figure 11.5: Total scope, Maximum sedimentation in the construction period.

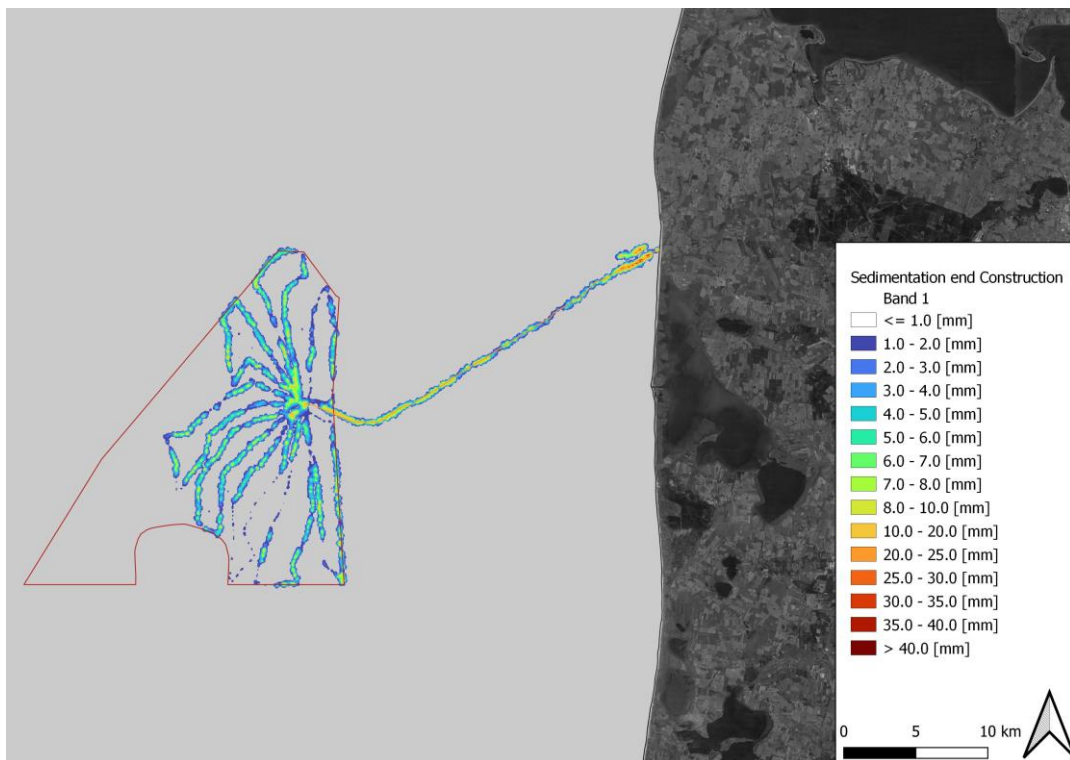


Figure 11.6: Total scope, Sedimentation at the end of the construction period.

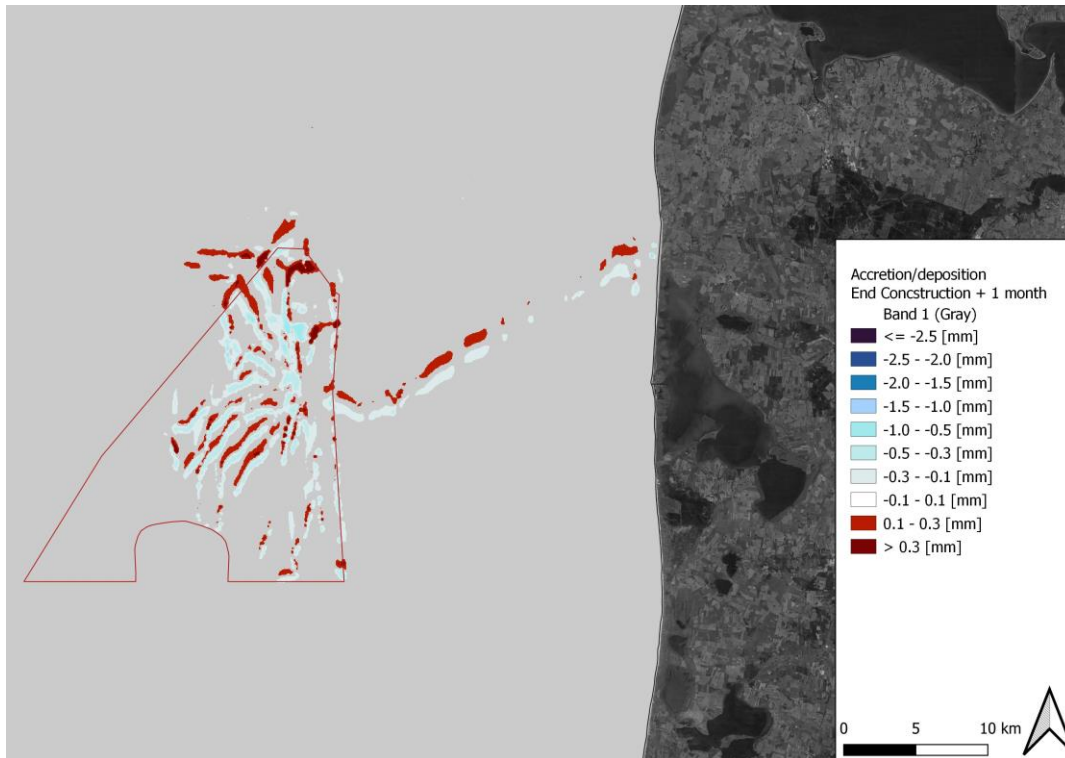


Figure 11.7: Accretion/deposition from the end of the construction period and 1 month ahead.

Table 11-4: Total scope, Selected sedimentation thickness as duration and affected areas (measured in hectares).

Sedimentation		Duration										
		6	12	1	2	1	2	3	4	8	12	16
		[hour]	[hour]	[day]	[day]	[week]						
1 mm	[ha]	13021	12854	12606	12246	11122	10101	9279	8564	6069	3904	1799
2 mm	[ha]	10457	10316	10117	9820	8869	7999	7309	6693	4610	2858	1229
5 mm	[ha]	8347	8201	7990	7683	6720	5853	5187	4599	2753	1424	471
10 mm	[ha]	4240	4106	3938	3682	2926	2310	1882	1531	690	264	43
20 mm	[ha]	398	382	361	334	261	205	166	135	52	14	2
50 mm	[ha]	0	0	0	0	0	0	0	0	0	0	0

Table 11-5: Export cable, Selected sedimentation thickness as duration and affected areas (measured in hectares).

Sedimentation		Duration										
		6	12	1	2	1	2	3	4	8	12	16
		[hour]	[hour]	[day]	[day]	[week]						
1 mm	[ha]	2175	2144	2102	2037	1853	1692	1557	1446	1060	718	337
2 mm	[ha]	1952	1922	1876	1815	1649	1489	1358	1254	877	554	227
5 mm	[ha]	1631	1604	1565	1505	1334	1174	1043	933	579	326	110
10 mm	[ha]	1215	1186	1144	1089	920	777	671	576	309	139	22
20 mm	[ha]	327	314	300	276	219	170	139	116	44	11	1
50 mm	[ha]	0	0	0	0	0	0	0	0	0	0	0

11.2. Scenario 2: cable burial without dredging

As for scenario 1, the longest duration with concentrations above 10 mg/l are found closest to the shore at landfall and is up to 25 days, see Figure 11.8 and Table 11-6. This is in range with the spill-related activities but due to the current and the wave activities, the sediments are kept in suspension before they are transported either along the shore or offshore. The former will be included in the natural longshore transport and will only contribute to an increased level of concentration close to the working area.

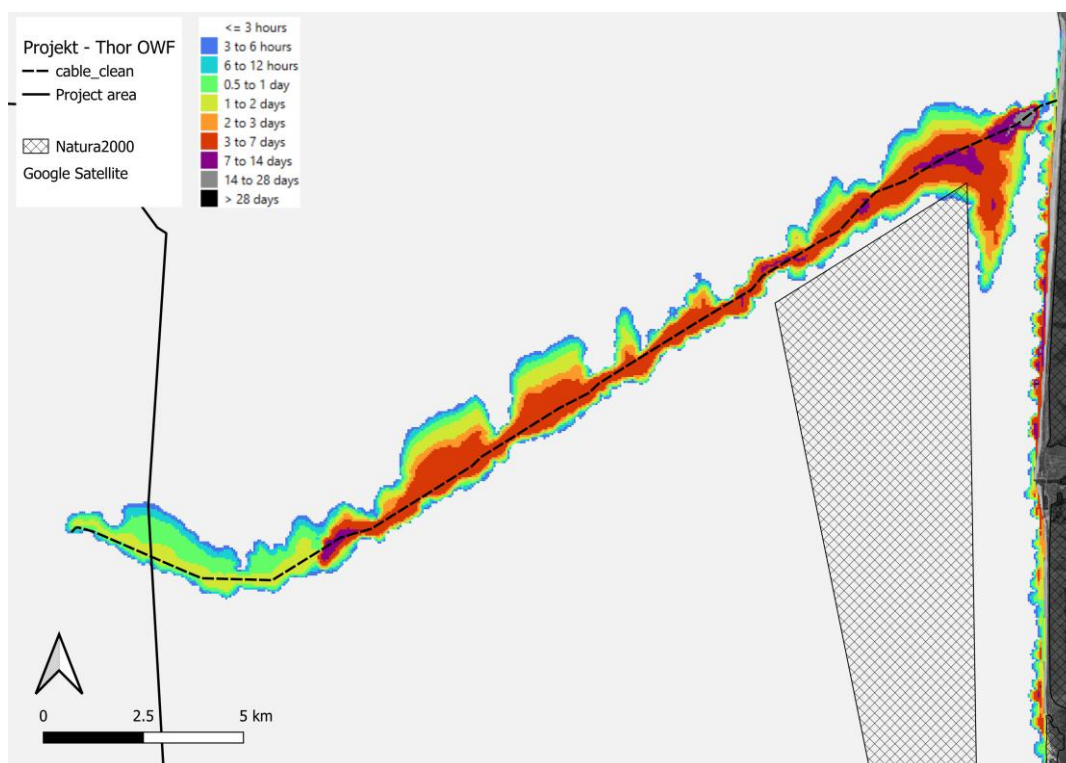


Figure 11.8: Export cable, Duration with concentrations above 10 mg/l (depth average).

Table 11-6: Export cable, Selected depth average concentrations as duration and affected areas (measured in hectares) in the entire water column (seabed to sea surface).

Concentration	[ha]	Duration										
		6	12	1	2	1	2	3	4	8	12	16
		[hour]	[hour]	[day]	[day]	[week]						
10 mg/l	[ha]	4419	3819	2897	1949	193	20	6	0	0	0	0
50 mg/l	[ha]	2106	1759	1385	977	109	19	6	0	0	0	0
100 mg/l	[ha]	1747	1503	1224	874	99	19	5	0	0	0	0
300 mg/l	[ha]	1360	1189	929	650	77	17	5	0	0	0	0
500 mg/l	[ha]	1154	977	748	519	71	17	5	0	0	0	0
1000 mg/l	[ha]	622	496	351	222	33	10	3	0	0	0	0

At the end of the construction period, the maximum sedimentation is up to 40 mm around 450 m from the shore but otherwise less than 20 mm and this only close to the alignment, Figure 11.9. Over time resuspension will reduce the impact e.g. 20 mm affects 277 ha for 6 hours and 3 ha for 16 weeks, Table 11-7.

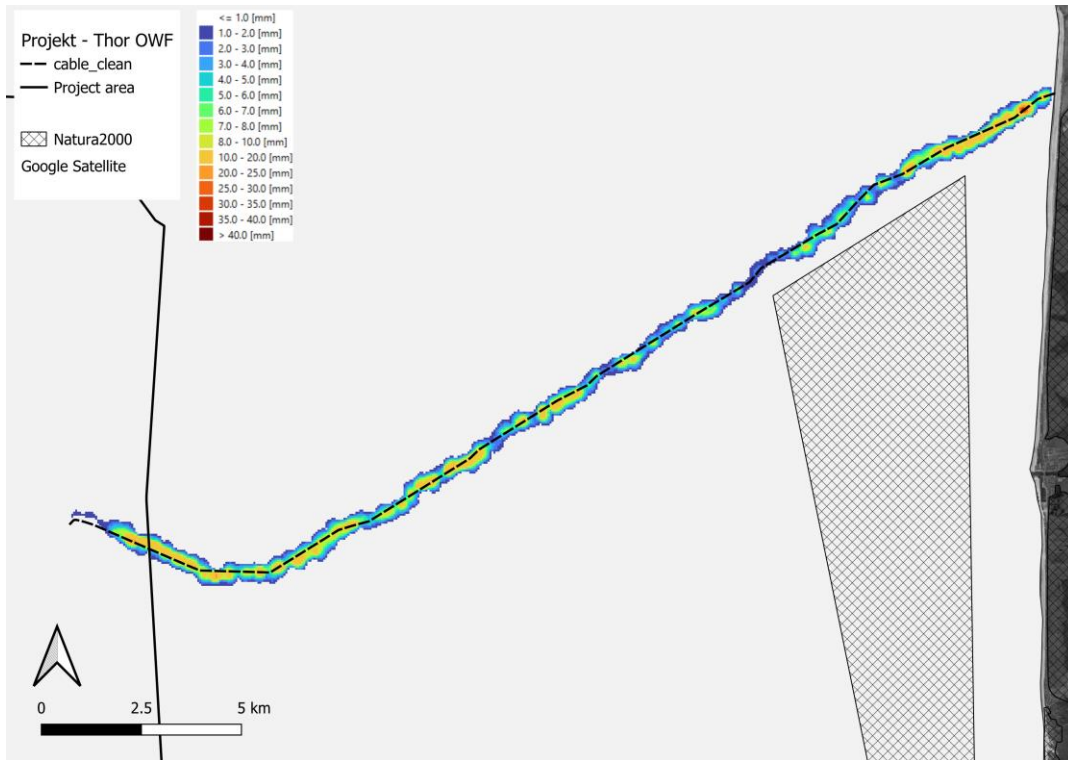


Figure 11.9: Export cable, Sedimentation at the end of the construction period.

Table 11-7: Export cable, Selected sedimentation thickness as duration and affected areas (measured in hectares).

Sedimentation		Duration										
		6	12	1	2	1	2	3	4	8	12	16
	[ha]	[hour]	[hour]	[day]	[day]	[week]						
1 mm	[ha]	1831	1807	1779	1731	1609	1482	1391	1307	1014	739	466
2 mm	[ha]	1642	1619	1591	1545	1430	1309	1219	1137	847	596	355
5 mm	[ha]	1483	1462	1430	1377	1244	1104	997	907	617	394	215
10 mm	[ha]	1103	1081	1046	991	828	698	609	534	311	159	63
20 mm	[ha]	277	261	248	221	154	106	80	63	25	9	3
50 mm	[ha]	0	0	0	0	0	0	0	0	0	0	0

12. Summary

The location of Thor OWF in the North Sea makes it exposed to severe weather which at present is observed in both the wind farm area and along the ECC corridor in the seabed morphology and sediment distribution: The former in the presence of seabed features offshore, and significant seasonal changes in the cross-shore profile nearshore. The latter is a lack of fine sediment and a limited amount of silt and clay in the sediment samples.

Construction

The construction work carried out in the coastal zone when constructing Thor OWF is taking place in areas with a highly dynamic morphology. Large seasonal changes in the seabed are observed at water depths up to around 10 meters below MSL.

This means, that some transportation of suspended sediments from dredging and jetting works is expected. However, due to the large areas with relatively coarse sediment grain sizes, the plumes of suspended sediments are relatively small in size, low in concentration and short in duration. Most of the released sediments fall directly through the water column and deposit onto the seabed. Hereafter, the sediments will be part of the natural sediment transportation. A month after construction, almost no visible sediment accretion/deposition is expected.

With regard to the two different scenarios for cable installation in the near shore area, the overall exposure from scenario 1 covers scenario 2 in terms of both sedimentation and suspended sediment concentrations, see Figure 12.1 and Figure 12.2. The small difference in sediment plume contours (Figure 12.1) between scenario 1 and scenario 2 in the nearshore area is negligible.

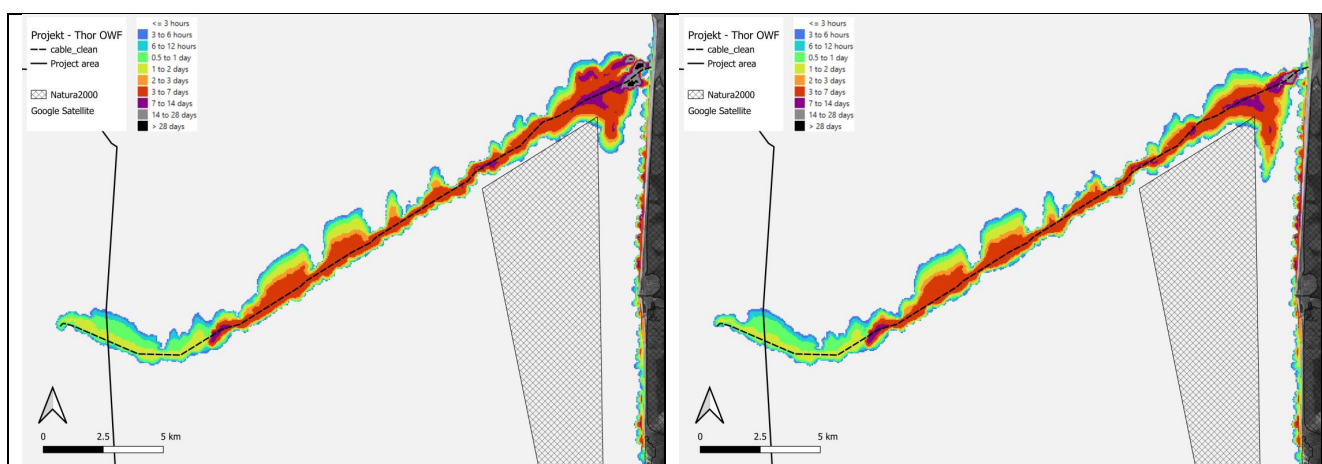


Figure 12.1: Duration of suspended sediment concentration above 10 mg/l. Left: scenario 1. Right: scenario 2.

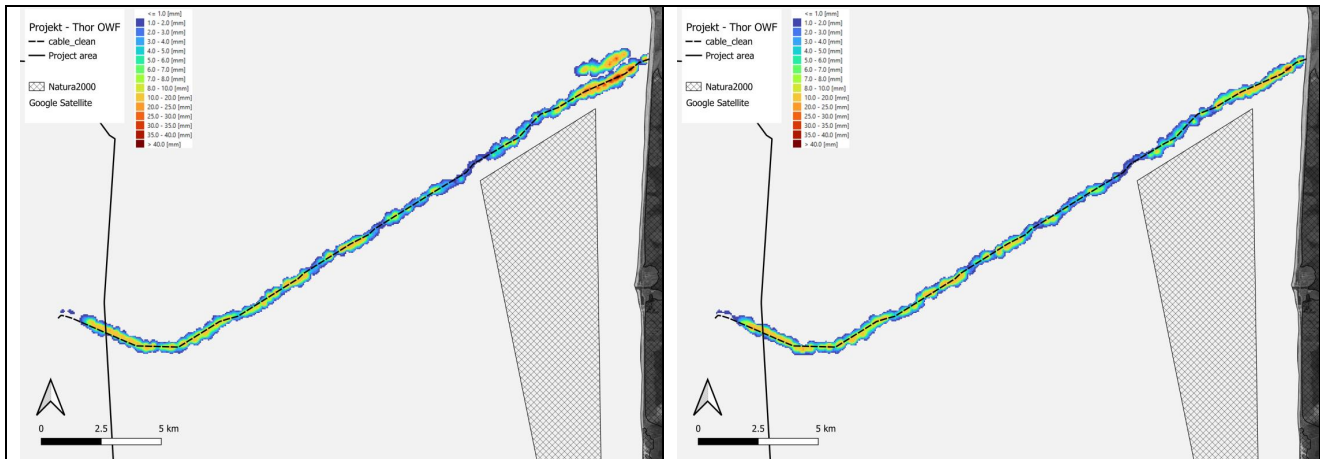


Figure 12.2: Sedimentation at the end of the construction period. Left: scenario 1. Right: scenario 2.

Operation

Based on the model results, limited changes in the current conditions are expected once the wind turbines are installed. The monopiles embedded in the seabed increased the hydraulic resistance locally in the WTG area, which has a small impact on the general current pattern. On average, a small local decrease in the current speed is expected in the area north of the wind farm up to 9mm/s. This is considered a small impact.

Furthermore, a small increase in the current speed is seen between the OWF and the coastline. The increase here in the average current speed is in the order of up to 6 mm/s, which again is considered a small impact. A small increase with the same magnitude of up to 6 mm/s is also observed at the western corner of the project area. The model results also show a small local blocking effect, however, this effect is only seen near the installed monopiles.

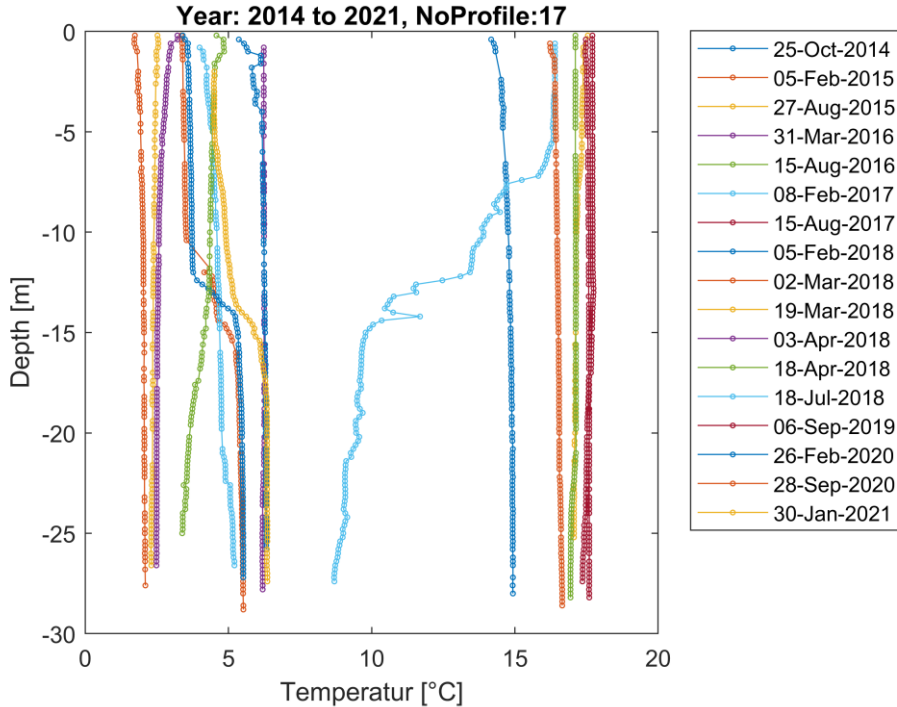
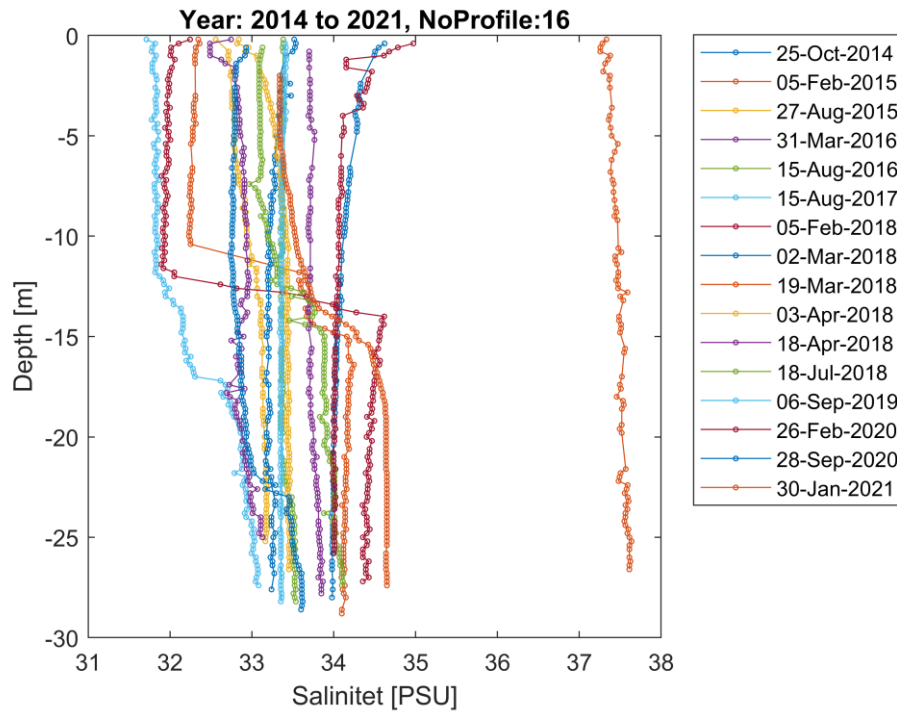
Based on the model results, some small changes in the wave conditions are also expected once the wind turbines are installed. This effect is mainly due to the wake of the wind turbines, where the wind energy is reduced. The local reduction in wind energy at the OWF wake results in a small reduction in the locally generated wind waves. The largest coastal impact on the average significant wave height is found around 12 km north of Hvidesande. Here the average significant wave height is reduced by 2 to 3 cm.

Since the main driver of longshore sediment transportation is the radiant stresses from wave breaking, the reduction in the significant wave height changes the sediment transportation patterns slightly. Looking at the northwards and southwards sediment transportation, the maximum change in the transportation rates as a consequence of the OWF is in the order of ± 2.5 depending on the specific location. However, at most of the stretches along the coast, the change in sediment transportation rates is between 0.0 and 0.5 %. Due to the large yearly variations in sediment transportation rates, the OWFs impact on sediment transportation is considered small.

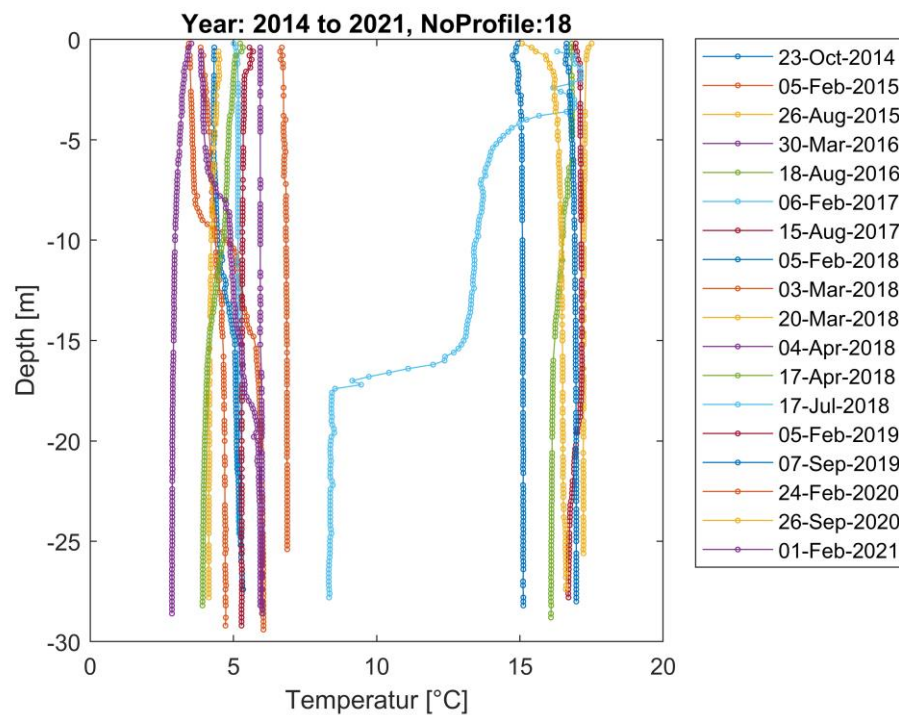
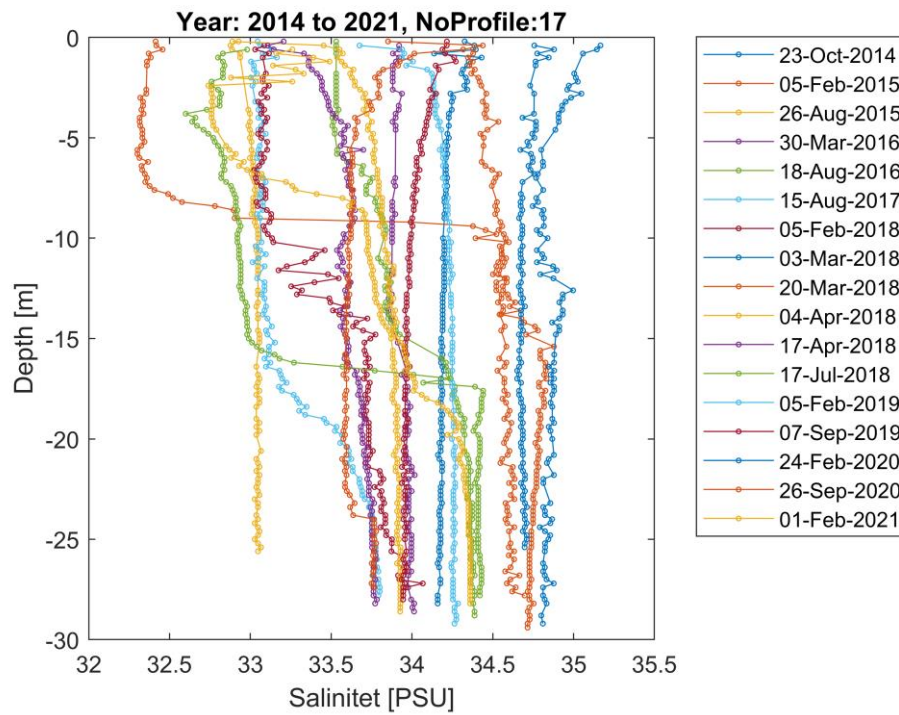
13. References

- BEK nr 803 af 14/06/2023. (n.d.). Bekendtgørelse om konsekvensvurdering vedrørende internationale naturbeskyttelsesområder samt beskyttelse af visse arter ved projekter om etablering m.v. af elproduktionsanlæg og elforsyningsnet på havet. Retrieved from <https://www.retsinformation.dk/eli/lta/2010/1476>
- British Oceanographic Data Centre. (2022, 09 28). Retrieved from https://www.bodc.ac.uk/data/hosted_data_systems/sea_level/uk_tide_gauge_network/processed/C-map. (2019, 12 01). *MIKE C-MAP*. (DHI) Retrieved from <https://www.mikepoweredbydhi.com/products/mike-c-map>
- Coastal Engineering Research Center. (1984). *Shore Protection Manual*. U.S. Army Engineer Waterways. Retrieved from <https://archive.org/details/shoreprotectionm01unit/mode/1up?ref=ol&view=theater>
- Danish Coastal Authority. (2022, April). Data - Cross shore profiles.
- Danish Coastal Authority. (2022b). *Kystatlas*. Retrieved from <https://kyst.dk/kyster-og-klima/vaerktoejer/kystatlas/>
- Danish Maritime Authority. (n.d.). *Energy systems*. Retrieved April 27, 2022, from <https://dma.dk/safety-at-sea/safety-of-navigation/construction-works-at-sea/energy-systems>
- DHI. (n.d.). Retrieved from www.mikepoweredbydhi.com: <https://www.mikepoweredbydhi.com/download/mike-2019>
- DMI. (2022). *DMI Frie Data*. Retrieved from <https://www.dmi.dk/friedata>
- ECMWF, C. C. (2019, 03 01). *Climate Data Store*. (ECMWF) Retrieved from <https://cds.climate.copernicus.eu/cdsapp#!/dataset/reanalysis-era5-single-levels?tab=form>
- EMODnet. (2021, 03 15). *Bathymetry*. Retrieved from [portal.emodnet-bathymetry.eu/#: portal.emodnet-bathymetry.eu/#](http://portal.emodnet-bathymetry.eu/#:portal.emodnet-bathymetry.eu/#)
- Jensen, N.O. (1983). *A note on wind generator interaction*. DTU.
- Lumborg. (2005). *Modelling the deposition, erosion, and flux of cohesive sediment through Øresund*. Journal of Marine systems.
- MarineSpace. (2022). *Technical Note - Thor Offshore Wind Farm Task 1 - Bed Morphology and Mobility*.
- Miljø- og Fødevarerministeriet. (2022, 01). *Overfladevandedatabasen, ODA*. Retrieved from <https://odaforalle.au.dk/login.aspx>
- MMT. (2020a). Thor Offshore Wind Farm. Site Investigation. Lot 1. Geophysical survey report.
- MMT. (2020b). Thor Offshore Wind Farm. Export cable route investigation. Lot 2. Geophysical survey report.
- MMT. (2020c). Thor Offshore Wind Farm. Hydrographic survey report.
- MMT. (2020d). Thor Offshore Wind Farm. Export cable route. Hydrographic survey report.
- NIRAS. (2023). *Miljøkonsekvensrapport for Thor Havvindmøllepark*.

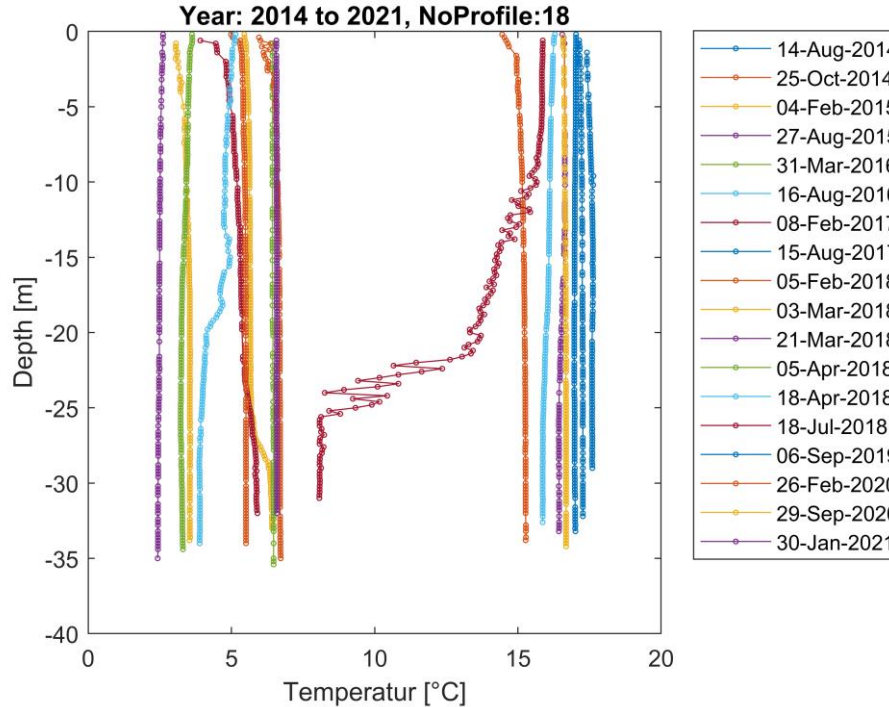
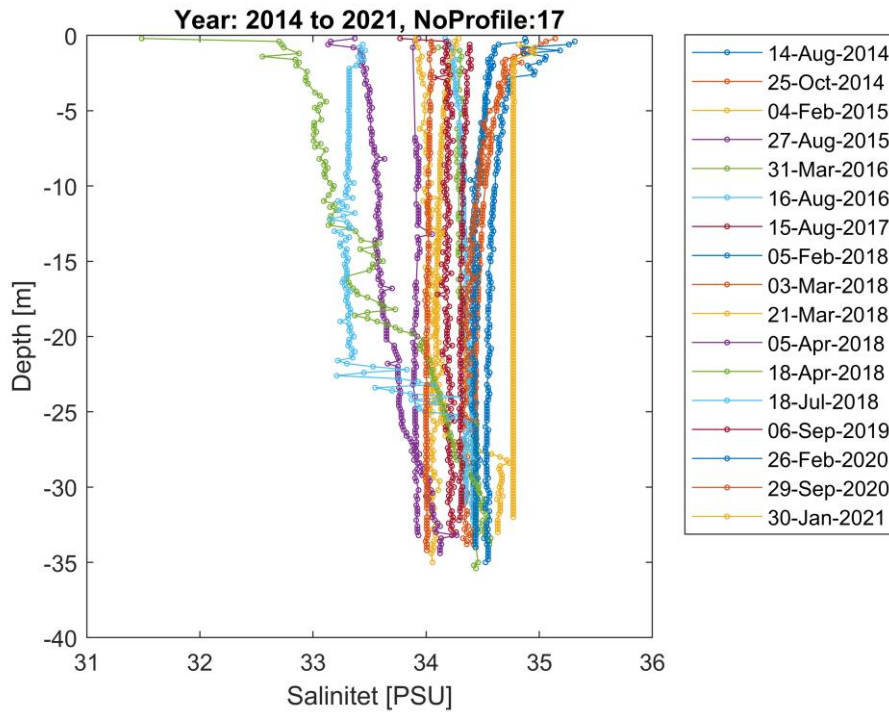
Appendix 1: DMU1035, salinity and temperature profiles



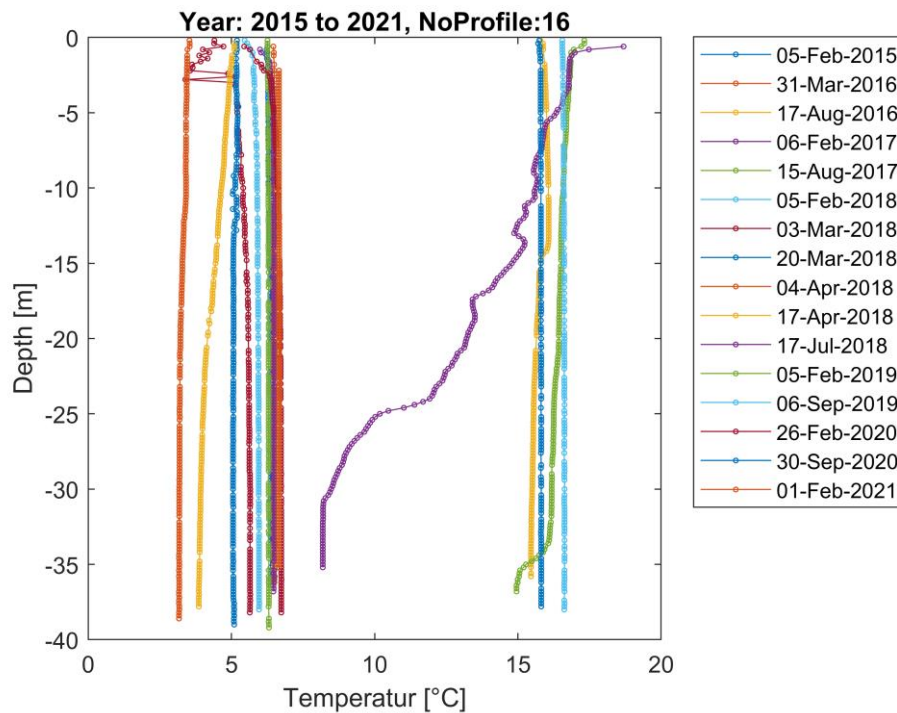
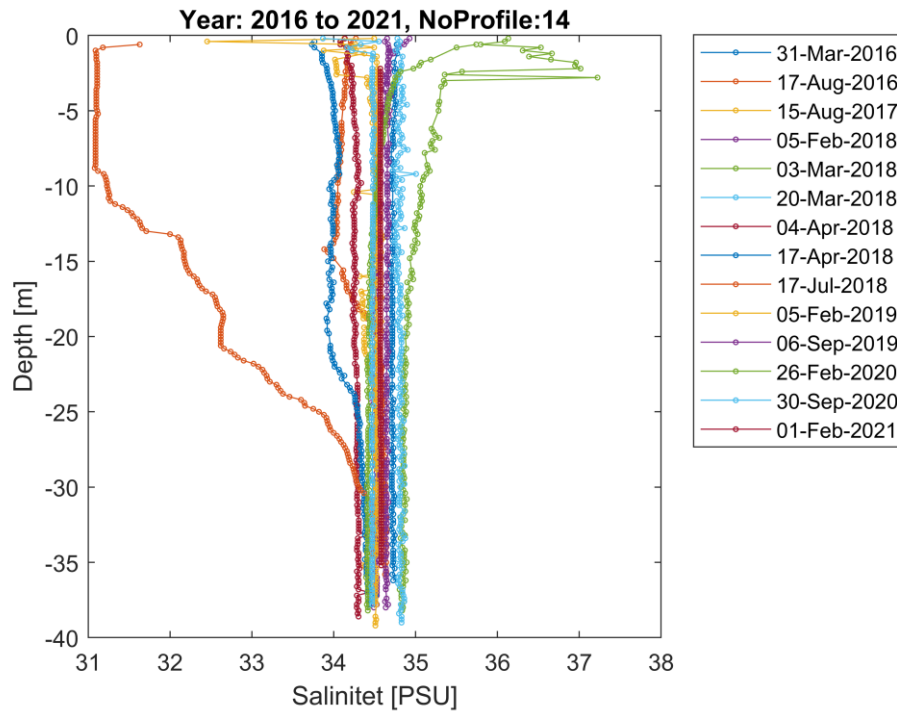
Appendix 2: DMU1023, salinity and temperature profiles



Appendix 3: DMU1072, salinity and temperature profiles



Appendix 4: DMU1025, salinity and temperature profiles



Appendix 5: Particle size distribution

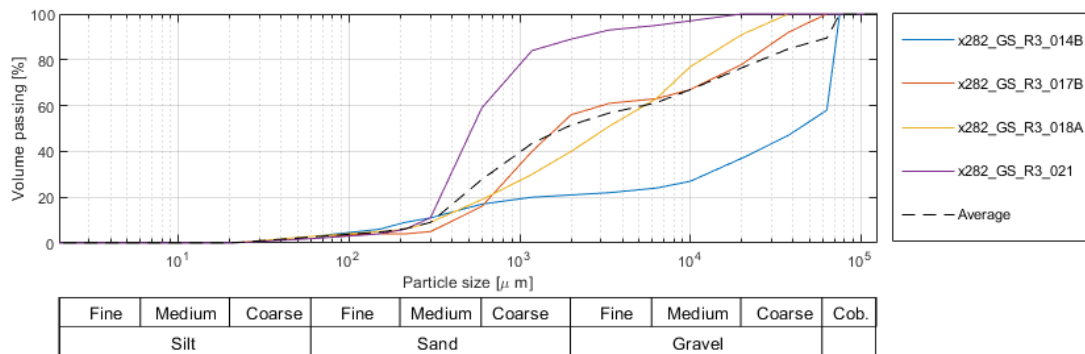


Figure 13.1: ECC gravel

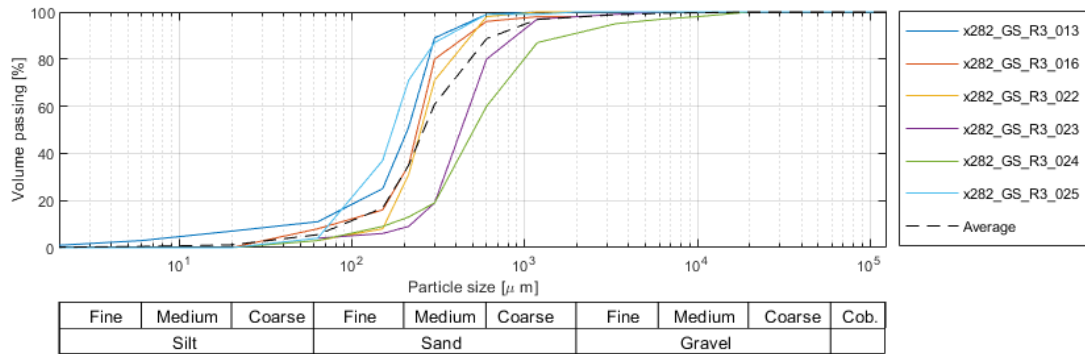


Figure 13.2: ECC sand

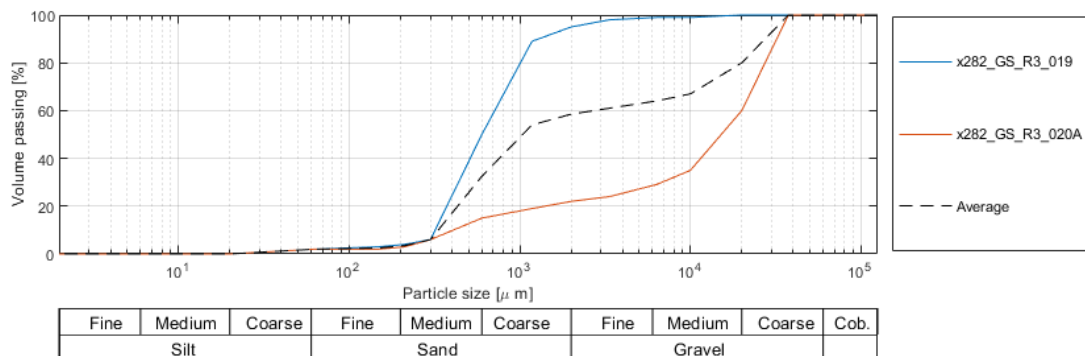


Figure 13.3: ECC Sandy Gravel

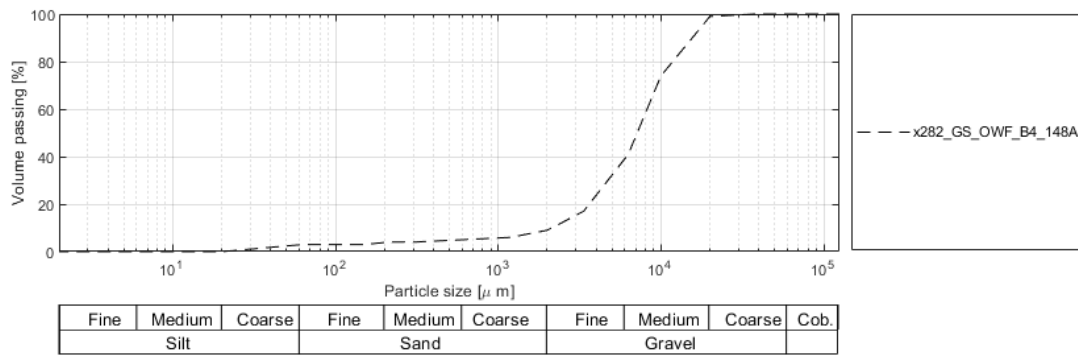


Figure 13.4: OWF Gravel

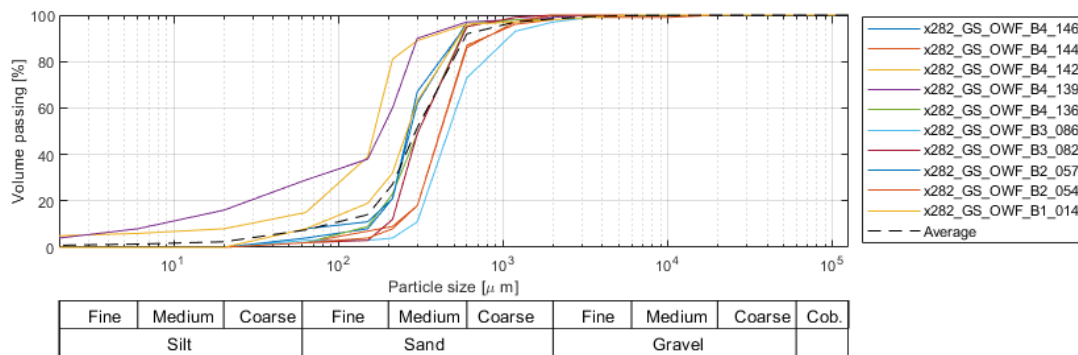


Figure 13.5: OWF Sand

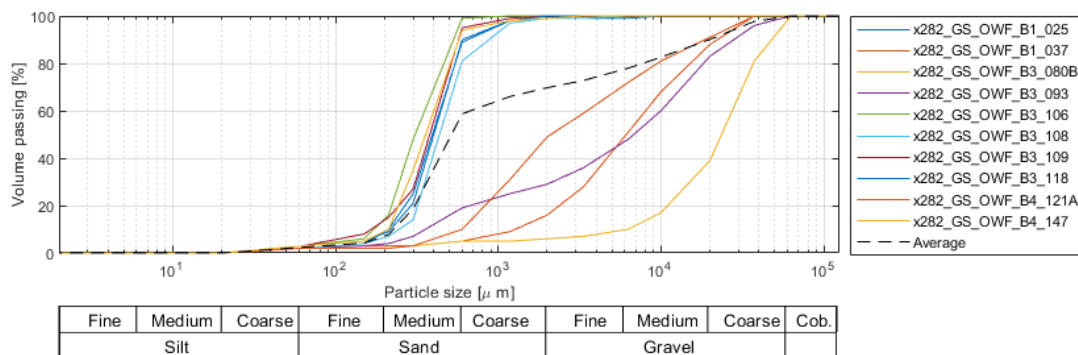
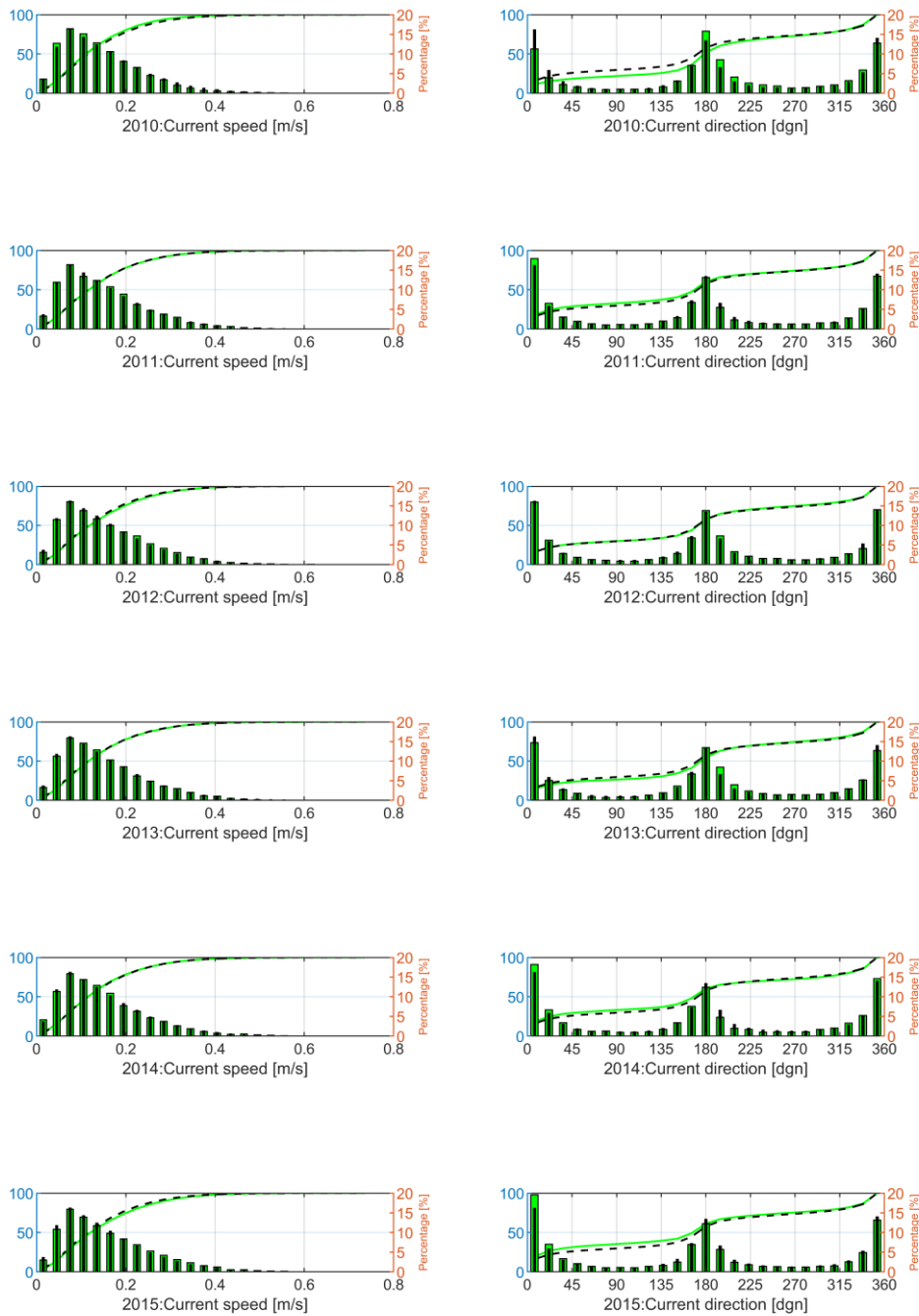
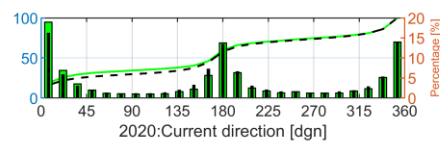
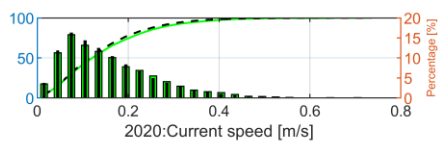
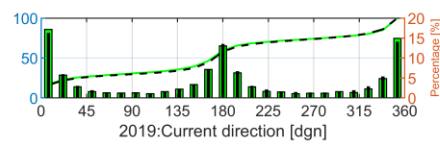
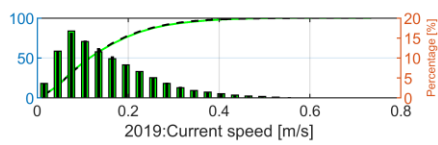
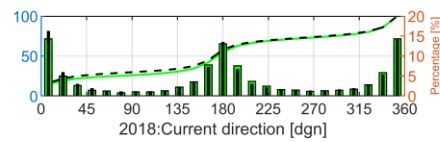
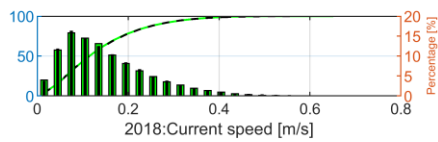
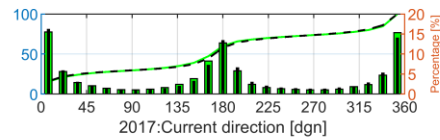
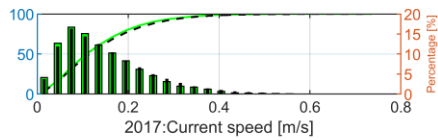
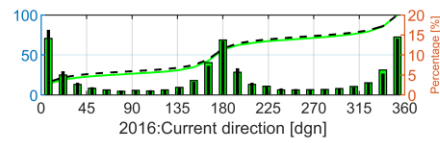
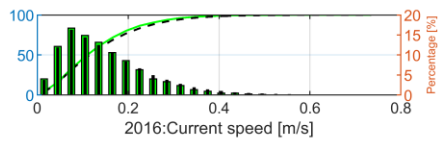


Figure 13.6: OWF Sandy gravel

Appendix 6: Yearly current distribution

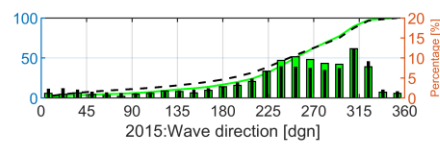
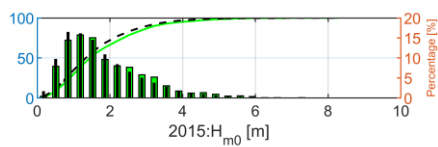
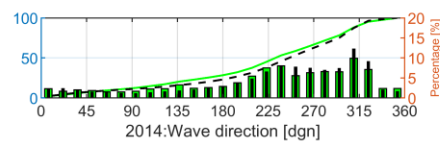
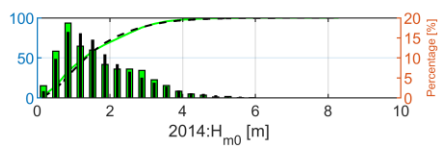
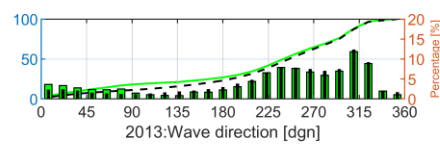
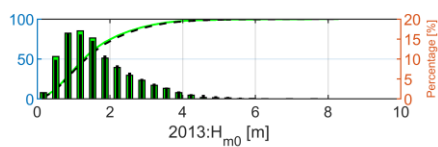
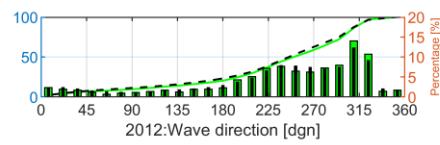
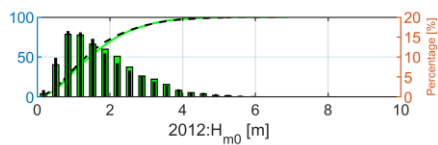
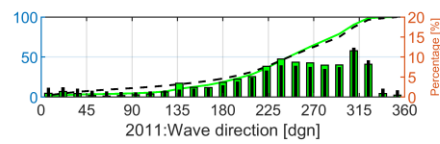
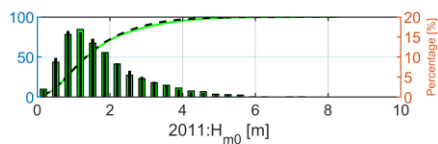
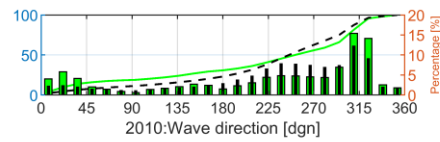
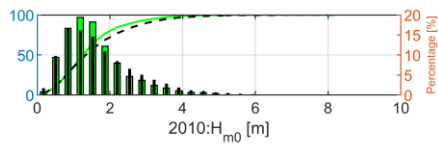
Green is the yearly distribution and black is the average.

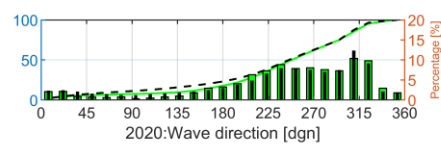
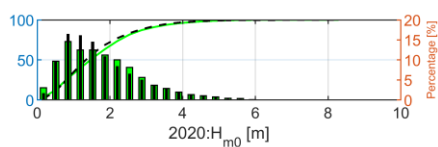
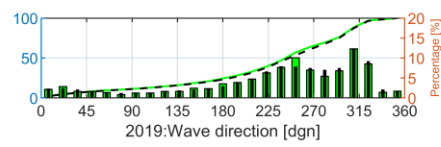
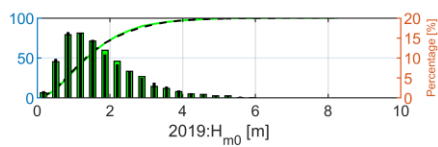
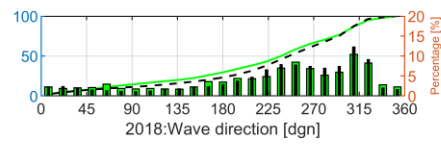
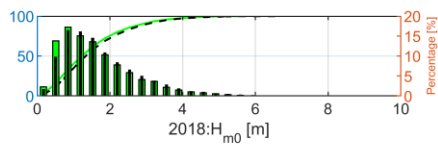
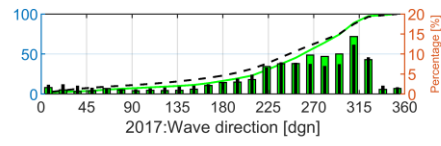
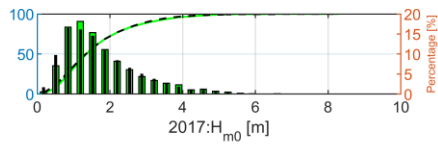
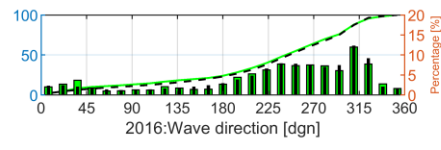
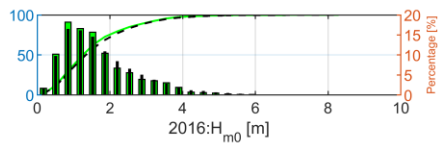




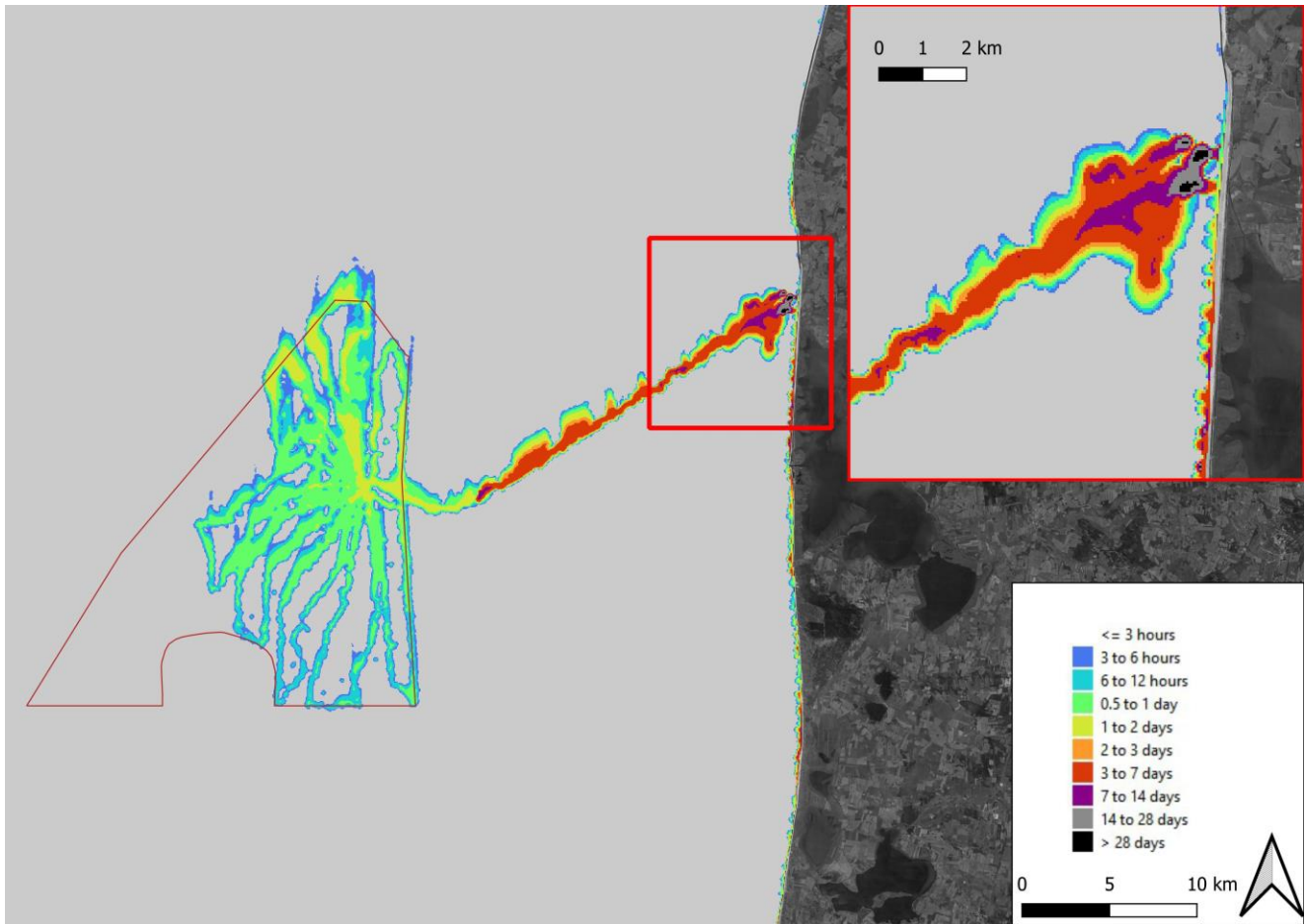
Appendix 7: Yearly wave distribution

Green is the yearly distribution and black is the average.

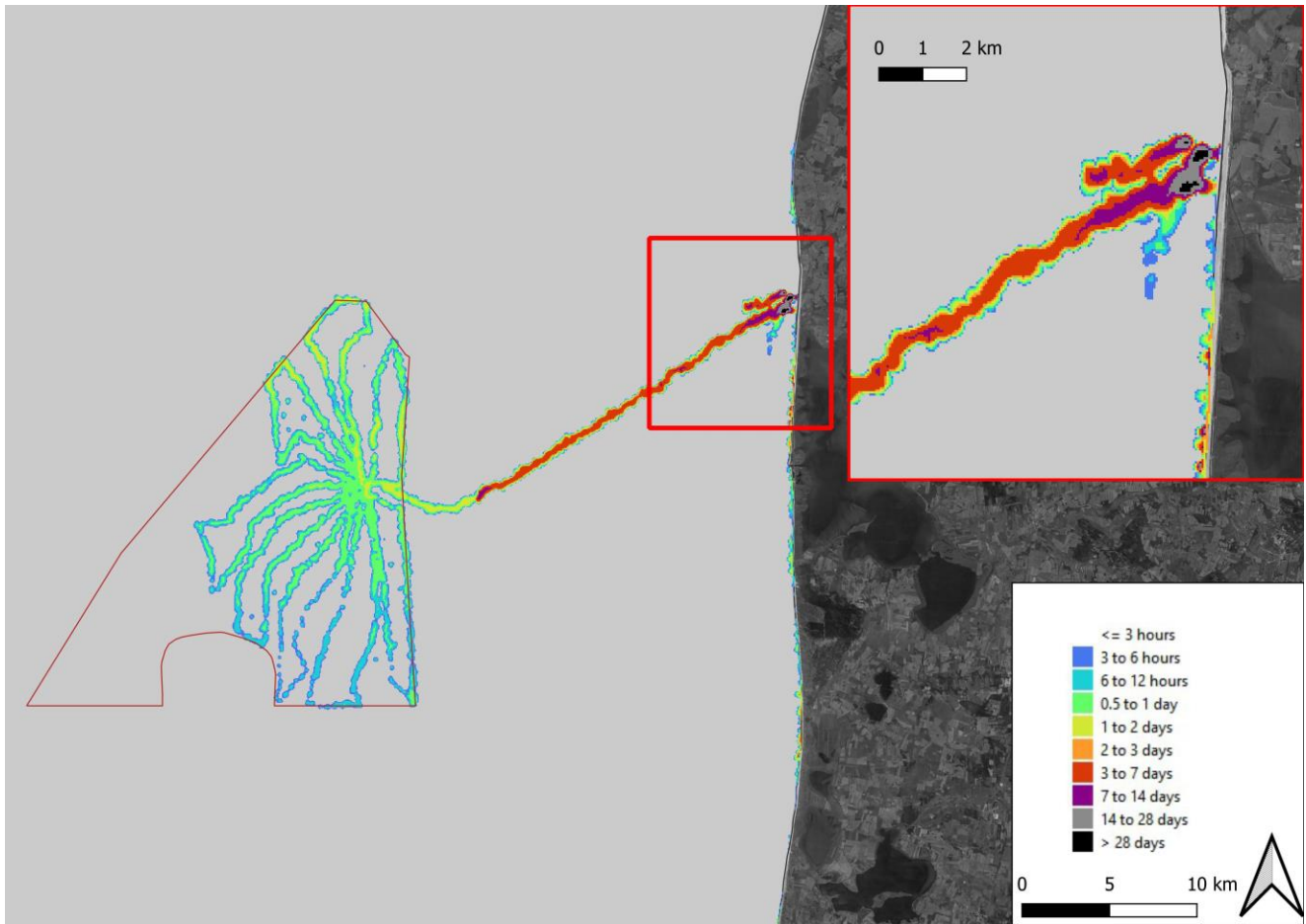




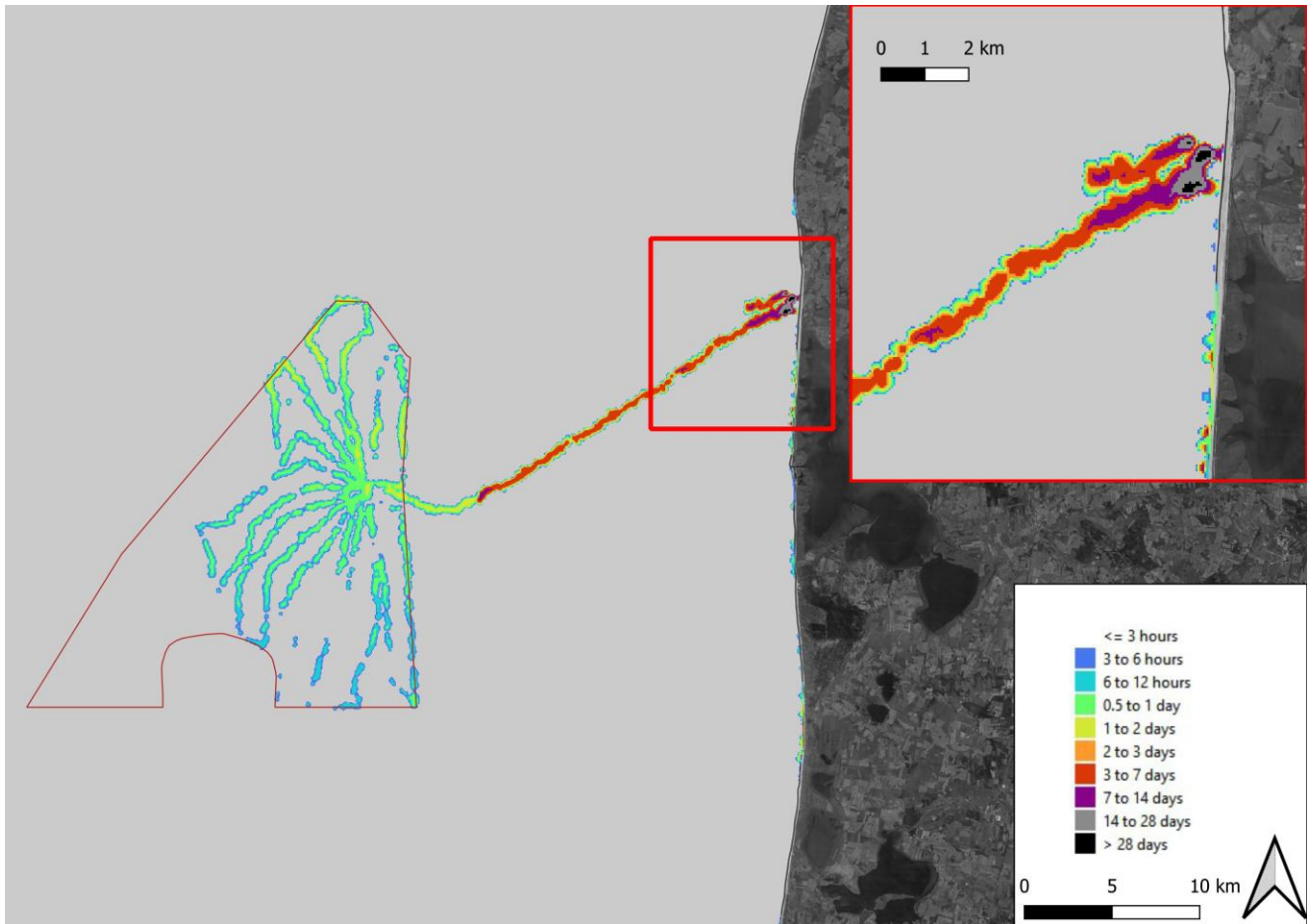
Appendix 8: Duration with sediment concentrations above 10 mg/l, depth average



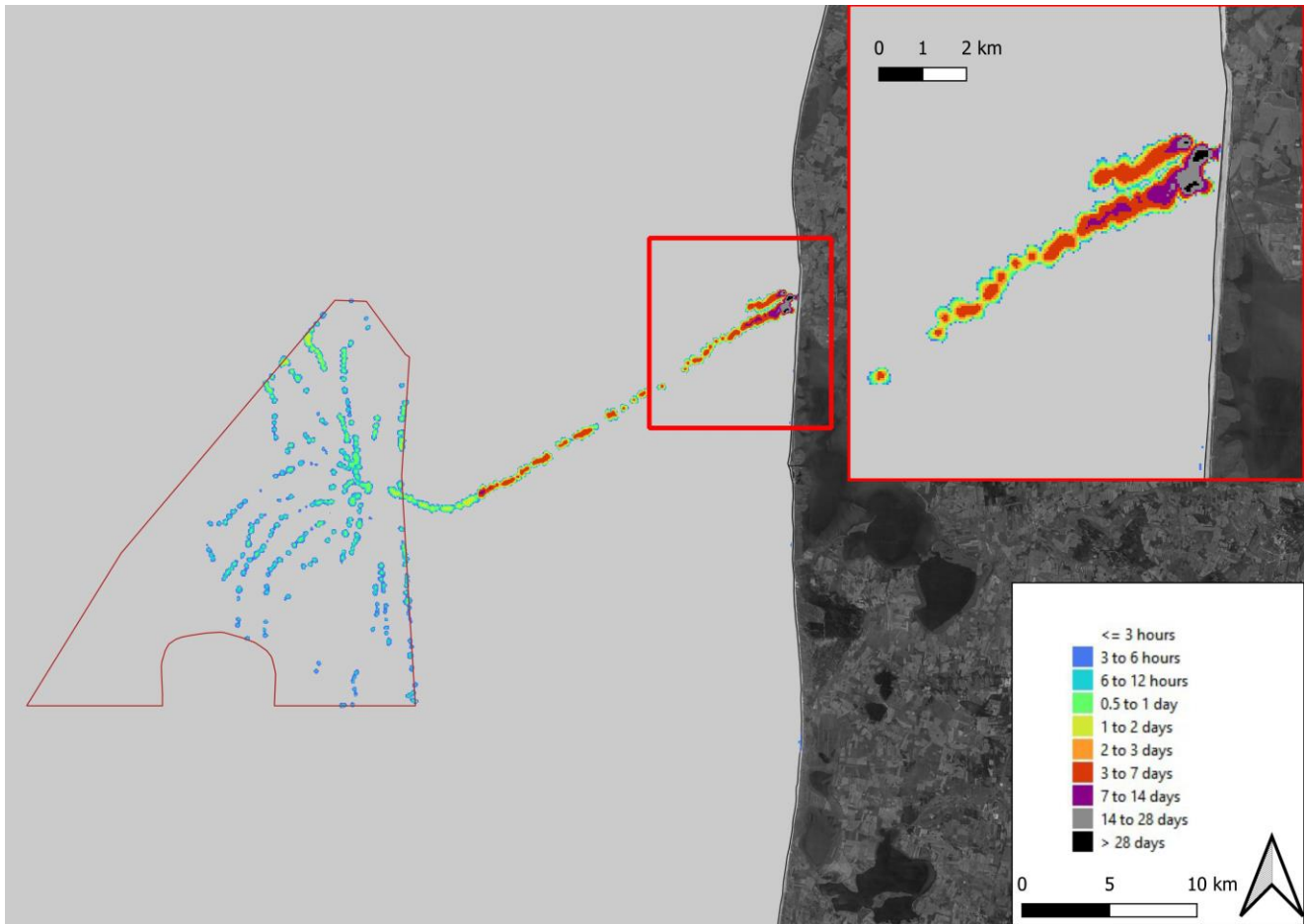
Appendix 9: Duration with sediment concentrations above 50 mg/l, depth average



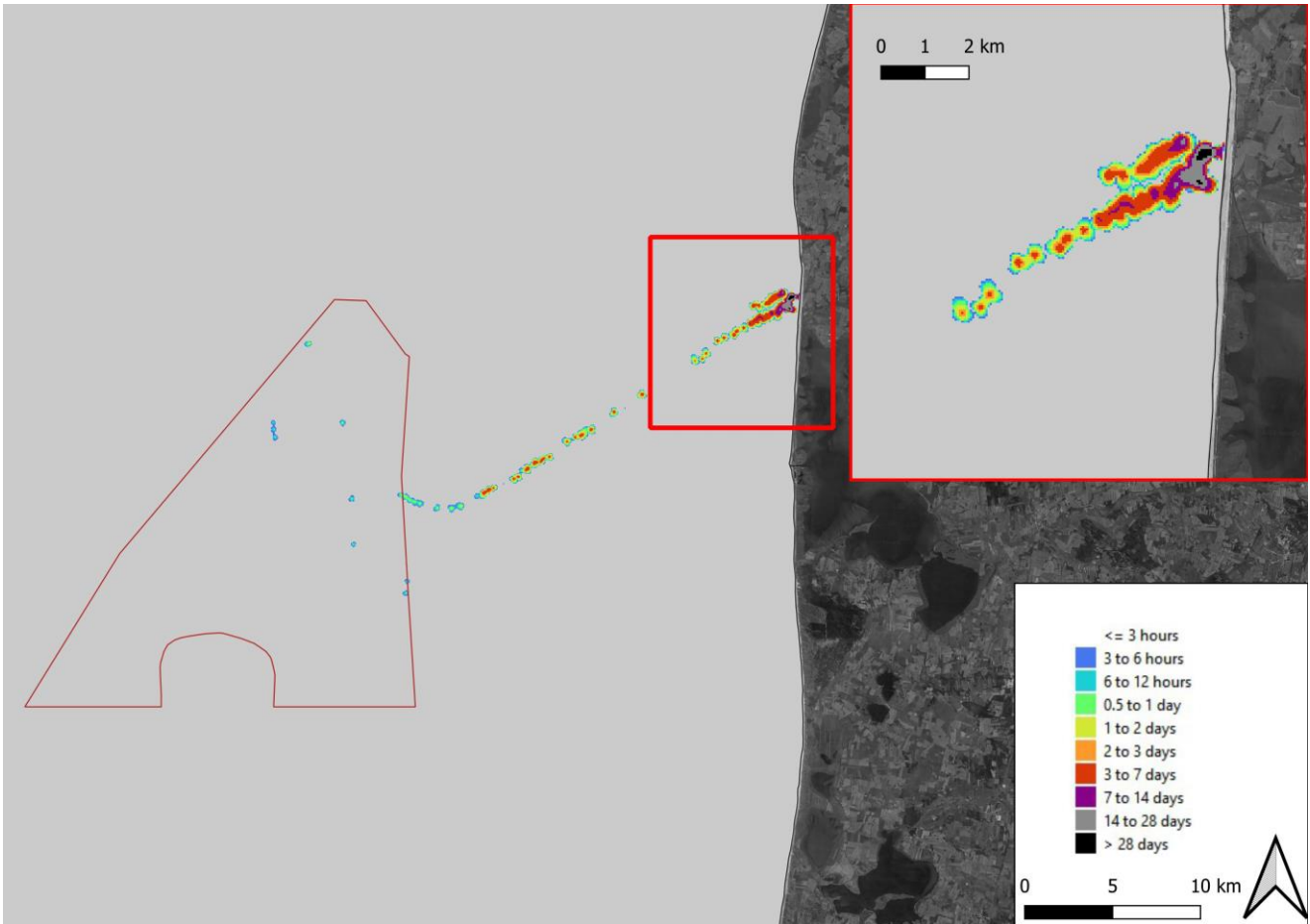
Appendix 10: Duration with sediment concentrations above 100 mg/l, depth average



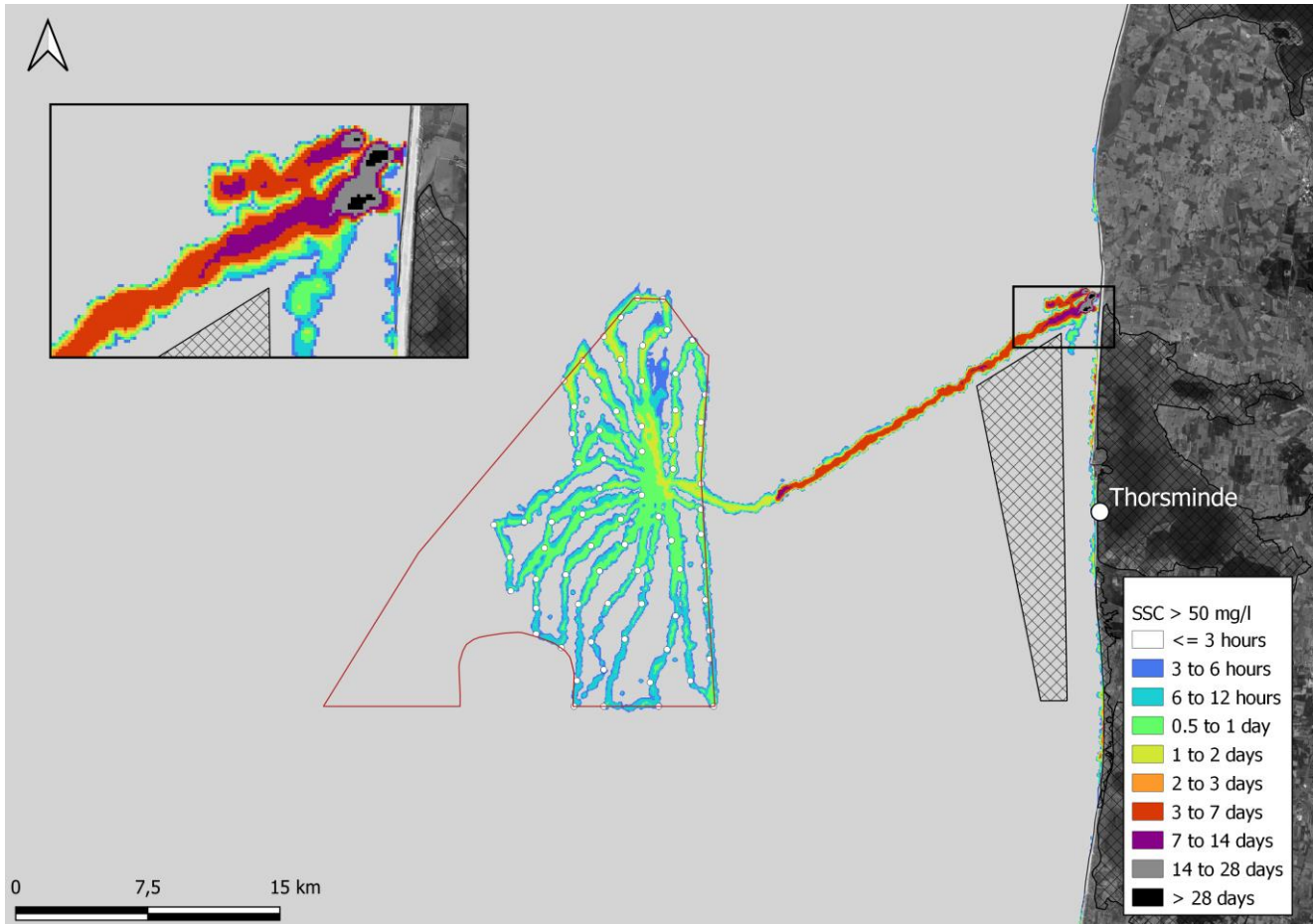
Appendix 11: Duration with sediment concentrations above 500 mg/l, depth average



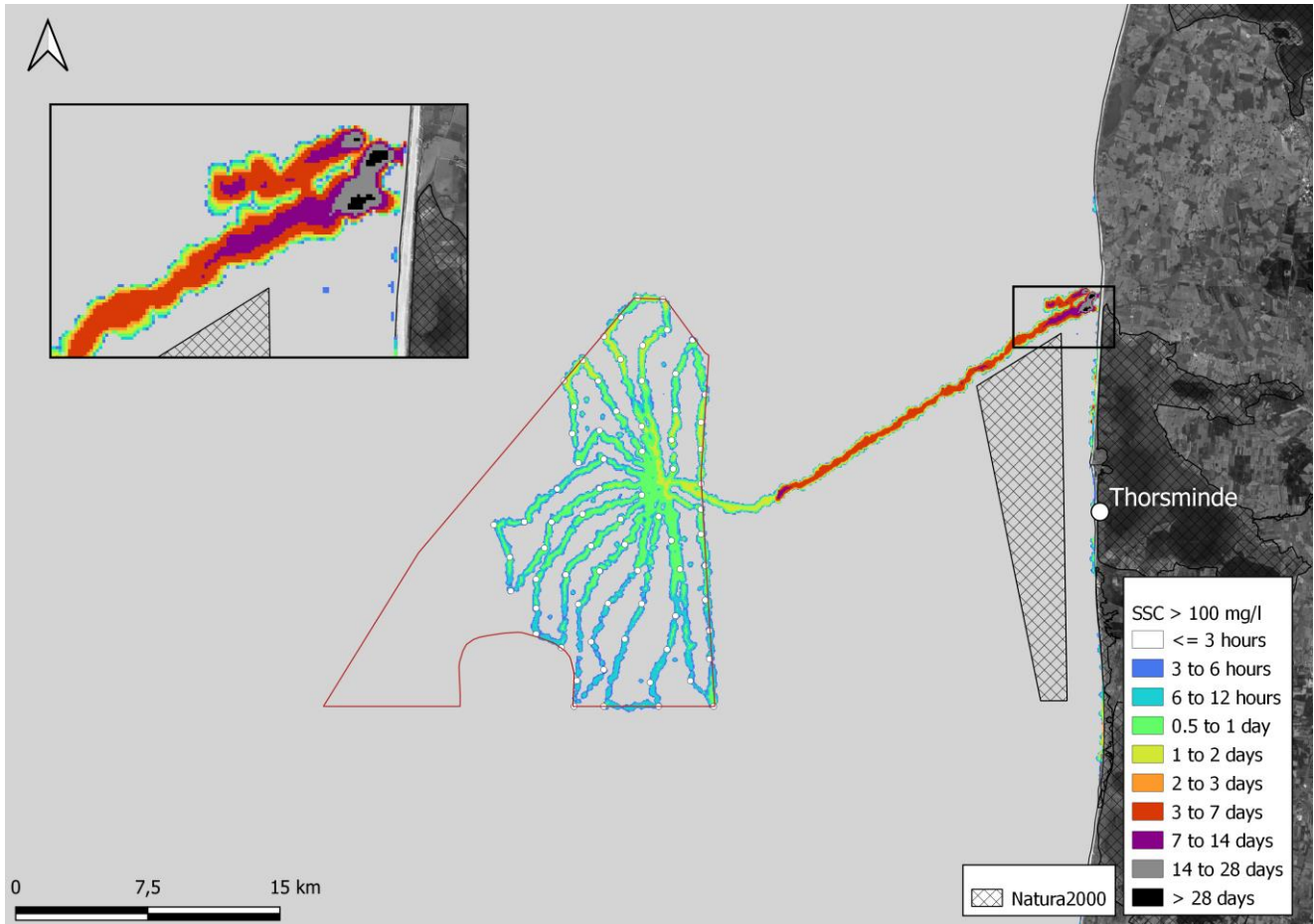
Appendix 12: Duration with sediment concentrations above 1000 mg/l, depth average



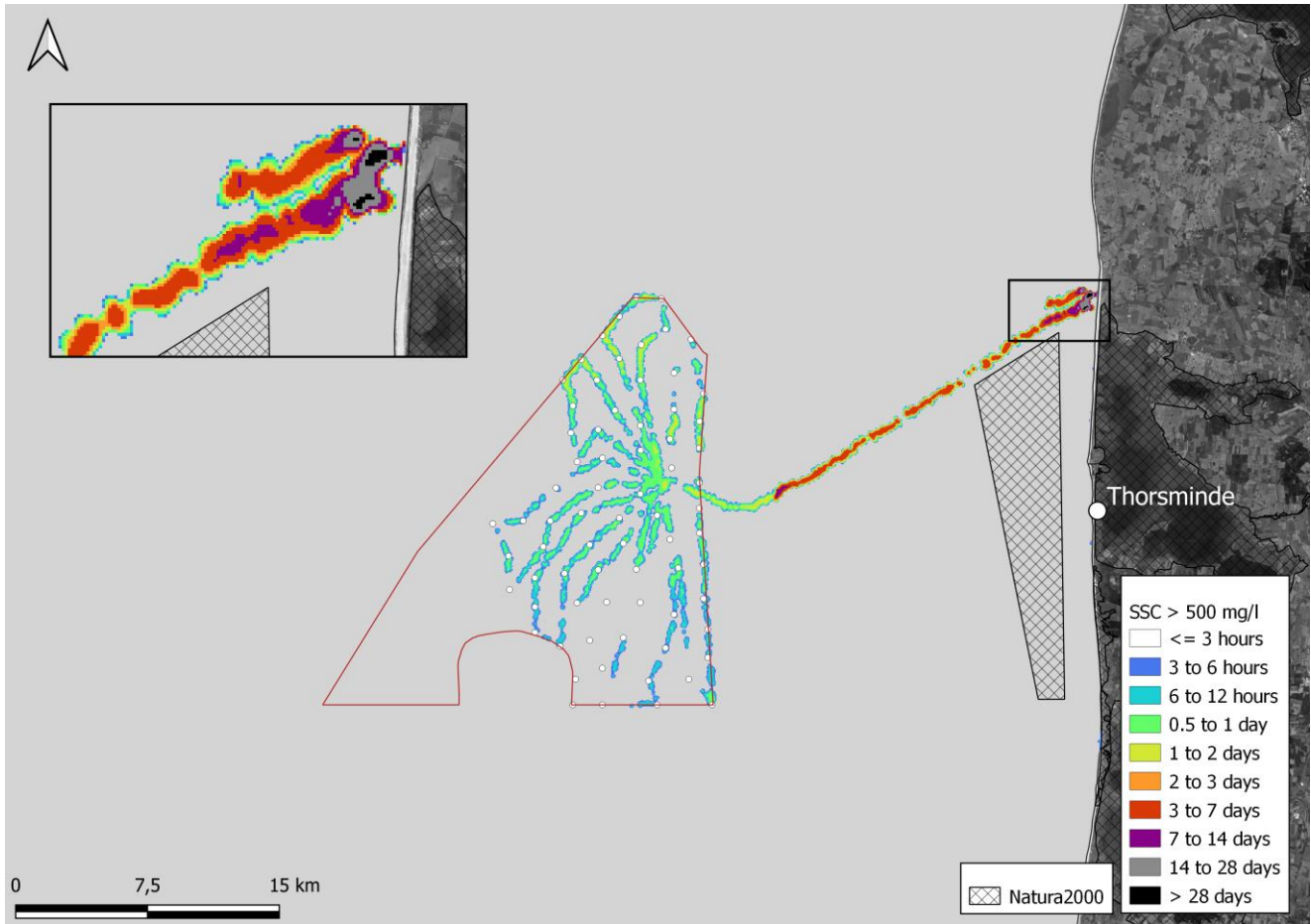
Appendix 13: Duration with sediment concentrations above 50 mg/l (bottom 10 meters)



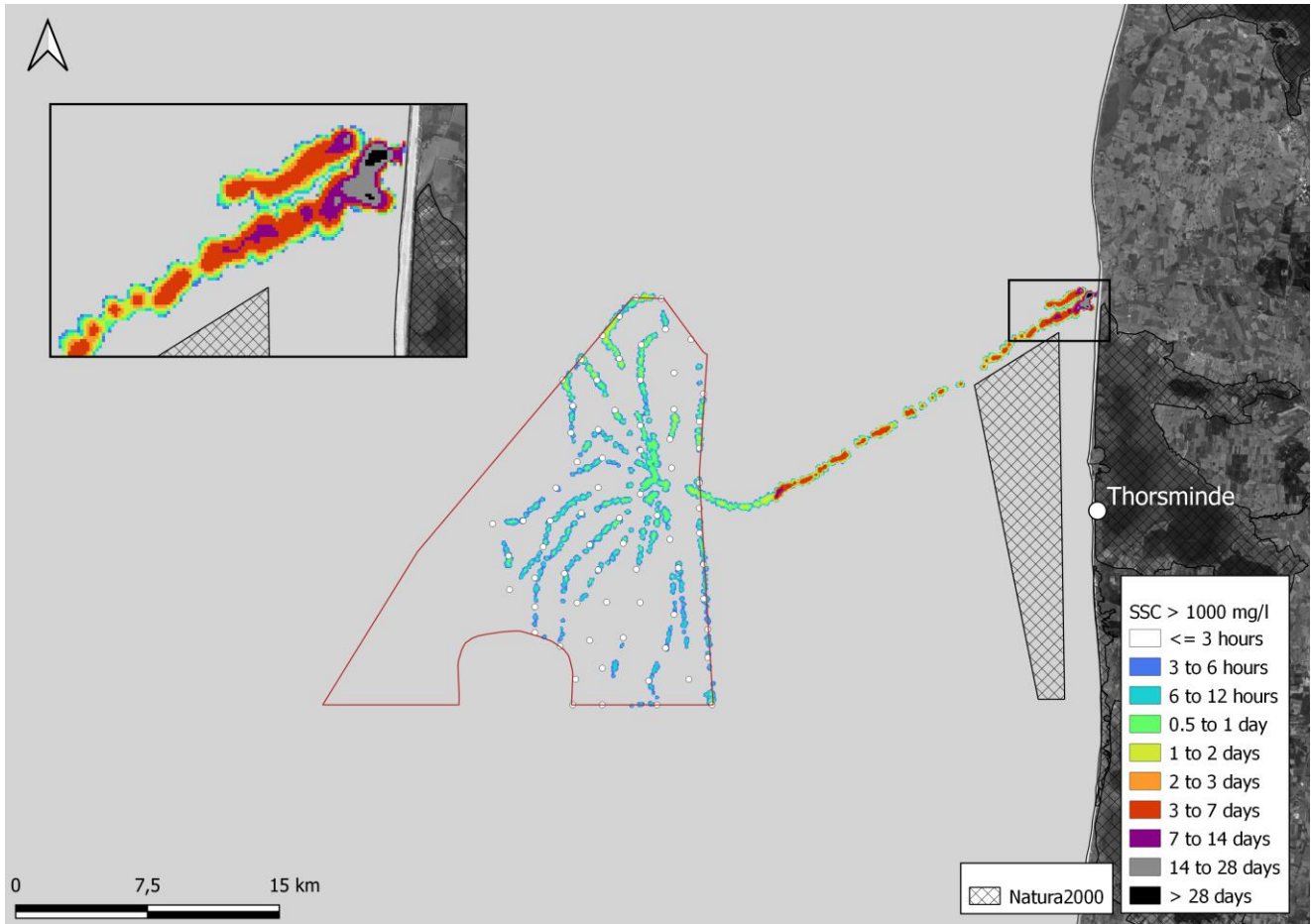
Appendix 14: Duration with sediment concentrations above 100 mg/l (bottom 10 meters)



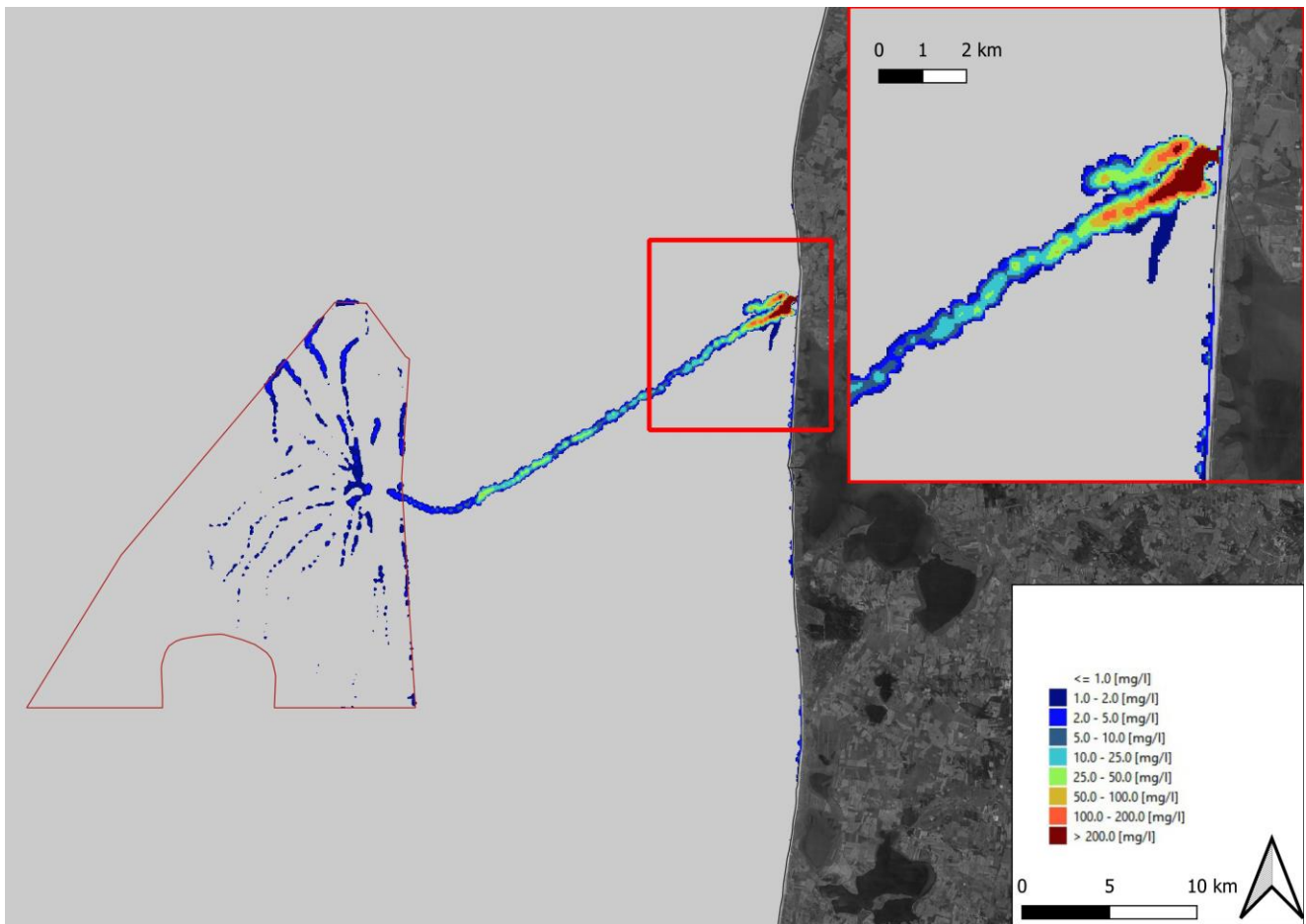
Appendix 15: Duration with sediment concentrations above 500 mg/l (bottom 10 meters)



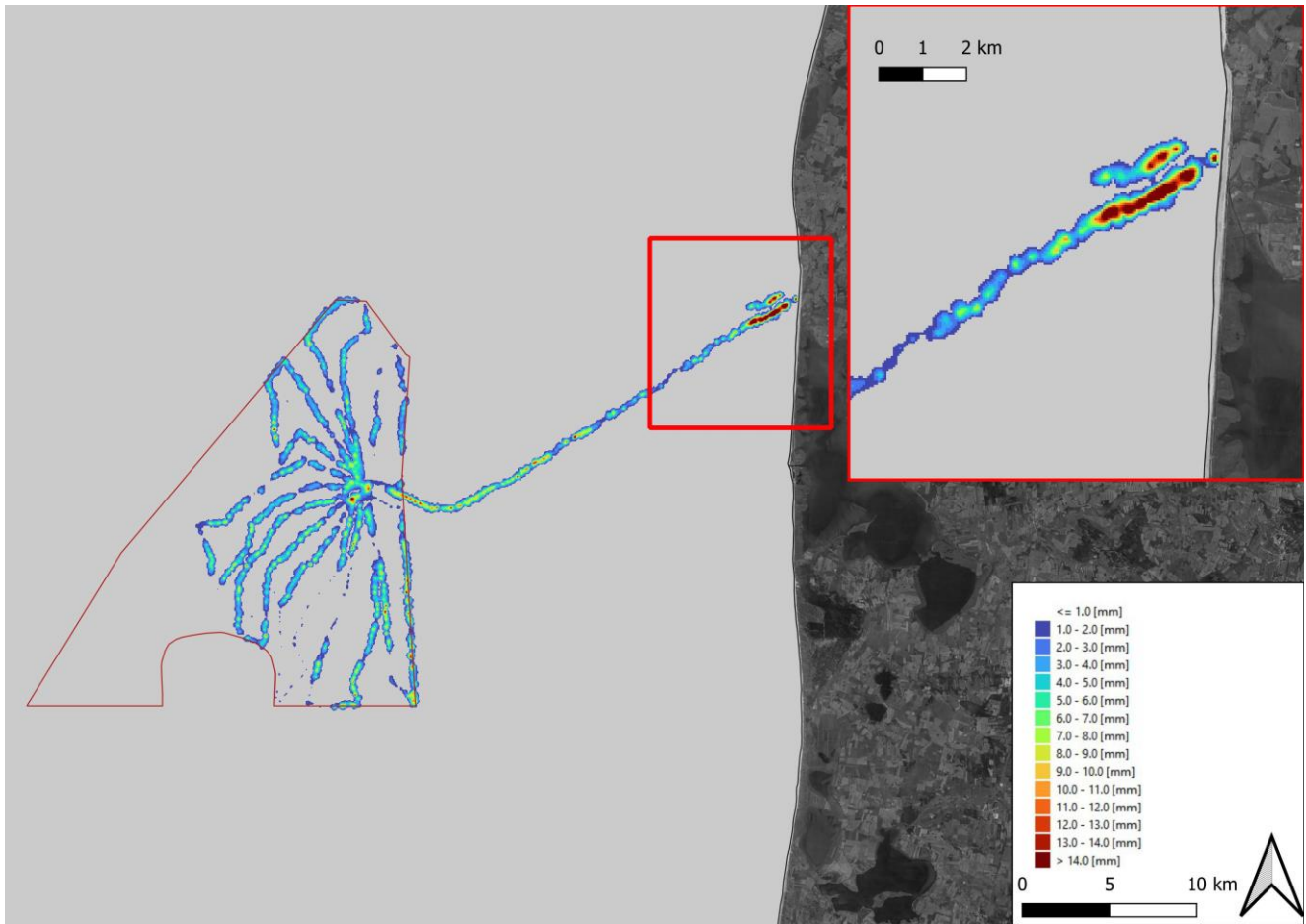
Appendix 16: Duration with sediment concentrations above 1000 mg/l (bottom 10 meters)



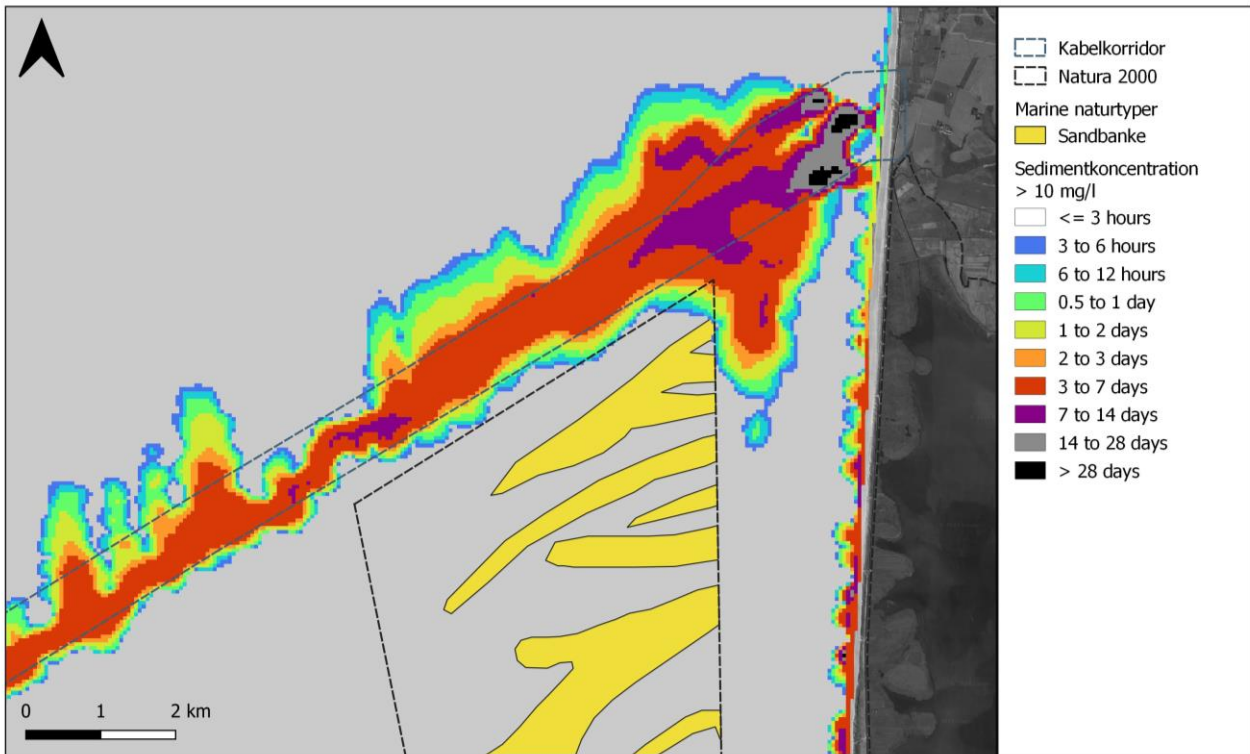
Appendix 17: Average sediment concentrations during construction, depth average



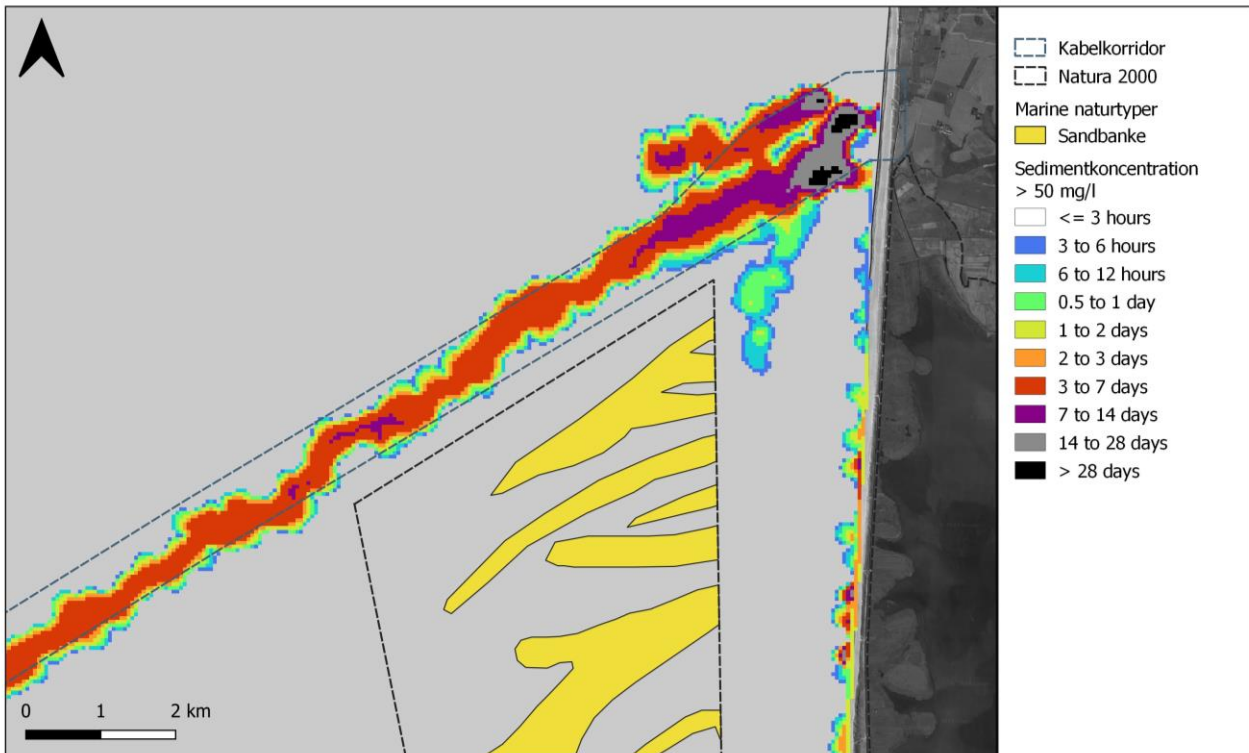
Appendix 18: Average sedimentation during construction



Appendix 19: Duration with sediment concentrations above 10 mg/l (bottom 10 m): Nearshore



Appendix 20: Duration with sediment concentrations above 50 mg/l (bottom 10 m):
Nearshore



Appendix 21: Maximum sedimentation in the construction period: Nearshore

